Universidade Federal De São Carlos
Centro De Ciências Exatas E De Tecnologia
Programa De Pós-Graduação Em Biotecnologia

Exploring the potential of eukaryotic microalgae: A biochemical, bioactive, and metabolomic study

Lucas Santos Solidade

Tese apresentada ao Programa de Pós-Gradução em Biotecnologia (PPGBIOTEC) como parte dos requisitos para obtenção do título Doutor em Ciências (Área de concentração: Biotecnologia).

Orientadora
Prof.ª. Dra. Ana Teresa Lombardi

Bolsista FAPESP (Processo: 2020/12508-2)

São Carlos – SP
2024

Lucas Santos Solidade

Exploring the potential of eukaryotic microalgae: A biochemical, bioactive, and metabolomic study

Tese apresentada ao Programa de Pós-Gradução em Biotecnologia (PPGBIOTEC) como parte dos requisitos para obtenção do título Doutor em Ciências (Área de concentração: Biotecnologia).

Orientador:
Prof.ª. Dra. Ana Teresa Lombardi

São Carlos
2024

ACKNOWLEDGMENTS

I am deeply grateful to my mother, Florisdete Borges Santos, and my grandmother, Hildete Borges Santos, for their lifelong support, which allowed me to pursue undergraduate and doctoral studies at public universities. To Vinicius Sousa Ferreira, I express my gratitude for his support and companionship throughout the Ph.D.

I extend my thanks to Professor Ana Teresa Lombardi for guiding me through this arduous journey, always willing to help and serve as a guide during the most challenging scientific moments. I am also grateful to Professors Clovis Wesley Oliveira de Souza and Ralph Urbatzka for welcoming me into their laboratories, sharing their knowledge, and providing guidance that was essential for the completion of this work.

To Professors Camila Manoel Crnkovic and Inessa Lacativa Bagatini, thank you for making your laboratory infrastructure available and for always being willing to answer questions and helping whenever possible.

My thanks also go to my colleagues from the various laboratories I have been part of: Lab Azul, the Laboratory of Microbiology and Pathology, the Blue Biotechnology Laboratory, Environment and Health, and the Algae Biotechnology Laboratory.

I would like to thank the Brazilian Federal Agency for Support and Evaluation of Graduate Education (CAPES) (Grant 88882.426529/2019-1) and the São Paulo Research Foundation (FAPESP) (Grants 2020/12508-2; 2018/07988-5) for the financial support that made this project possible. I also extend my thanks to UFSCar and the Graduate Program in Biotechnology for providing the necessary infrastructure.

Finally, I am grateful to all the scientists who have dedicated their careers to the construction of knowledge. Each of them, through their articles, dissertations, theses, and experiments contributed small building blocks that helped pave the road of knowledge I have traveled to reach this point.

To all, thank you very much!

"*If I have seen further, it is by standing on the shoulders of giants.*"

Isaac Newton

Resumo

Microalgas são microorganismos fotossintetizantes unicelulares, cuja utilização remonta à antiguidade. Elas se destacam por sua capacidade de acumular proteínas, ácidos graxos poli-insaturados, pigmentos e compostos bioativos com potencial nutricional e industrial. Este estudo teve como objetivo principal explorar microalgas eucarióticas de água doce avaliando sua composição química, bem como suas potenciais aplicações nos setores nutracêutico, da bioenergia e farmacêuticos. Para isso, foram avaliadas 26 diferentes espécies de microalgas, das quais 12 tiveram suas composições bioquímicas caracterizadas. As microalgas *Pediastrum* sp. e *Chlorella emersonii* apresentaram as composições macromoleculares mais promissoras para estudos de viabilidade industrial, com taxas de crescimento superiores às demais algas, de 0,96 e 0,90 d^{-1}, e teor proteico superior a 60%. *Pediastrum* sp. também se destacou pelo maior percentual de ácidos graxos poli-insaturados e por sua atividade antioxidante superior, o que a torna promissora como fonte nutricional. Quanto à atividade antimicrobiana, a microalga *C. emersonii* foi capaz de inibir as bactérias Gram-positivas *Staphylococcus aureus* e *Enterococcus faecalis*. Após fracionamento, seu potencial antimicrobiano foi incrementado, com as frações B e C mostrando a capacidade de inibir o crescimento de *S. aureus* em até 50 $\mu g.mL^{-1}$ e *S. mutans* até 25 $\mu g.mL^{-1}$. A análise metabólica dessas frações indicou a presença significativa de ácidos graxos poli-insaturados, possivelmente responsáveis pela atividade antimicrobiana, além de compostos secundários que necessitam de mais investigação. Observou-se também a atividade antiobesidade dos extratos, com potencial redutor de lipídios, anti-inflamatório e inibidor de apetite nas microalgas *S. bibraianum* e *Dictyosphaerium* sp. *S. bibraianum* demonstrou a maior atividade redutora de lipídios, reduzindo as reservas lipídicas em até 50%, enquanto *Dictyosphaerium* sp. apresentou a maior atividade inibidora do apetite (70% de inibição) e anti-inflamatória (95% de inibição). A análise metabolômica revelou metabólitos, como derivados da clorofila e lipídios polares, associados a essas bioatividades. Os ensaios também indicaram ausência de citotoxicidade dos extratos. Assim conclui-se que as microalgas *C. emersonii*, *Pediastrum* sp. e *Dictyosphaerium* sp. mostram-se promissoras para aplicações nutracêuticas e farmacêuticas. Elas podem ser exploradas futuramente para aplicações industriais, destacando-se das demais algas avaliadas.

Palavras chaves: Aplicações nutricionais; Antiobesidade; Antimicrobiano; Microalgas de água doce.

Abstract

Microalgae are unicellular photosynthetic microorganisms whose use dates back to ancient times. They stand out for their ability to accumulate proteins, polyunsaturated fatty acids, pigments, and bioactive compounds with nutritional and industrial potential. This study aimed to explore freshwater eukaryotic microalgae by evaluating their chemical composition, as well as their potential applications in the nutraceutical, bioenergy and pharmaceutical sectors. For this purpose, 26 different species of microalgae were evaluated, of which 12 had their biochemical compositions characterized. The microalgae *Pediastrum* sp. and *Chlorella emersonii* presented the most promising macromolecular compositions for industrial feasibility studies, with growth rates higher than the other algae (0.96 and 0.90 d^{-1}) and protein content greater than 60%. *Pediastrum* sp. also stood out for its higher percentage of polyunsaturated fatty acids and superior antioxidant activity, making it promising as a nutritional source. Regarding antimicrobial activity, the microalga *C. emersonii* was able to inhibit the Gram-positive bacteria *Staphylococcus aureus* and *Enterococcus faecalis*. After fractionation, its antimicrobial potential increased, with fractions B and C showing the ability to inhibit the growth of *S. aureus* at concentrations of up to 50 µg.mL^{-1} and *S. mutans* at up to 25 µg.mL^{-1}. Metabolic analysis of these fractions indicated the significant presence of polyunsaturated fatty acids, likely responsible for the antimicrobial activity, as well as secondary compounds that require further investigation. The anti-obesity activity of the extracts was also observed, with lipid-reducing, anti-inflammatory, and appetite-suppressing potential in the microalgae *S. bibraianum* and *Dictyosphaerium* sp. *S. bibraianum* demonstrated the highest lipid-reducing activity, reducing lipid reserves by up to 50%, while *Dictyosphaerium* sp. exhibited the greatest appetite-suppressing (70% inhibition) and anti-inflammatory activity (95% inhibition). Metabolomic analysis revealed metabolites such as chlorophyll derivatives and polar lipids associated with these bioactivities. The assays also indicated an absence of cytotoxicity in the extracts. In conclusion, the microalgae *C. emersonii*, *Pediastrum* sp., and *Dictyosphaerium* sp. show promise for nutraceutical and pharmaceutical applications. They may be further explored for future industrial applications, standing out from the other algae evaluated in this study.

Keywords: Nutritional applications; Anti-obesity; Antimicrobial; Freshwater microalgae.

LIST OF FIGURES

General Introduction

Chapter 1: Biochemical characterization of 12 freshwater microalgae reveals *Pediastrum* sp. as a promising species for nutrition and *Dimorphococcus* sp. for biofuels.

LIST OF TABLES

General Introduction

Chapter 1: Biochemical characterization of 12 freshwater microalgae reveals *Pediastrum* sp. as a promising species for nutrition and *Dimorphococcus* sp. for biofuels.

LIST OF ABBREVIATIONS AND ACRONYMS

AMDIS	Automated mass spectral deconvolution & identification system
ANOVA	Analysis of variance
AOCS	American oil chemists' society
ARA	Arachidonic acid
BG11	Blue green medium
Chl a	Chlorophyll a
Chl b	Chlorophyll b
Chl c	Chlorophyll c
Chl a/b	Chlorophyll a/b ratio
DCM	Dichloromethane
DGTSA	Diacylglyceryltrimethylhomo
DHA	Docosahexaenoic acid
DMEM	Dulbecco's Eagle's medium
EPA	Eicosatetraenoic acid
FAMEs	Fatty acid methyl esters
GAE	Gallic acid equivalent
GNPS	Global natural products social molecular networking
HPLC	High performance liquid chromatography
LC-HRESIMS/MS	Liquid chromatography-high resolution electrospray ionization tandem mass spectrometry
MeCN	Acetonitrile
MeOH	Methanol
MIC	Minimal inhibitory concentration
MUFAS	Monounsaturated fatty acids
NPA	Natural product atlas
PCA	Principal component analysis
PUFAS	Polyunsaturated fatty acids
SFAS	Saturated fatty acids
SQDG	Sulfoquinovosyl diacylglycerol
TC	Total Carotenoids concentration
TPC	Total phenolic content
WC	Freshwater medium for the culturing microalgae
μ_{max}	Maximum Growth rate
ω3	Omega 3
ω6	Omega 6
ω6/3	Omega 6/3 ratio

SUMMARY

OVERVIEW

This Doctorate thesis is divided into 3 chapters, each one dealing with specific subjects, all of them related to microalgae biotechnology, advancing the present knowledge related to the prospection and applications of microalgae and their extracts.

Microalgae are diverse organisms from a morphological, environmental, and chemical perspective. Although their applications in the food and pharmaceutical industries are widely recognized, the groups that have been explored remain limited to a small number compared to the total number of known species. Therefore, searching for new strains with promising potential helps expand our understanding of microalgae diversity and their biotechnological applications.

Various bioproducts can be derived from microalgae, including biomass, which is valuable on its own, and specific molecules like proteins, carbohydrates, lipids, and carotenoids. These metabolites have direct applications in areas such as food, biofuels, and pharmaceuticals. Although commercially valuable, the real treasure lies in their chemical potential. Unlike plants and bacteria, microalgae have been underexplored regarding their chemical diversity, making them a promising source for the discovery of new bioactive molecules. This potential includes antimicrobial activity, which is particularly relevant in the light of the recent rise of antibiotic-resistant bacteria. Other applications involve molecules that benefit human health, with direct impacts on metabolism. These include potential treatments for non-communicable chronic diseases and related comorbidities. Examples of these applications are the development of anti-inflammatory, anti-obesity, and appetite suppressant drugs, among others.

While the discovery of new molecules is crucial, traditional drug discovery methods are slow and expensive, limiting their efficiency in meeting industry needs. By integrating modern approaches, such as advanced analytical technologies and computational methods, the discovery of unique molecules can be accelerated, reducing the likelihood of rediscovering known compounds. One strategy to achieve this involves using disease models, such as cell cultures and more complex organisms like zebrafish embryos. Zebrafish offer several advantages: their development closely mimics that of fully developed organisms, they do not require ethical approval, and they are cost-effective and easy to maintain.

Considering that microalgae have high physiological plasticity, in this research we have used microalgae physiology concepts, such as strictly controlled culture conditions to grow the cells, focusing on reproducible results, combined with modern screening techniques and computational analysis to prospect for new compounds with diverse applications. The first chapter provides information on the physiology and biochemical composition such as its constitutive biomolecules (lipids, proteins and carbohydrates) of 12 microalgae strains. The second and third chapters aims at prospecting bioactivity of extracts from the microalgae studied in chapter 1, including 14 additional species. This increase in the number of species aimed to expand the biological diversity, and a total of 26 microalgal strains were subjected to sequential extraction using two solvents, resulting in a total of 52 different extracts. In chapter 2, we explore the antimicrobial potential of these extracts against some pathogenic bacteria, while in chapter 3 anti-inflammatory, anti-obesity and appetite suppressant activity were investigated. The present study should make an important contribution to the growing area of microalgae biotechnology by exploring the potential applicability of understudied microalgae strains.

1. General Introduction

1.1. Microalgae: Commercial Applications and Bioactive Potential

Microalgae are a diverse group of photosynthetic microorganisms, which can be unicellular or colonies. The term "microalgae" is a general term used to include various organisms that exhibit such characteristics. The groups commonly referred to as microalgae include the taxonomic Phylum Glaucophyta, Chlorophyta, Rhodophyta, Excavata (class: Euglenophyceae), Rhizaria, Cryptista, Stramenopiles, Alveolata, Haptophyta and Cyanophyta (SEXTON; LOMAS, 2018). There is considerable debate surrounding the classification of blue-green algae (Cyanobacteria), which are often classified as a separate group because they are procaryotic, and photosynthetic microorganisms, which share with the eucaryotic microalgae the same ecological niche. However, in the present work cyanobacteria will be included in the microalgae group.

Microalgae play a crucial ecological role in the environment. They have chlorophyll a and perform photosynthesis, thus act as significant carbon fixers. It has been reported that microalgae are capable of absorbing 10 to 50 times more carbon dioxide (CO_2) than terrestrial plants if they were distributed in the same area as the plants (WANG et al., 2008). Globally, they contribute to the regulation and maintenance of atmospheric CO_2 levels. This process, known as biological carbon pump, is characterized by the conversion of the inorganic carbon into particulate organic carbon through photosynthesis (RICOUR et al., 2023) in the ocean. This organic matter then sinks, transporting carbon to deep ocean zones. Some of this carbon is consumed and returns as inorganic carbon, while a portion remains trapped in deep regions (>1000 m). This process helps to increase the concentration of available carbon in the ocean by approximately 1700 pentagrams (Pg) and helps maintain atmospheric CO_2 levels (WILSON et al., 2022).

In addition to their ecological importance, microalgae began to gain biotechnological relevance in the 1940s in Germany, where large-scale cultures of diatoms were conducted aiming at using them as fuel (BARBOSA et al., 2023). However, it was not until the 1970s in Japan that the industrial production of Chlorella for food purposes began, despite the high costs of the product at the time (PULZ; SCHEIBENBOGEN, 2006). Its use as a food source persisted, and today, Chlorella is one of the main genera used in food, along with Spirulina (BARBOSA et al., 2023). Other groups are used as sources of carotenoids and/or lipids. In this case, industrial production is

mainly limited to few species of microalgae (DUMAY; MORANÇAIS, 2016). Table 1 is a short list of microalgae genus in the commerce nowadays.

Table 1. General groups of microalgae and their potential industrial applications.

Microalgae	Phylum	Application or bioproduct	Reference
Chlorella sp.	Chlorophyta	Food	(RICHMOND, 2003)
		Carotenoid	(LIU; CHEN, 2014)
		Wastewater treatment	
Arthrospira sp.	Cyanobacteria	Food	(RICHMOND, 2003)
		Phycobiliproteins	
		Aquaculture	(BELAY; KATO; OTA, 1996)
		Bioinoculants	(ARAHOU et al., 2023)
Dunaliella sp.	Chlorophyta	βS-carotene	
		Food	(RICHMOND, 2003)
		Phytoene	
		Biorremediation	
Haematococcus sp.	Chlorophyta	Astaxantin	(RICHMOND, 2003)
		Food colorant	
		Cosmetics	(OSLAN et al., 2021)
Porphyridium sp.	Rhodophyta	Polysaccharide	(RICHMOND, 2003)
Nannochoropsis sp.	Heterokontophyta	Aquaculture	
Nostoc sp.	Cyanobacteria	Aquaculture	
Botryococcus sp.	Chlorophyta	Biofuels	(ESTEVAM et al., 2022)

The literature describes several characteristics that make microalgae promising organisms for industrial use, among them the ability to fix atmospheric CO_2, high photosynthetic performance, rapid growth, and the production of specific compounds (GUEDES; AMARO; MALCATA, 2011). Their protein content can vary, reaching up to 80% of their dry biomass (JANSSEN; WIJFFELS; BARBOSA, 2022). Another aspect to mention is their amino acid composition, which according to WILLIAMSON et al. (2024) are rich in essential amino acids. Polyunsaturated fatty acids (PUFAs) such as omega-3 and omega-6 are essential fatty acids produced by algae as well (SED; CICCI; BRAVI, 2017). Some microalgae may accumulate considerable lipid content relative to dry biomass, reaching up to 60% (MORALES; AFLALO; BERNARD, 2021). Pigments are a class

of molecules that may be of industrial interest and are accumulated by microalgae. Some of these are lutein, carotenoids, phycocyanin. Altogether, they have different uses in the society. The first two have pharmaceutical and nutraceutical applications (SHEGOKAR; MITRI, 2012), while the last can be used as natural colorant. Thanks to these applications, microalgae biomass has become of interest for various industrial sectors.

Considering bioenergy, microalgae are of particular interest due to the wide range of products that can be derived from their biomass, such as biomethane, biohydrogen, bioethanol, and, notably, biodiesel, which has gained significant attention (BORA et al., 2024). Various microalgal species have been studied for this purpose, including *Nanochloropsis* sp. and *Chlorella* sp. (SATI et al., 2019). The rationale for choosing microalgae as source of biofuel lies in the quality of their oil, which is comparable to that of plants and considered suitable for biodiesel production (CHEN et al., 2018). Additionally, microalgae offer greater versatility than plants, as they can be cultivated throughout most of the year, do not compete with agricultural food production, and require proportionally less water (RUANE; SONNINO; AGOSTINI, 2010). The main advantage of microalgae, however, is their ability to accumulate large amounts of lipids, with a productivity per hectare superior to that of palm and soybeans (BARBOSA et al., 2023).

It is evident that the different biomolecules from microalgae offer numerous potential applications. Several authors have been exploring the concept of a biorefinery for microalgae, where biomass can be used to obtain a wide variety of products (BHATTACHARYA; GOSWAMI, 2020; FERNÁNDEZ et al., 2021). Table 2, presented below, lists some microalgae and their biochemical composition related to total proteins, carbohydrates and lipids. Besides the primary metabolites, microalgae produce secondary metabolites. These are classified as non-essential for cell maintenance, but their presence provides advantages, such as resistance to predators or environmental stress (Cardozo et al., 2007; Hassan et al., 2019; Martín et al., 2005). Related to biotechnology, such metabolites have high added value due to their potential use in the industry of fine chemicals. Their value lies in the biological effect they may exert, thus a valuable biomass for commercial production, potentially costing up to 10 times more (ACIÉN FERNÁNDEZ, 2019). In general, the metabolites produced by microalgae have bioactive potential (ABREU; MARTINS; NUNES, 2023), however most of them have been underexplored and its majority can be considered as new compounds (OLAIZOLA, 2003).

Table 2. General biochemical composition of different microalgae. The content of proteins, carbohydrates and lipids is reported as % of dry matter.

Algae	Group	Proteins	Carbohydrates	Lipids	Reference
Botryococcus braunii	Chlorophyta	41.70	20.00	30.20	(Ferreira et al., 2021)
Chlamydomonas nivalis	Chlorophyta	33.40	38.40	22.20	(Verspreet et al., 2021)
Chlorella fusca	Chlorophyta	32.00	24.00	12.00	(Silva et al., 2023)
Chlorella vulgaris	Chlorophyta	37.53	47.43	9.54	(Nordin et al., 2022)
Desmodesmus brasiliensis	Chlorophyta	42.20	32.70	14.50	(Ferreira et al., 2021)
Dunaliella salina	Chlorophyta	29.50	-	23.00	(Chen et al., 2020)
Kirchneriella lunaris	Chlorophyta	58.95	7.62	15.95	(Santhakumaran et al., 2018)
Monoraphidium griffithii	Chlorophyta	44.36	13.68	14.27	(Santhakumaran et al., 2018)
Myrmecia bisecta	Chlorophyta	45.52	11.37	12.68	(Santhakumaran et al., 2018)
Neochloris oleoabundans	Chlorophyta	13.50	12.33	24.12	(Sánchez-Saavedra et al., 2023)
Oocystis lacustris	Chlorophyta	43.77	12.47	16.49	(Santhakumaran et al., 2018)
Pseudococcomyxa simplex	Chlorophyta	35.89	8.23	23.78	(Santhakumaran et al., 2018)
Pseudotetradesmus quaternaries	Chlorophyta	35.02	8.74	27.17	(Santhakumaran et al., 2018)
Radiococcus nimbatus	Chlorophyta	21.01	12.62	16.05	(Santhakumaran et al., 2018)
Tetraselmis suecica	Chlorophyta	40.20	20.80	28.50	(Verspreet et al., 2021)
Tetrastrum komarekit	Chlorophyta	40.85	4.58	28.07	(Santhakumaran et al., 2018)
Aphanocapsa marina	Cyanobacteria	11.21	42.40	26.24	(Sánchez-Saavedra et al., 2023)
Nostoc sphaeroides	Cyanobacteria	50.80	14.50	15.10	(Verspreet et al., 2021)
Phormidium sp.	Cyanobacteria	10.84	40.32	28.70	(Sánchez-Saavedra et al., 2023)
Spirulina platensis	Cyanobacteria	42.80	21.50	5.50	(Matos et al., 2016)
Isochrysis galbana	Haptophyta	14.36	11.09	13.38	(Sánchez-Saavedra et al., 2023)
Cymbella sp.	Heterokontophyta	42.46	18.09	24.98	(Sánchez-Saavedra et al., 2023)
Heterococcus sp.	Heterokontophyta	15.39	21.95	5.01	(Sánchez-Saavedra et al., 2023)
Nannochloropsis gaditana	Heterokontophyta	46.20	15.80	31.90	(Verspreet et al., 2021)
Phaeodactylum tricornutum	Heterokontophyta	39.00	15.40	14.90	(Matos et al., 2016)
Galdieria sulphuraria	Rhodophyta	43.95	5.91	14.11	(Montenegro-Herrera et al., 2022)
Porphyridium tricornutum	Rhodophyta	38.80	11.00	20.50	(Verspreet et al., 2021)
Tisochrysis lutea	Haptophyta	42.90	8.60	27.90	(Verspreet et al., 2021)

Regarding the activities of biomolecules synthesized by microalgae, astaxanthin is an example that in addition to having a potent antioxidant activity (greater than other carotenoids such as lutein or β-carotene, Naguib, 2000) has a protective effect by inhibiting pathways associated with cancer development and inducing apoptosis in an oral cancer model in hamsters (KAVITHA et al., 2013). Still, on the potential antitumor application of microalgae, the polysaccharide from *Porphyridium cruentum* was able to extend the survival time by up to 15 days in mice grafted with Graffi tumor cells (GARDEVA et al., 2009).Another polysaccharide, this time from *Synechococcus* sp., also showed a promising effect as anti-tumor activity, inducing apoptosis in colon cancer cells (SRIMONGKOL et al., 2023). Hielscher-Michael et al. (2016) identified a group of sulfolipids in *Scenedesmus* sp. microalgae that is capable of inhibiting glutaminyl cyclase, an enzyme associated with the development and worsening of Alzheimer's disease. Yang et al. (2022) observed inhibitory effects on inflammatory activity in macrophages associated with the presence of linoleic and linolenic acids from *Chlorella* sp. Additionally, 1-palmitoyl-sn-glycero-3-phosphocholine, identified in *Cylindrotheca closterium*, exhibited potent anti-inflammatory activity by inhibiting the release of tumor necrosis factor-α (TNF-α) (LAURITANO et al., 2020).

The metabolites produced by some microalgae have also shown antimicrobial activity. A study evaluating 675 extracts from different cyanobacteria groups found that alpha-linolenic acid and other polyunsaturated fatty acids were associated with the inhibition of microbial growth and biofilm formation (CEPAS et al., 2019). This pattern has also been identified in *Scenedesmus obliquus*, showing activity against *Pseudomonas aeruginosa*, *Escherichia coli*, and *Staphylococcus aureus* in extracts rich in polyunsaturated fatty acids (CATARINA GUEDES et al., 2011). Shaima et al. (2022) identified some compounds associated with fatty acids and phytols in extracts from *Chlorella* sp. and *Scenedesmus* sp. that had antimicrobial potential.

1.2. Metabolomics: A Strategy for Discovering New Compounds

With the advancement of analytical techniques, new approaches have emerged to enhance information processing. These have made possible to evaluate massive quantities of cellular products, including genes, proteins, and metabolites, which became known as "the omics sciences" (ROESSNER; BOWNE, 2009). Among them, the science that focuses on evaluating metabolites

present in a cell type, tissue, or biological fluid is known as metabolomics, which can be classified as either targeted or untargeted (ALONSO; MARSAL; JULIÃ, 2015).

For the study of the metabolome, equipment such as nuclear magnetic resonance (NMR) or mass spectrometry (MS), usually coupled with liquid or gas chromatography, can be used (ROESSNER; BOWNE, 2009). Regardless of the equipment, a common feature in this context is the generation of a massive amount of data that usually needs multivariate analyses, such as Principal Component Analysis (PCA) or Partial Least Squares Discriminant Analysis (PLS-DA) for processing and prioritizing the obtained metabolites (PLS-DA) (WORLEY; POWERS, 2012). Considering mass spectrometry analysis, in 2012 a form of data visualization known as molecular networking was introduced. This method initially used in proteomics studies (GUTHALS et al., 2012), was later introduced in the analysis of metabolites from living microbial colonies (WATROUS et al., 2012), helping the advancement of the technique.

The development of molecular networks revolutionized the way information is conveyed, and mass spectrometry data are evaluated. A molecular network is constructed by pairwise comparison and alignment of mass spectra, seeking to identify precursor spectra with similar mass-to-charge (*m/z*) values and fragmentation patterns, thus obtaining a consensus spectrum. It also evaluates spectra that exhibit similarities to each other. To this similarity is assigned a cosine score ranging from 0 to 1, with 1 representing identical ion. In this way, observed metabolites that are similar are grouped into a molecular network, where the nodes usually represent a possible metabolite, and the edges represent connections between metabolites that show a degree of similarity (ARON et al., 2020; QUINN et al., 2017). To illustrate this process, Figure 1 shows the construction of a molecular network.

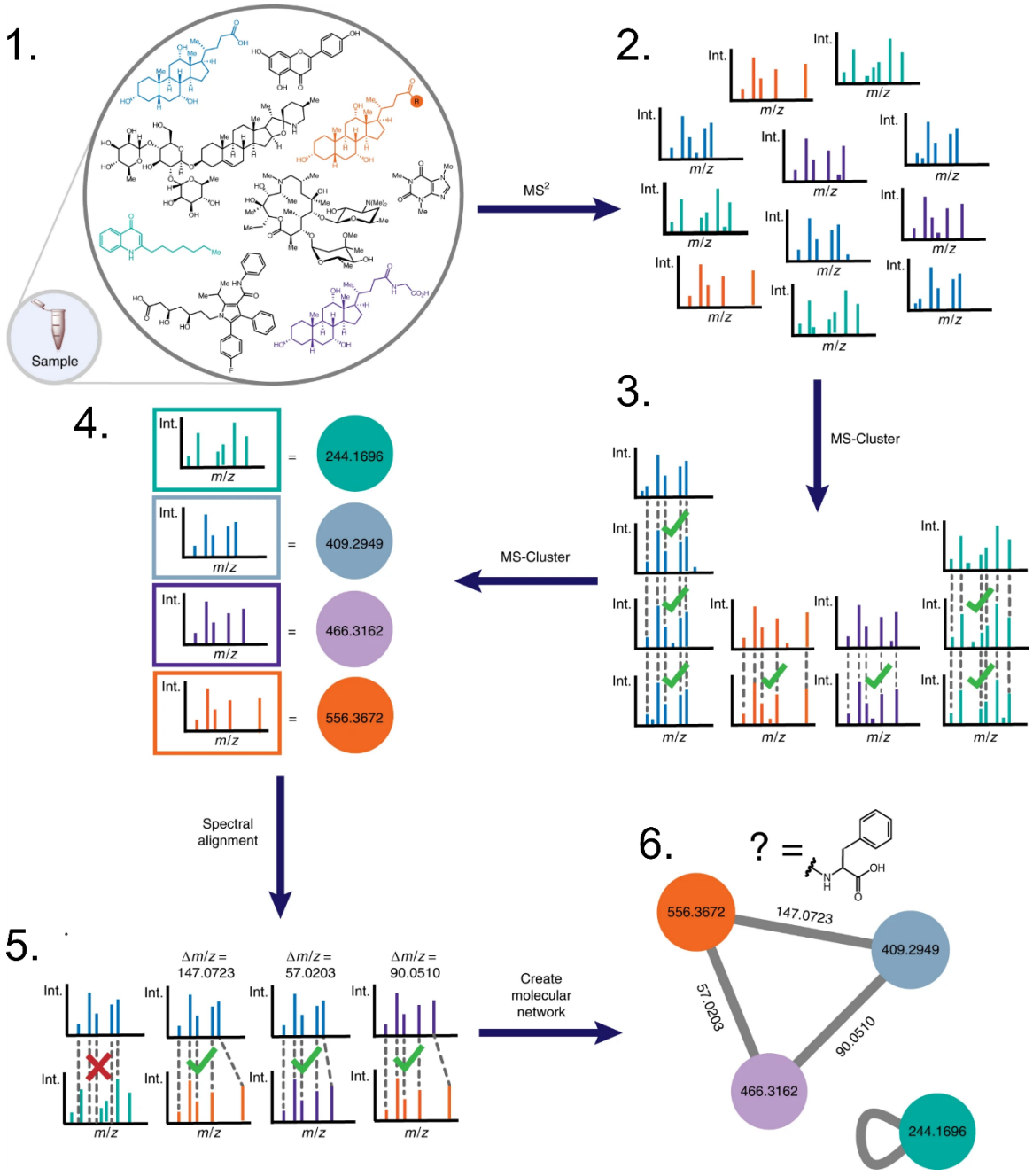

Figure 1. The colors in the diagram represent the transition from molecules in a sample (1) to nodes in a molecular network (6). The process begins with the acquisition of MS^2 spectra for all ionized molecules (2). MS-Cluster aligns each MS^2 spectrum with others in the dataset, merging mass spectra from identical compounds into a single node or consensus cluster due to the high similarity of their precursor and fragment ions (3). Spectral alignment allows for similarity searches even when precursor ion masses differ (4), using a modified cosine score that accounts for ions differing by the mass difference of the precursor ions (5). Structurally related molecules, are represented by separate nodes interconnected by edges (6). Source: Aron et al. (2020), adapted.

Considering such strategy, the Global Natural Products Social Molecular Networking (GNPS, http://gnps.ucsd.edu) was launched in 2014 (WANG et al., 2016). This platform aims to share, analyze, store, and compare MS and MS^2 data, allowing the annotation of compounds, the generation of molecular networks, and other associated tools (ARON et al., 2020; QIN et al., 2022). Rapidly, other tools were developed to complement molecular network analyses, such as feature-based molecular networking(NOTHIAS et al., 2020).Bioactive-based molecular networking (NOTHIAS et al., 2018), and ion identity molecular networking (SCHMID et al., 2021). These approaches have accelerated the discovery and annotation of bioactive compounds in the research of natural, with numerous successful studies.

1.3. Application of zebrafish in drug discovery

With advancements in drug discovery and development, modern approaches as high throughput screening (HTS) (GIACOMOTTO; SÉGALAT, 2010), has been widely used (GIACOMOTTO; SÉGALAT, 2010); JANZEN, 2014). The process of discovering and developing new drugs is laborious and time-consuming, and the use of model organisms is an efficient way to accelerate it in a complex system. It serves as an adequate model for studying absorption, distribution, metabolism, and excretion in the organism. Mammalian models are expensive, require large infrastructure and significant time for maintenance (ZON; PETERSON, 2005), making them less suitable for high-throughput drug screenings. This has led to the exploration of alternatives such as enzyme assays or two- and three-dimensional cell cultures (ZHANG et al., 2012). However, these do not fully reflect biological complexity, making phenotype-based screening more appealing as it captures the phenotypic complexity of organisms, providing more accurate responses in real organism (MACRAE; PETERSON, 2015). Thus, organisms easier to maintain and with shorter life cycles, such as the zebrafish, even though physiologically simpler, have been suggested.

The use of zebrafish (*Danio rerio*) as a model for physiological studies presents several advantages over the use of other organisms. The advantages include rapid embryogenesis, which is completed in 72 hours, with organs fully developed by 96 hours. The embryos can be completely transparent and are easy to manipulate. Additionally, due to their small size, embryos can be housed in 96- to 384-well plates (DELVECCHIO; TIEFENBACH; KRAUSE, 2011). Another

significant advantage is their genetic similarity to humans, with 70% of their genome being similar to that of humans and more than 80% of proteins associated with diseases being conserved (HOWE et al., 2013). Figure 2 shows embryos in the two development periods used in this work.

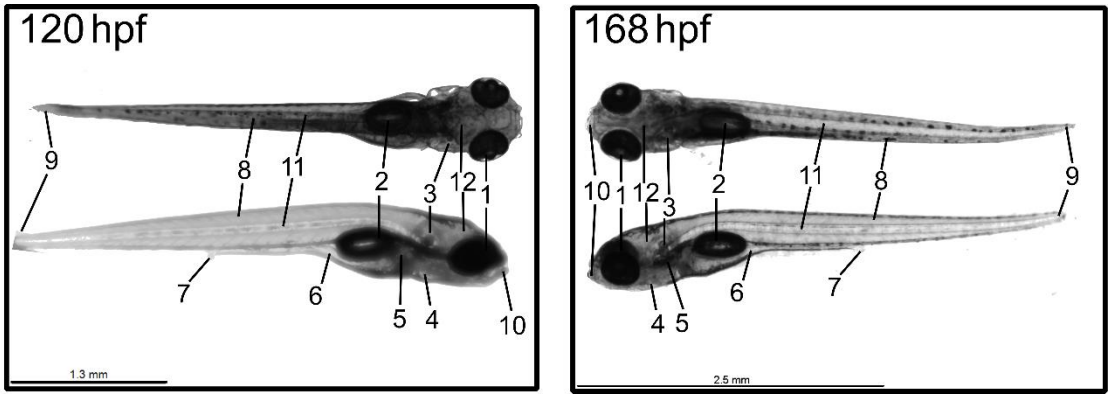

Figure 2. Anatomy of zebrafish embryos at two developmental stages: 120 hours post-fertilization (hpf) and 168 hpf. The highlighted parts represent: 1. Eyes, 2. Swim bladder, 3. Otolith, 4. Heart, 5. Liver, 6. Intestine, 7. Urogenital opening, 8. Dorsal fin, 9. Caudal fin, 10. Mouth, 11. Spinal cord, 12. Cerebellum.

These characteristics enable zebrafish to be used in various applications, including genetic, behavioral, embryonic development, toxicological, and pharmacological studies (PATTON; ZON; LANGENAU, 2021). In many cases, zebrafish serve as a more similar model than rats, as demonstrated in the case of thalidomide. In zebrafish models, thalidomide has effects similar to those observed in humans, unlike the observed in rats, where the compound does not produce the same adverse effects (PATTON; ZON; LANGENAU, 2021). Zebrafish is also used to understand non-communicable diseases (NCDs), known as chronic diseases, including conditions such as obesity, cancer, diabetes, cardiovascular, and respiratory diseases (WORLD HEALTH ORGANISATION, 2023). Currently, these diseases are the leading cause of death globally, with the risk being particularly high in low- and middle-income populations (BENNETT et al., 2018). While a healthy lifestyle and balanced diet are effective in their treatment, pharmacological therapy is often necessary (CASTRO et al., 2016).

The zebrafish model has already been identified as suitable for the study of obesity and chronic diseases (GIACOMOTTO; SÉGALAT, 2010). Jones et al. (2008) demonstrated that it is

possible to evaluate the effect of molecules on zebrafish metabolism using Nile Red as a stain for neutral lipids. Subsequent studies have confirmed this methodology and adapted, optimized, and applied it to the study of both purified compounds and crude extracts or fractions (FREITAS et al., 2019; MARTELLI et al., 2024; NOINART et al., 2017; REGUEIRAS et al., 2021; RIBEIRO et al., 2023; URBATZKA et al., 2018). Regarding appetite, Otis & Farber (2016) established a protocol to access feeding and monitor intake using egg yolk liposomes containing fluorescent dye. This allowed the quantification of appetite levels in zebrafish embryos from the seventh day after fertilization. Other protocols have also been developed for studies on molecules with anticancer (TERRIENTE; PUJADES, 2013), toxicity and diabetes activities (SCHOLZ et al., 2008).

2. Hypothesis

Thus, this work was based on two main hypotheses:

- Different groups of microalgae have distinct biochemical compositions, which can result in different applications, offering alternatives to microalgae traditionally used in the food and biofuel industries.

- Eukaryotic microalgae can produce unique metabolites with potential biological effects, such as antimicrobial, antitumor, antiobesity, and appetite suppressant compounds, without showing toxicity in cell models.

3. Objectives

This study aimed at evaluating and exploring freshwater eukaryotic microalgae for biotechnological purposes. This was performed by assessing their chemical composition considering lipids, proteins, carbohydrates, and secondary metabolites, as well as their potential applications in the nutraceutical, bioenergy, and pharmaceutical sectors.

4. References

ABIUSI, F. et al. Mixotrophic cultivation of Galdieria sulphuraria for C-phycocyanin and protein production. **Algal Research**, v. 61, p. 102603, jan. 2022.

ABREU, A. P.; MARTINS, R.; NUNES, J. Emerging Applications of Chlorella sp. and Spirulina (Arthrospira) sp. **Bioengineering**, v. 10, n. 8, p. 955, 11 ago. 2023.

ALONSO, A.; MARSAL, S.; JULIÃ, A. Analytical Methods in Untargeted Metabolomics: State of the Art in 2015. **Frontiers in Bioengineering and Biotechnology**, v. 3, 5 mar. 2015.

ARON, A. T. et al. Reproducible molecular networking of untargeted mass spectrometry data using GNPS. **Nature Protocols**, v. 15, n. 6, p. 1954–1991, 13 jun. 2020.

BARBOSA, M. J. et al. Hypes, hopes, and the way forward for microalgal biotechnology. **Trends in Biotechnology**, v. 41, n. 3, p. 452–471, mar. 2023.

BECKER, E. W. Micro-algae as a source of protein. **Biotechnology Advances**, v. 25, n. 2, p. 207–210, mar. 2007.

BENNETT, J. E. et al. NCD Countdown 2030: worldwide trends in non-communicable disease mortality and progress towards Sustainable Development Goal target 3.4. **The Lancet**, v. 392, n. 10152, p. 1072–1088, set. 2018.

BHATTACHARYA, M.; GOSWAMI, S. Microalgae – A green multi-product biorefinery for future industrial prospects. **Biocatalysis and Agricultural Biotechnology**, v. 25, p. 101580, maio 2020.

BORA, A. et al. Microalgae to bioenergy production: Recent advances, influencing parameters, utilization of wastewater – A critical review. **Science of The Total Environment**, v. 946, p. 174230, out. 2024.

BOROWITZKA, M. A. Chapter 3 - Biology of Microalgae. In: LEVINE, I. A.; FLEURENCE, J. (Eds.). Microalgae in Health and Disease Prevention. **Academic Press**, 2018. p. 23–72.

CARDOZO, K. H. M. et al. Metabolites from algae with economical impact. **Comparative Biochemistry and Physiology Part C: Toxicology & Pharmacology**, v. 146, n. 1–2, p. 60–78, 2007.

CASTRO, M. et al. Obesity: The Metabolic Disease, Advances on Drug Discovery and Natural Product Research. **Current Topics in Medicinal Chemistry**, v. 16, n. 23, p. 2577–2604, 2016.

CATARINA GUEDES, A. et al. Microalgal and cyanobacterial cell extracts for use as natural antibacterial additives against food pathogens. **International Journal of Food Science and Technology**, v. 46, n. 4, p. 862–870, 2011.

CEPAS, V. et al. Inhibition of Bacterial and Fungal Biofilm Formation by 675 Extracts from Microalgae and Cyanobacteria. **Antibiotics**, v. 8, n. 2, p. 77, 12 jun. 2019.

CHEN, J. et al. The potential of microalgae in biodiesel production. **Renewable and Sustainable Energy Reviews**, v. 90, p. 336–346, jul. 2018.

CHEN, Y.; WANG, C.; XU, C. Nutritional evaluation of two marine microalgae as feedstock for aquafeed. **Aquaculture Research**, v. 51, n. 3, p. 946–956, 19 mar. 2020.

DELVECCHIO, C.; TIEFENBACH, J.; KRAUSE, H. M. The Zebrafish: A Powerful Platform for In Vivo , HTS Drug Discovery. **ASSAY and Drug Development Technologies**, v. 9, n. 4, p. 354–361, ago. 2011.

DUMAY, J.; MORANÇAIS, M. Proteins and Pigments. **Seaweed in Health and Disease Prevention**. Elsevier, 2016. p. 275–318.

FERNÁNDEZ, F. G. A. et al. The role of microalgae in the bioeconomy. **New Biotechnology**, v. 61, p. 99–107, mar. 2021.

FREITAS, S. et al. Chlorophyll Derivatives from Marine Cyanobacteria with Lipid-Reducing Activities. **Marine Drugs**, v. 17, n. 4, p. 229, 17 abr. 2019.

GARDEVA, E. et al. Cancer Protective Action of Polysaccharide, Derived from Red Microalga Porphyridium Cruentum — A Biological Background. **Biotechnology & Biotechnological Equipment**, v. 23, n. sup1, p. 783–787, 15 jan. 2009.

GIACOMOTTO, J.; SÉGALAT, L. High-throughput screening and small animal models, where are we? **British Journal of Pharmacology**, v. 160, n. 2, p. 204–216, 26 maio 2010.

GUEDES, A. C.; AMARO, H. M.; MALCATA, F. X. Microalgae as sources of carotenoids. **Marine Drugs**, v. 9, n. 4, p. 625–644, 2011.

GUTHALS, A. et al. The spectral networks paradigm in high throughput mass spectrometry. **Molecular BioSystems**, v. 8, n. 10, p. 2535, 2012.

HASSAN, Q. P.; BHAT, A. M.; SHAH, A. M. **Bioprospecting actinobacteria for bioactive secondary metabolites from untapped ecoregions of the northwestern himalayas**. New and Future Developments in Microbial Biotechnology and Bioengineering: Microbial Secondary Metabolites Biochemistry and Applications. Elsevier B.V., 2019. p. 77–85.

HIELSCHER-MICHAEL, S. et al. Natural Products from Microalgae with Potential against Alzheimer's Disease: Sulfolipids Are Potent Glutaminyl Cyclase Inhibitors. **Marine Drugs**, v. 14, n. 11, p. 203, 2 nov. 2016.

HOWE, K. et al. The zebrafish reference genome sequence and its relationship to the human genome. **Nature**, v. 496, n. 7446, p. 498–503, 25 abr. 2013.

JANZEN, W. P. Screening Technologies for Small Molecule Discovery: The State of the Art. **Chemistry & Biology**, v. 21, n. 9, p. 1162–1170, set. 2014.

JONES, K. S. et al. A high throughput live transparent animal bioassay to identify non-toxic small molecules or genes that regulate vertebrate fat metabolism for obesity drug development. **Nutrition & Metabolism**, v. 5, n. 1, p. 23, 27 dez. 2008.

KAVITHA, K. et al. Astaxanthin inhibits NF-κB and Wnt/β-catenin signaling pathways via inactivation of Erk/MAPK and PI3K/Akt to induce intrinsic apoptosis in a hamster model of oral

cancer. **Biochimica et Biophysica Acta (BBA) - General Subjects**, v. 1830, n. 10, p. 4433–4444, out. 2013.

LAURITANO, C. et al. Lysophosphatidylcholines and Chlorophyll-Derived Molecules from the Diatom Cylindrotheca closterium with Anti-Inflammatory Activity. **Marine Drugs**, v. 18, n. 3, p. 166, 17 mar. 2020.

MACRAE, C. A.; PETERSON, R. T. Zebrafish as tools for drug discovery. **Nature Reviews Drug Discovery**, v. 14, n. 10, p. 721–731, 11 out. 2015.

MARTELLI, F. et al. Lactic acid fermented microalgae and cyanobacteria as a new source of lipid reducing compounds: assessment through zebrafish Nile red fat metabolism assay and untargeted metabolomics. **Food & Function**, v. 15, n. 10, p. 5554–5565, 2024.

MATOS, Â. P. et al. Chemical Characterization of Six Microalgae with Potential Utility for Food Application. **Journal of the American Oil Chemists' Society**, v. 93, n. 7, p. 963–972, 27 jul. 2016.

MONTENEGRO-HERRERA, C. A. et al. Single-cell protein production potential with the extremophilic red microalgae Galdieria sulphuraria: growth and biochemical characterization. **Journal of Applied Phycology**, v. 34, n. 3, p. 1341–1352, 22 jun. 2022a.

MONTENEGRO-HERRERA, C. A. et al. Single-cell protein production potential with the extremophilic red microalgae Galdieria sulphuraria: growth and biochemical characterization. **Journal of Applied Phycology**, v. 34, n. 3, p. 1341–1352, 22 jun. 2022b.

MORALES, M.; AFLALO, C.; BERNARD, O. Microalgal lipids: A review of lipids potential and quantification for 95 phytoplankton species. **Biomass and Bioenergy**, v. 150, p. 106108, jul. 2021.

NAGUIB, Y. M. A. Antioxidant Activities of Astaxanthin and Related Carotenoids. **Journal of Agricultural and Food Chemistry**, v. 48, n. 4, p. 1150–1154, 1 abr. 2000.

NOINART, J. et al. A New Ergosterol Analog, a New Bis-Anthraquinone and Anti-Obesity Activity of Anthraquinones from the Marine Sponge-Associated Fungus Talaromyces stipitatus KUFA 0207. **Marine Drugs**, v. 15, n. 5, p. 139, 16 maio 2017.

NORDIN, N. et al. Effect of photo-autotrophic cultural conditions on the biomass productivity and composition of Chlorella vulgaris. **Biofuels**, v. 13, n. 2, p. 149–159, 7 fev. 2022.

NOTHIAS, L.-F. et al. Bioactivity-Based Molecular Networking for the Discovery of Drug Leads in Natural Product Bioassay-Guided Fractionation. **Journal of Natural Products**, v. 81, n. 4, p. 758–767, 27 abr. 2018.

NOTHIAS, L.-F. et al. Feature-based molecular networking in the GNPS analysis environment. **Nature Methods**, v. 17, n. 9, p. 905–908, 24 set. 2020.

OLAIZOLA, M. Commercial development of microalgal biotechnology: From the test tube to the marketplace. **Biomolecular Engineering**, v. 20, n. 4–6, p. 459–466, 2003.

OTIS, J. P.; FARBER, S. A. High-fat Feeding Paradigm for Larval Zebrafish: Feeding, Live Imaging, and Quantification of Food Intake. **Journal of Visualized Experiments**, n. 116, 27 out. 2016.

PATTON, E. E.; ZON, L. I.; LANGENAU, D. M. Zebrafish disease models in drug discovery: from preclinical modelling to clinical trials. **Nature Reviews Drug Discovery,** v. 20, n. 8, p. 611–628, 11 ago. 2021.

PULZ, O.; SCHEIBENBOGEN, K. **Photobioreactors: Design and performance with respect to light energy input.** Bioprocess and Algae Reactor Technology, Apoptosis. Springer Berlin Heidelberg, 2006. p. 123–152.

QIN, G.-F. et al. MS/MS-Based Molecular Networking: An Efficient Approach for Natural Products Dereplication. **Molecules**, v. 28, n. 1, p. 157, 24 dez. 2022.

QUINN, R. A. et al. Molecular Networking As a Drug Discovery, Drug Metabolism, and Precision Medicine Strategy. **Trends in Pharmacological Sciences**, v. 38, n. 2, p. 143–154, fev. 2017.

REGUEIRAS, A. et al. Potential Anti-Obesity, Anti-Steatosis, and Anti-Inflammatory Properties of Extracts from the Microalgae Chlorella vulgaris and Chlorococcum amblystomatis under Different Growth Conditions. **Marine Drugs**, v. 20, n. 1, p. 9, 22 dez. 2021.

RIBEIRO, T. et al. Metabolite Profile Characterization of Cyanobacterial Strains with Bioactivity on Lipid Metabolism Using In Vivo and In Vitro Approaches. **Marine Drugs**, v. 21, n. 9, p. 498, 19 set. 2023.

RICOUR, F. et al. Century-scale carbon sequestration flux throughout the ocean by the biological pump. **Nature Geoscience**, v. 16, n. 12, p. 1105–1113, 27 dez. 2023.

ROESSNER, U.; BOWNE, J. What is metabolomics all about? **BioTechniques**, v. 46, n. 5, p. 363–365, 25 abr. 2009.

RUANE, J.; SONNINO, A.; AGOSTINI, A. Bioenergy and the potential contribution of agricultural biotechnologies in developing countries. **Biomass and Bioenergy**, v. 34, n. 10, p. 1427–1439, 2010.

SÁNCHEZ-SAAVEDRA, M. P.; CASTRO-OCHOA, F. Y. Bioprospecting for Lipid Production of Eleven Microalgae Strains for Sustainable Biofuel Production. **BioEnergy Research**, v. 17, n. 2, p. 1118–1132, 18 out. 2023.

SANTHAKUMARAN, P.; KOOKAL, S. K.; RAY, J. G. Biomass yield and biochemical profile of fourteen species of fast-growing green algae from eutrophic bloomed freshwaters of Kerala, South India. **Biomass and Bioenergy**, v. 119, p. 155–165, dez. 2018.

SATI, H. et al. Microalgal lipid extraction strategies for biodiesel production: A review. **Algal Research**, v. 38, p. 101413, mar. 2019.

SCHMID, R. et al. Ion identity molecular networking for mass spectrometry-based metabolomics in the GNPS environment. **Nature Communications**, v. 12, n. 1, p. 3832, 22 jun. 2021.

SCHOLZ, S. et al. The zebrafish embryo model in environmental risk assessment—applications beyond acute toxicity testing. **Environmental Science and Pollution Research**, v. 15, n. 5, p. 394–404, 25 jul. 2008.

SED, G.; CICCI, A.; BRAVI, M. Extraction and purification of exopolysaccharides from exhausted Arthrospira platensis (Spirulina) culture systems. **Chemical Engineering Transactions**, 2017.

SHAIMA, A. F. et al. Unveiling antimicrobial activity of microalgae Chlorella sorokiniana (UKM2), Chlorella sp. (UKM8) and Scenedesmus sp. (UKM9). **Saudi Journal of Biological Sciences**, v. 29, n. 2, p. 1043–1052, 2022.

SHEGOKAR, R.; MITRI, K. Carotenoid lutein: A promising candidate for pharmaceutical and nutraceutical applications. **Journal of Dietary Supplements**, v. 9, n. 3, p. 183–210, 2012.

SILVA, J. C. et al. Biomass, photosynthetic activity, and biomolecule composition in Chlorella fusca (Chlorophyta) cultured in a raceway pond operated under greenhouse conditions. **Journal of Biotechnology**, v. 367, p. 98–105, abr. 2023.

SRIMONGKOL, P. et al. Sulfated polysaccharides derived from marine microalgae, Synechococcus sp. VDW, inhibit the human colon cancer cell line Caco-2 by promoting cell apoptosis via the JNK and p38 MAPK signaling pathway. **Algal Research**, v. 69, p. 102919, jan. 2023.

TERRIENTE, J.; PUJADES, C. Use of Zebrafish Embryos for Small Molecule Screening Related to Cancer. **Developmental Dynamics**, v. 242, n. 2, p. 97–107, 22 fev. 2013.

URBATZKA, R. et al. Lipid reducing activity and toxicity profiles of a library of polyphenol derivatives. **European Journal of Medicinal Chemistry**, v. 151, p. 272–284, maio 2018.

VERSPREET, J. et al. Nutritional Profiling and Preliminary Bioactivity Screening of Five Micro-Algae Strains Cultivated in Northwest Europe. **Foods**, v. 10, n. 7, p. 1516, 1 jul. 2021.

WANG, B. et al. CO2 bio-mitigation using microalgae. **Applied Microbiology and Biotechnology**, v. 79, n. 5, p. 707–718, 1 jul. 2008.

WANG, M. et al. Sharing and community curation of mass spectrometry data with Global Natural Products Social Molecular Networking. **Nature Biotechnology**, v. 34, n. 8, p. 828–837, 9 ago. 2016.

WATROUS, J. et al. Mass spectral molecular networking of living microbial colonies. **Proceedings of the National Academy of Sciences**, v. 109, n. 26, 26 jun. 2012.

WILLIAMSON, E. et al. Microalgae: potential novel protein for sustainable human nutrition. **Trends in Plant Science**, v. 29, n. 3, p. 370–382, mar. 2024.

WILSON, J. D. et al. The biological carbon pump in CMIP6 models: 21st century trends and uncertainties. **Proceedings of the National Academy of Sciences**, v. 119, n. 29, 19 jul. 2022.

WORLD HEALTH ORGANIZATION. **Noncommunicable Diseases**. Disponível em: <https://www.who.int/news-room/fact-sheets/detail/noncommunicable-diseases>. Acess: 14.10.2024

WORLEY, B.; POWERS, R. Multivariate Analysis in Metabolomics. **Current Metabolomics**, v. 1, n. 1, p. 92–107, 1 nov. 2012.

YANG, L. et al. Anti-Inflammatory Effect of Acetone Extracts from Microalgae Chlorella sp. WZ13 on RAW264.7 Cells and TPA-induced Ear Edema in Mice. **Frontiers in Marine Science**, v. 9, 5 jul. 2022.

ZHANG, D. et al. Preclinical experimental models of drug metabolism and disposition in drug discovery and development. **Acta Pharmaceutica Sinica** B, v. 2, n. 6, p. 549–561, dez. 2012.

ZON, L. I.; PETERSON, R. T. In vivo drug discovery in the zebrafish. N**ature Reviews Drug Discovery**, v. 4, n. 1, p. 35–44, jan. 2005.

Chapter 1: Biochemical characterization of 12 freshwater microalgae reveals *Pediastrum* sp. as a promising species for nutrition and *Dimorphococcus* sp. for biofuels.

Abstract

Microalgae have gained prominence in food, feed, and biofuels due to their capacity to produce economically valuable biomolecules and mitigate CO_2. However, only a limited number of species are industrially produced nowadays. This study evaluated the biochemical composition of 12 eukaryotic microalgae kept under controlled laboratory conditions, focusing on proteins, carbohydrates, lipids, fatty acid composition, pigments, and antioxidant potential. The results showed that five microalgae had 60% PUFAs: *C. obovata*, *Pediastrum* sp., *S. leptocladium*, *S. pantanale*, and 80% for *W. botryoides*, with alpha-linolenic acid (C18:3n3) as the predominant one, followed by linoleic acid (C18:2n6). The highest antioxidant potential was detected in S. leptocladium (43% DPPH radical inhibition). Overall, we propose *Pediastrum* sp. as a promising nutritional source with high total proteins (52%), polyunsaturated fatty acids (>60%), significant antioxidant potential, and pigment production, and *Dimorphococcus* sp. as a potential organism for biodiesel production, with 28% lipids rich in saturated and monounsaturated fatty acids. This investigation highlights the biotechnological potential of understudied 12 microalgae species.

Keywords: Biomolecules; Nutraceutical; Biodiesel; Algae Physiology.

1. Introduction

Microalgae are organisms with photosynthetic capacity that present a positive impact on reducing greenhouse gas from the atmosphere, particularly carbon dioxide (CO_2) (BEARDALL; RAVEN, 2016; WANG et al., 2008). They have attributes such as high growth rates and biomolecule production such as proteins, carbohydrates, lipids and high value-added compounds, some of them produced exclusively by microalgae (BOROWITZKA, 2013; YAP et al., 2021). Altogether such properties lead to industrial interest in microalgae as their application in human and animal food, pharmaceuticals, agriculture and energy are possible from the biomass (FERNÁNDEZ et al., 2021). Compared to plant sources, microalgae have a higher production capacity per hectare, with up to 10 times more proteins, carbohydrates and lipids than soy (BARBOSA et al., 2023). Many species are known as good protein producers, where *Chlorella vulgaris* and *Liminospira platensis* are the most used. They can accumulate up to 50 - 70% of their biomass as proteins (JANSSEN; WIJFFELS; BARBOSA, 2022). Others have the advantage of lipid accumulation, up to 50% of its dry biomass, and under stress conditions, some strains can increase it to about 70% (GRIFFITHS; HARRISON, 2009; MORALES; AFLALO; BERNARD, 2021).

Fatty acid profiles produced by microalgae vary among different groups, and for most of them, palmitic and oleic acid production are the most common (LI-BEISSON et al., 2019). Monounsaturated and saturated fatty acids are proposed for biodiesel production (BREUER et al., 2012). Some microalgae fatty acids are valuable because they are important nutritional sources of the omega 3 and 6 groups, alpha-linolenic, linoleic, eicosapentaenoic acids (EPA), and docosahexaenoic acid (DHA). They are especially valuable as they are synthesized in small quantities in humans and their constant consumption is important to maintain healthy conditions (CASTRO; TOCHER; MONROIG, 2016; TOCHER, 2015). Another class of valuable molecules

for human consumption produced by microalgae are carotenoids, precursors of vitamins and a natural antioxidant (GOSWAMI; AGRAWAL; VERMA, 2021). For example, *Dunaliella salina* and *Haematococcus pluvialis* produce considerable amounts of carotenoids under specific growth conditions. *H. pluvialis* is a great producer of astaxanthin. In order to meet global demand, more than 300 tons of biomass per year are produced (LAFARGA; CLEMENTE; GARCIA-VAQUERO, 2020).

As a consequence of the necessity of new natural products for human and animal life microalgae production has increased recently, reaching more than 10,000 tons of dry biomass per year (RICHMOND; HU, 2013). Despite this growth, commercial activity is still concentrated in just 5 genera: *Liminospira, Chlorella, Dunaliella, Aphanizomenon* and *Haematococcus* (DUMAY; MORANÇAIS, 2016), although a large number of known microalgae species has been estimated to be around 50,000 (RICHMOND; HU, 2013). Several reasons justify this restriction on the number of algae in the market, such as legislation, lack of knowledge of the biochemical composition and optimum growth conditions for a variety of strains, as well as the economic viability for large-scale production. Currently, only 8 species in the USA, 13 in the European Union and 7 in China are authorized for consumption (FU et al., 2021). Therefore, prospecting microalgae for their growth and biochemical composition can be a promising way to offer industries new opportunities related to strains with commercial relevance. In the present research, 12 microalgae species were prospected revealing their potential as sources of total proteins, carbohydrates and lipids, fatty acid composition, and antioxidant activity under laboratory-controlled growth condition.

2. Material and Methods

2.1. Cultures

The strains used were obtained from the freshwater microalgae culture collection at the Federal University of São Carlos (CCMA-UFSCar) and the Freshwater Microalgae Culture Collection of the Institute of Biological Sciences at the Federal University of Rio Grande (FURG). In the culture collections, the algae are kept in WC medium (GUILLARD, 1975). However, for the experiments, they were adapted to the BG11 medium (STANIER et al., 1979) because it is a nutrient richer medium that supports higher biomass. Those that did not adapt to BG11 were maintained in WC. Before the experiments, the saturating light intensity (E_k) for each strain investigated was determined through rapid light curves using a PhytoPAM (Heinz-Walz Effeltrich, Germany) instrument. Through preliminary cultivation under the same conditions as those used for this experiment, the growth curve was performed and the end of the exponential growth for each microalga was determined.

For the microalgae growth, 1 L Houx-type flasks (267 mm x 122 mm x 56 mm), containing the appropriate medium for each species. It was autoclaved at 121 ºC for 20 min, and the unialgal cultures in exponential growth phase were inoculated at a final concentration of 5.10^{-4} cels/mL The cultures (batch mode) were maintained under the respective E_k, with constant aeration with filtered (0.22 µm) atmospheric air and a 12h/12h light/dark photoperiod. The algae were grown to the point of maximum biomass accumulation and end of the exponential growth phase. Cultures were monitored for bacterial contamination sice they were unialgal, not axenic. For this daily samples were obtained and inspected under an optical microscope. For microalgae growth monitoring, *in vivo* chlorophyll a fluorescence and absorption at 684 nm were performed. A Turner fluorometer (Turner, USA) was used for the *in vivo* chlorophyll a fluorescence and a

spectrophotometer (NANOCOLOR® UV/VIS - MACHEREY-NAGEL, Germany) for absorbance. The specific (maximum) growth rate (μ) was calculated based on a linear regression fit of the fluorescence data, by plotting the natural logarithm of *in vivo* fluorescence (Y axis) against cultivation time (X axis). The slope of the obtained line represents the specific, or maximum, growth rate in the exponential growth phase. Three experimental replicates were performed for every species.

2.2. Rapid Light Curves

Different species os photosynthetic microalgae may have different light requirements. Thus, it was necessary to define the best light intensity for each organism being studied and, for this rapid light curves (RLC) were performed. A pulse amplitude modulated fluorometer (Phyto-PAM, Walz – Germany) was used using the standard conditions therein. After 20 minutes of dark adaptation, the microalgae were exposed to increasing pulses of photosynthetically active radiation (PAR) ranging from 0 to 2000 μmol photons $m^{-2}s^{-1}$ at 20 second intervals. The relative electron transport rate (rETR) was calculated by multiplying the PAR by the effective quantum yield at each intensity. The curve was fitted using the mathematical model proposed by Platt et al. (1981), yielding the maximum relative electron transport rate (rETRmax, μmol electrons m^{-2} s^{-1}) and α, the initial part of the curve where just light is limiting photosynthesis (μmol electrons m^{-2} s^{-1} [μmol photons m^{-2} s^{-1}]$^{-1}$). The saturating irradiance (E_k) was calculated as rETRmax / α.

2.3. Dry biomass and Biomolecules

Dry biomass was determined by filtering 5 mL of culture through a 0.22 μm cellulose acetate filter (Whatman, England) of known mass, then the filters were dried in an oven (40 ºC) until constant mass and weighed in a microanalytical balance with 10^{-6} g precision (XPE26 - METTLER TOLEDO, Switzerland).

Biomolecules were determined in exponentially growing cells because in the stationary phase of batch cultures, uncontrolled environmental factors may act on cell physiology, affecting its biochemical composition. As this study investigates different microalgae strains, examining them during the exponential growth phase can ensure a consistent comparison among all organisms, as the reasons for a batch culture entering the stationary phase may vary from species to species. Total protein content was determined based on quantification with the Folin reagent, adapted for microplates (SLOCOMBE et al., 2013). Absorbance was determined in a microplate spectrophotometer (Epoch - Biotech, USA). The method used is described in Slocombe et al. (2013) and the cells were digested according to Price (1965). Total carbohydrates concentration was determined according to Albalasmeh et al. (2013), which is based on the digestion of the cells by sulfuric acid. The total lipid content was determined by gravimetry according to Parrish (1999), a modification of the Folch et al. (1957). The results obtained are expressed as the percentage of biomolecules in relation to dry biomass weight (% DW).

Photosynthetic pigments were determined on the last experimental day, as were the other biomolecules. To do this, 3 mL of biomass was filtered through a 0.22 µm cellulose acetate filter (Whatman, England) and dissolved in dimethyl sulfoxide (P.A., Synth, Brazil) for pigment extraction. After 10 minutes, the absorbance was registered in a spectrophotometer (NANOCOLOR® UV/VIS - MACHEREY-NAGEL, Germany). For the Chlorophyta and Charophyta the concentrations of the pigments (chlorophyll a, b and carotenoids) were calculated as described in SHOAF; LIUM (1976) and WELLBURN (1994), while for the Xanthophyceae (chorophyll a and c1, c2) as in Ritchie et al. (2021) and for the Cryptophyta (chorophyll a and c2) as in Ritchie et al. (2022). The results are presented in $\mu g.mL^{-1}$.

2.4. Fatty acids profile

To determine the fatty acids profile, the direct transesterification methodology proposed by SOARES et al. (2014) was used. The preparation of fatty acid methyl esters (FAMEs) was performed using lyophilized biomass (Solab© SL - 404). The methyl esters were collected in vials and dried under a nitrogen stream. For analysis, they were solubilized in heptane 99% (Exodo Científica, Brazil). An Agilent 7890 gas chromatograph coupled to an Agilent 5975 mass spectrometer (Agilent Technologies, Inc. USA) with an Agilent HP-5MS column (5% Phenyl Methyl Silox 30 m x 250 μm x 0.25 μm) was used to analyze the FAMEs. They were conducted with 70 eV electron impact energy as the electron energy, ion source temperature at 230 °C, and transfer line temperature at 280 °C. Injections were made using a micro syringe (Agilent - AG5181-1267), the injection volume was 1 μL in a splitless mode with an injector temperature of 120 °C. Helium 5.0 (>99.999%) was used as the carrier gas at a pressure of 15,926 psi in a total flow of 1.924 $mL.min^{-1}$. The initial temperature was 70 °C for the first 10 minutes and heated at a constant rate of 5 $°C.min^{-1}$ until 250 °C, remaining constant thereafter up to the end of the run. The identification of FAMEs was based on the FAME MIX C8-C24 standard (Supelco Product number 18918) and with the help of the NIST11.L library (National Institute of Standards and Technology), AMDIS 32 Analysis software (Automated Mass Spectral Deconvolution & Identification System) associated with the mass spectra files present in the AOCS "Lipid library" of the Scottish Crop Science Research Institute (http://www.lipidlibrary.com.uk/índex.html). Fatty acid normalization was based on the integrated peak area.

2.5. Antioxidant activity and total polyphenols

For antioxidant activity, methanolic extracts using HPLC grade methanol (J.T. Baker, UK) were prepared from the lyophilized microalgae biomass in a ratio of 50 mg of biomass per mL of methanol. After adding the solvent, the solution was shaken in a vortex shaker (Gehaka© AV-2)

for 1 minute with glass beads (3 mm in diameter) to facilitate cell rupture. After the extraction step, the samples were centrifuged in a refrigerated centrifuge at 2486 g and 10 ºC (Thermo Scientific© Sorvall ST16-R) for 15 minutes. The extraction was repeated three times, and the supernatant was collected and used to analyze antioxidant activity and total polyphenols. The DPPH (2,2-diphenyl-1-picrylhydrazyl) radical reduction activity determination was performed according to the methodology described in BRAND-WILLIAMS; CUVELIER; BERSET (1995), adapted for microplates. The calculation was made according to equation 1.

$$DPPH\ Scavenging\ activity\ (\%) = \frac{(Abs_{control} - Abs_{sample})}{Abs_{control}} .\ 100 \qquad \text{(Eq. 1)}$$

Total polyphenols assay was performed using the Folin-Ciocalteu according to Zhang et al. (2006) method adapted to the microplate. The analysis was carried out with extracts in 1:10 ratio using 60 µL of sample, followed by 60 µL of 1:1 Folin-Ciocalteu reagent (Sigma-Aldrich, 2N, Switzerland) and 80 µL of 7.5% sodium carbonate solution. The solution was incubated at room temperature for 2 hours and then absorbance was determined at 750 nm in a spectrophotometer (NANOCOLOR® UV/VIS - MACHEREY-NAGEL, Germany). For the blanks, only microalgae extracts in 1:10 ratio were used with the same final volume as the quantified samples. The values were calculated according to a calibration curve made with gallic acid and expressed in gallic acid equivalents per gram of biomass ($mgEq.g^{-1}$).

2.6. Statistical analysis

Statistical analysis was performed using one-way analysis of variance (ANOVA) and compared using Tukey's test with a significance level of 95%. The Shapiro-Wilk tests for normality and Levene's test for homogeneity of variances were performed. RStudio version 2023.03.0, with R 4.2.2 and the stats and agricolae packages were used for statistics, ggplot2 for graphics, Factoshiny and missMDA for the principal component analysis.

3. Results

3.1. Growth rates and biomass

The exponential phase of the microalgae ranged from 4 to 6 days depending on the species. Table 1 shows specific growth rates, biomass, and the light intensity used to grow the cultures, which corresponds to the saturating irradiance (E_k) obtained for each species.

Table 1. Microalgae species, E_k (µmol photons.m^{-2}.s^{-1}), and maximum growth rate (d^{-1}) based on *in vivo* chlorophyll a fluorescence, and final biomass (mg.L^{-1}) in the cultures, culture time (days) for harvesting and culture media. Values represent the mean (n=3) and the standard deviation of the mean (in parentheses). For growth rate and biomass, the same letters identify groups with no statistically significant difference ($p<0.05$). All algae belong to the Class Chlorophyceae, except *Cryptomonas obovata* that is a Cryptophyceae and *Ophyocytium* sp., a Xanthophyceae.

Microalgae	Ek	Maximum Growth Rate	Final Biomass	Culture Time	Culture Media
CCMA323-*Chlorella emersonii*	312.00 (3.13)	0.91 (0.00)^{a}	128.5(6.50)^{bc}	4	BG-11
CCMA148-*Cryptomonas obovata*	182.00 (2.50)	0.39 (0.15)^{de}	73.3(15.0)^{d}	5	WC
CCMA262-*Desmodesmus brasiliensis*	208.05 (8.61)	0.65(0.04)^{b}	157.6(36.6)^{ab}	5	BG-11
CCMA571-*Dimorphococcus* sp.	197.79 (13.32)	0.44(0.02)^{de}	127.2(2.20)^{bc}	6	WC
CCMA553-*Ophiocytium* sp.	254.18 (1.27)	0.34(0.00)^{ef}	129.5(2.10)^{bc}	6	WC
CH007-*Pediastrum* sp.	246.26 (6.61)	1.06(0.02)^{a}	153.3(19.8)^{ab}	4	BG-11
CCMA498-*Raphidocelis sp.*	180.00 (11.30)	0.63(0.03)^{bc}	129.8(7.10)^{bc}	5	BG-11
CCMA655-*Radiococcus* sp.	243.29 (11.37)	0.53(0.02)^{bcd}	159.6(22.3)^{ab}	5	WC
CCMA200-*Staurastrum leptocladium*	192.96 (30.85)	0.20(0.02)^{f}	190.7(8.50)^{a}	5	WC
CCMA382-*Staurastrum pantanale*	213.42 (10.22)	0.39(0.07)^{de}	68.5(3.30)^{d}	5	WC
CCMA307-*Tetranephris brasiliensis*	154.65 (4.04)	0.68(0.06)^{b}	85.9(8.20)^{cd}	5	BG-11
CCMA311-*Westella botryoides*	200.13 (10.20)	0.48(0.00)^{cde}	57.5(2.40)^{d}	5	BG-11

Growth rates ranged from 0.20 ± 0.5 d^{-1} to 1.06 ± 0.02 d^{-1}. Among the microalgae, *Pediastrum* sp. and *C. emersonii* presented statistically similar growth rates. It was observed that biomass production (Table 1) did not follow growth rate, e.g., the strain with the highest growth rate did not necessarily result in the highest amount of dry biomass. *S. leptocladium* presented the highest biomass concentration, despite exhibiting the lowest growth rate among the analyzed algae.

3.2. Biochemical composition

In this study, some species produced a high protein content, e.g., above 50%, as shown in Figure 1. *C. emersonii*, *Radiococcus* sp., *Dimorphococcus* sp., and *Pediastrum* sp. were the species that produced significant amounts of proteins, with over 50% of their dry biomass; the highest was 63% for *C. emersonii*. However, other microalgae also show promising potential for proteins, such as *Radiococcus* sp., with 58% as proteins, *Pediastrum* sp. 52%, while in the others, the total protein content ranged from 30 to 40%.

The carbohydrate content was the highest in *S. pantanale* (40%) as shown in Figure 1B, a value almost equivalent to that of its total proteins. Despite the slightly lower average, *S. leptocladium* presented statistically equivalent amounts of carbohydrates. *Radiococcus* sp. also stood out from the others, with a content of 24% carbohydrates. The other microalgae had contents ranging from 5% to 15% in their composition. Regarding the total lipid content (Figure 1C), *Dimorphococcus* sp. excelled with the highest value, at 28%, followed by *S. pantanale* (25%). *W. botryoides*, *T. brasiliensis*, and *S. leptocladium* that had approximately 20%. The other species had contents lower than 15%, recalling here that such values were obtained in exponentially growing cells.

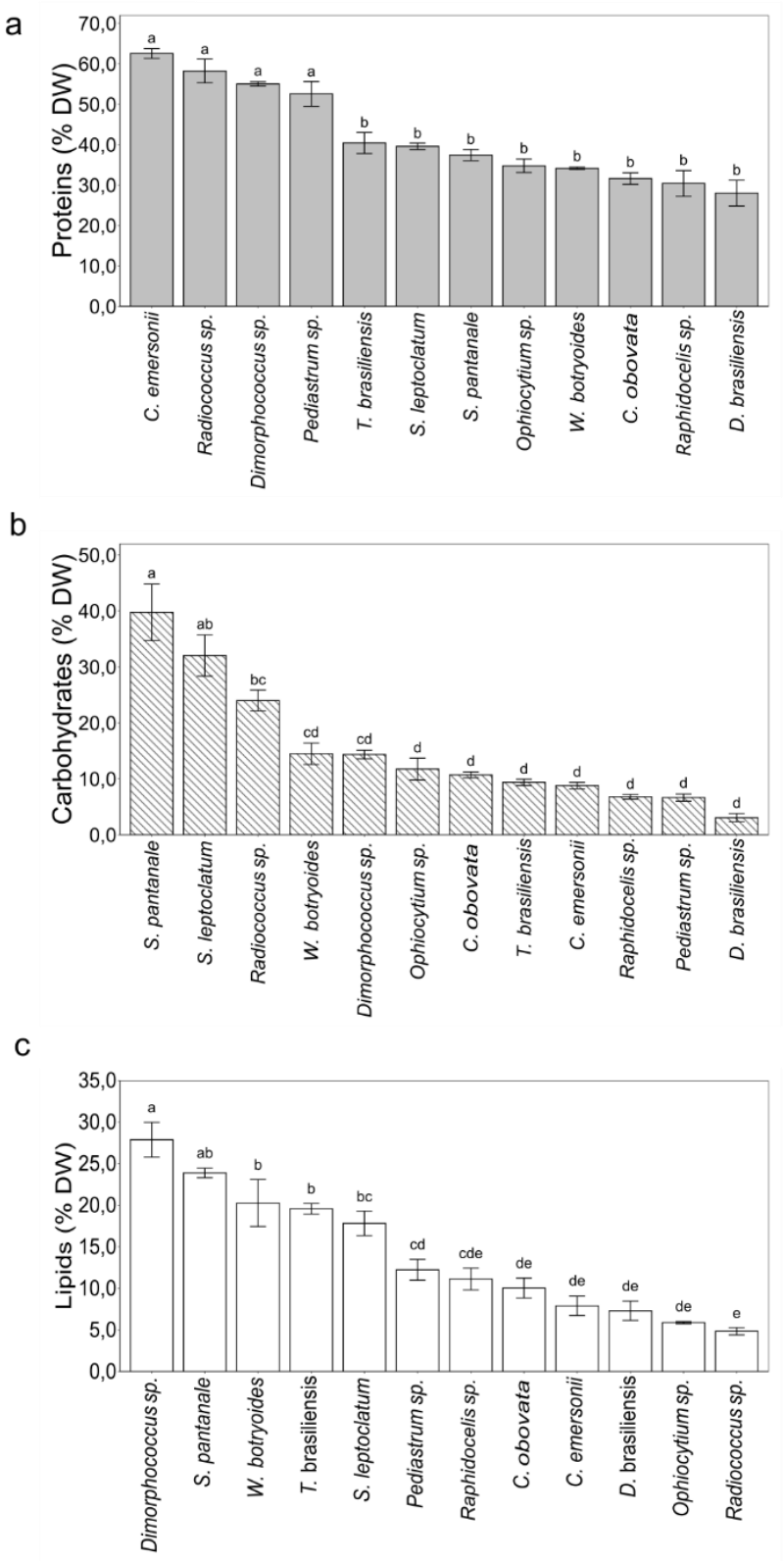

Figure 1. Composition of biomolecules of the 12 microalgae in percentage of dry biomass (DW). A: total proteins, B: total carbohydrates, C: total lipids. Same letters represent no statistical difference (ANOVA, $p < 0.05$). Error bars represent the standard deviation of the mean ($n = 3$).

3.3. Fatty acid profile

Table 2 shows the percentage values of each fatty acid in relation to the total, while Figure 2 shows the sum of saturated fatty acids (SFA), monounsaturated fatty acids (MUFA), and polyunsaturated fatty acids (PUFA). The values of ω3 and ω6 and the ω6:3 ratio are also presented.

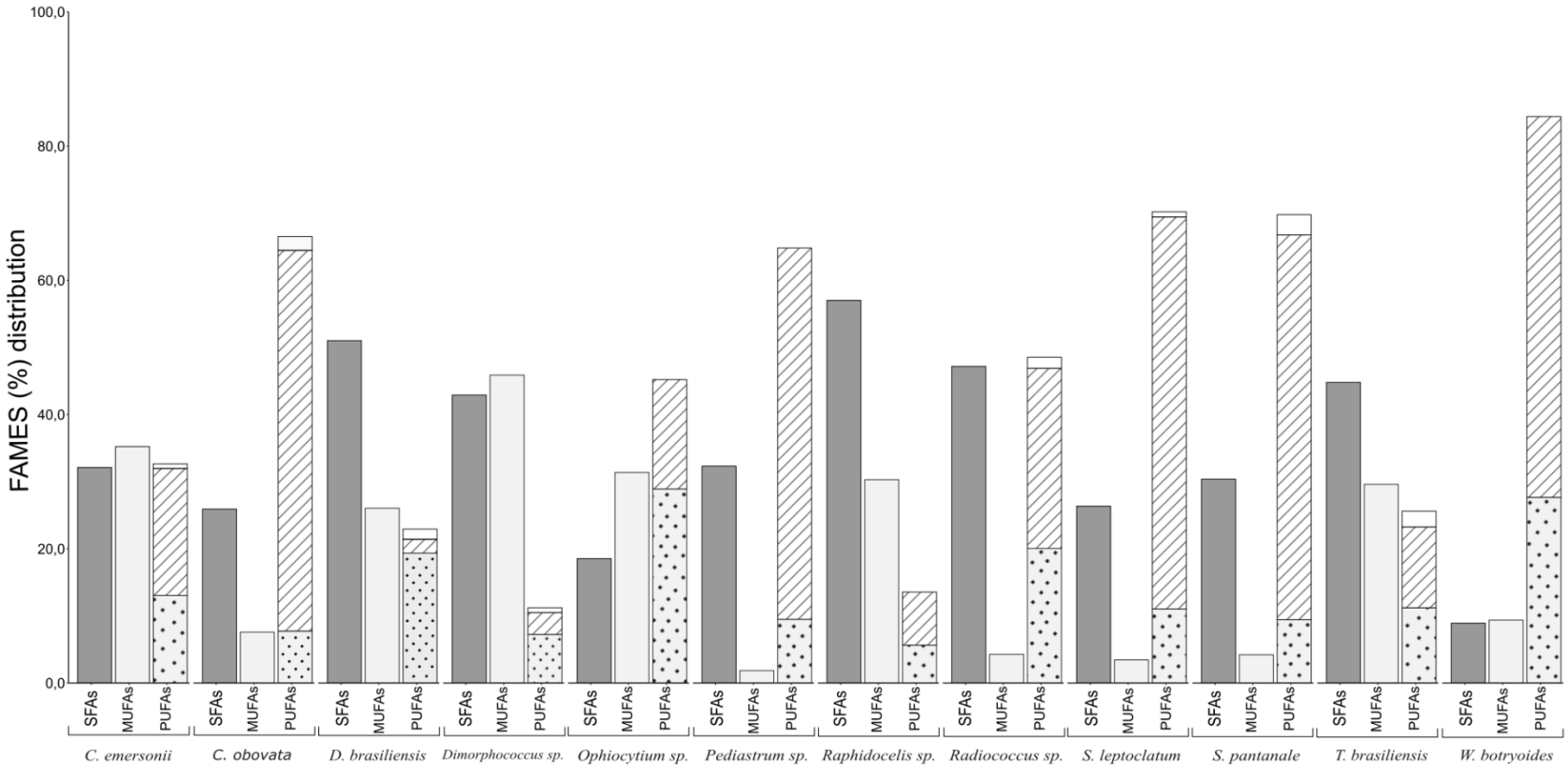

Figure 2. Distribution of fatty acid classes, SFAs (dark gray), MUFAs (light gray), and PUFAs, in which the presence of ω6 is represented as dots, ω3 as stripes, and other PUFAs as plain white. Values represent the means (n=3).

Table 2. Fatty acid profile in the 12 prospected freshwater microalgae. Values are presented as % of the total fatty acids and total content of omegas 3 (ω3) and 6 (ω6), and omega 6/3 ratio (ω6/3). Values represent the mean and standard deviations in parentheses (n = 3). The same letters represent means with no statistically significant differences (p-value < 0.05).

FAMES	*C. emersonii*	*C. obovata*	*D. brasiliensis*	*Dimorphococcus* sp.	*Ophiocytium* sp.	*Pediastrum* sp.	*Radiococcus* sp.	*Raphidoceli s sp.*	*S. leptocladium*	*S. pantanale*	*T. brasiliensis*	*W. botryoides*
C16:0	27.71 (14.59)^{cd}	22.01 (4.52)^{d}	47.87 (5.22)^{a}	40.86 (1.44)^{abc}	12.48 (0.35)^{a}	28.82 (3.75)^{bcd}	45.11 (2.02)^{ab}	48.73 (4.47)^{a}	24.88 (0.62)^{cd}	28.72 (3.15)^{cd}	39.15 (0.24)^{abc}	4.42 (7.66)^{e}
C16:1(n-7)	0.67 (0.19)^{c}	7.46 (4.33)^{b}	0.25 (0.44)^{c}	-	22.23 (3.69)^{a}	-	0.41 (0.36)^{c}	3.15 (0.05)^{bc}	3.44 (0.11)^{bc}	1.33 (0.73)^{c}	2.42 (0.15)^{bc}	5.73 (3.93)^{bc}
C16:1(n-9)	-	-	-	-	-	-	-	1.5 (0.05)^{a}	-	0.69 (0.64)^{b}	-	-
C16:2(n-4)	-	-	-	-	10.53 (1.89)^{a}	-	-	-	-	-	-	-
C16:2(n-6)	-	0.21 (0.22)^{bc}	-	0.48 (0.24)^{bc}	-	0.70 (0.17)^{bc}	0.39 (0.34)^{bc}	-	1.98 (0.17)^{a}	0.91 (0.71)^{b}	0.20 (0.06)^{bc}	-
C16:3(n-3)	-	1.15 (0.19)^{ef}	0.58 (0.36)^{ef}	-	-	3.31 (0.22)^{d}	4.88 (0.05)^{c}	1.25 (0.89)^{ef}	15.76 (0.2)^{a}	12.57 (1.38)^{b}	1.82 (0.04)^{e}	-
C16:4(n-3)	16.35 (7.60)^{a}	9.82 (2.55)^{ab}	1.01 (1.10)^{c}	-	-	8.68 (1.90)^{b}	4.37 (1.70)^{bc}	3.92 (1.37)^{bc}	-	-	10.06 (0.00)^{ab}	-
C18:0	3.20 (0.09)^{bcd}	2.54 (0.01)^{cde}	3.14 (0.28)^{bcd}	2.05 (0.20)^{cde}	6.06 (0.52)^{a}	2.09 (1.65)^{cde}	1.82 (0.23)^{de}	4.38 (0.71)^{ab}	1.21 (0.05)^{e}	1.66 (0.49)^{de}	3.66 (0.15)^{bc}	4.50 (0.01)^{ab}
C18:1(n-9)	34.56 (6.37)^{a}	-	-	-	9.14 (6.89)^{b}	-	-	-	-	-	-	-
C18:1(n-7)	-	-	24.61 (2.47)^{b}	45.88 (0.65)^{a}	-	1.05 (0.27)^{cd}	3.44 (0.69)^{c}	24.81 (2.04)^{b}	-	-	27.18 (0.02)^{b}	3.63 (0.44)^{c}
C18:1(n-5)	-	-	1.19 (0.30)^{b}	-	-	-	-	-	-	2.2 (0.88)^{a}	-	-
C18:2(n-6)	13.00 (0.36)^{c}	7.49 (1.30)^{de}	19.18 (1.96)^{b}	7.29 (0.21)^{de}	6.33 (0.44)^{de}	8.82 (0.97)^{d}	20.14 (0.57)^{b}	5.32 (0.7)^{e}	8.17 (0.58)^{d}	8.55 (1.18)^{d}	11.99 (0.24)^{c}	27.09 (1.04)^{a}
C18:3(n-6)	-	-	1.09 (0.3)^{b}	-	-	-	-	-	0.93 (0.22)^{b}	2.96 (0.47)^{a}	0.3 (0.09)^{c}	-

Table 2. cont. Fatty acid profile in the 12 prospected freshwater microalgae. Values are presented as % of the total fatty acids and total content of omegas 3 (ω3) and 6 (ω6), and omega 6/3 ratio (ω6/3). Values represent the mean and standard deviations in parentheses (n = 3). The same letters represent means with no statistically significant differences (p-value < 0.05).

FAMES	*C. emersonii*	*C. obovata*	*D. brasiliensis*	*Dimorphococcus* sp.	*Ophiocytium* sp.	*Pediastrum* sp.	*Radiococcus* sp.	*Raphidocelis sp.*	*S. leptocladium*	*S. pantanale*	*T. brasiliensis*	*W. botryoides*
C18:3(n-3)	-	46.81 (4.66)^{b}	-	-	-	42.37 (2.75)^{b}	15.08 (0.79)^{e}	-	33.13 (0.54)^{c}	33.08 (4.36)^{c}	-	54.62 (3.63)^{a}
C18:4(n-3)	3.12 (1.27)^{cd}	0.36 (0.20)^{fg}	1.06 (0.28)^{efg}	3.44 (0.4)^{cd}	-	1.89 (0.29)^{def}	3.67 (0.37)^{c}	2.21 (0.55)^{cde}	9.24 (0.57)^{a}	7.35 (1.09)^{b}	1.24 (0.08)^{efg}	-
C20:4(n-6)	-	-	-	-	15.21 (0.23)^{a}	-	-	-	0.83 (0.07)^{b}	-	-	-
C20:5(n-3)	-	0.46 (0.05)^{b}	-	-	12.7 (0.28)^{a}	-	-	-	0.12 (0.03)^{c}	-	-	-
C22:0	-	0.81 (0.05)^{b}	-	-	-	1.08 (0.26)^{b}	0.24 (0.1)^{c}	2.36 (0.38)^{a}	-	-	0.86 (0.1)^{b}	-
C22:1	-	-	-	-	-	-	0.43(0.04)^{a}	-	-	-	-	-
C22:6(n-3)	-	-	-	-	1.59 (0.27)^{a}	-	-	-	-	-	-	-
C24:0	1.21 (0.19)^{b}	0.23 (0.06)^{de}	-	-	-	0.34 (0.22)^{cd}	-	1.54 (0.02)^{a}	0.17 (0.02)^{de}	-	0.55 (0.09)^{c}	-
C24:1	-	-	-	-	-	0.8(0.2)^{a}	-	-	-	-	-	-
ω3	18.93 (6.35)	56.74 (3.67)	2.06 (0.51)	3.26 (0.26)	16.31 (0.80)	55.35 (2.48)	26.83 (2.23)	7.93 (2.09)	58.41 (1.05)	57.33 (1.55)	12.05 (0.01)	56.75 (0.58)
ω6	13.04 (0.24)	7.52 (0.70)	19.36 (1.41)	6.91 (0.12)	28.90 (1.08)	9.36 (0.50)	20.05 (0.46)	5.62 (0.52)	11.03 (0.48)	9.43 (0.35)	11.19 (0.24)	27.64 (0.41)
ω6/3	0.81 (0.41)^{b}	0.14 (0.01)^{b}	10.00 (2.65)^{a}	2.23 (0.21)^{b}	1.77 (0.06)^{b}	0.17 (0.02)^{b}	0.76 (0.16)^{b}	0.76 (0.08)^{b}	0.19 (0.02)^{b}	0.16 (0.01)^{b}	0.93 (0.32)^{b}	0.49 (0.00)^{b}

The lipid profile of the 12 microalgae (Table 2) shows the identification of 22 fatty acids, mainly PUFAs. Five microalgae had contents of 60% PUFAs: *C. obovata*, *Pediastrum* sp., *S. leptocladium*, *S. pantanale*, and *W. botryoides*. Alpha-linolenic acid (C18:3n3) was the predominant component, followed by linoleic acid (C18:2n6) (Table 3). Less common FAMEs for freshwater microalgae are eicosapentaenoic (EPA), docosahexaenoic (DHA), and arachidonic (ARA) acids. Although some other algae have presented these PUFAs, only in *Ophiocytium* sp. EPA (C20:5n3), DHA (C22:6n3), and ARA (C20:4n6) were they detected at concentrations higher than 1%. This microalga presented an ARA content of 15%, 1.3% for DHA, and 13% for EPA.

Regarding MUFAs, *Dimorphococcus* sp. had the highest content (49%), mainly consisting of vaccenic acid (C18:1n7). *Ophiocytium* sp. had the second highest content, rich in palmitoleic acid (16:1n7). *C. emersonii* stood out in relation to the amount of oleic acid (C18:1n9), which made up 34% of its 35% of monounsaturated lipids. This alga presented almost the same amount of SFAs, mainly comprising palmitic acid (C16:0), which was the most common SFA observed, especially for *Raphidocelis sp.* and *D. brasiliensis*, whose oils mainly consist of SFAs.

Among the ω3 and ω6 fatty acids, the highest production of ω3 was observed in the *Staurastrum* group of algae, where they were found to be predominant compared to ω6. The highest ω6 contents were found in *W. botryoides* and *Ophyocytium* sp. This favorable concentration of ω3 was responsible for decreasing the ω6:3 ratio, which ranged from 0.1 to 2 in the studied microalgae. The only exception was *D. brasiliensis*, with an ω6:3 ratio of 10.0 ± 2.6.

3.4. Pigments and antioxidants

The concentration of the photosynthetic pigments, chlorophyll a, chlorophyll (Chl b, $c_{1\&2}$) and carotenoids, the antioxidant activity, and total polyphenols are shown in Table 3.

Table 3. Pigment composition, chlorophyll a (Chl a), chlorophyll (Chl b, $c_1\&_2$), carotenoids (TC), the ratio of chlorophyll a to b (chl a/b), total polyphenols content (TPC) and scavenging activity by DPPH (DPPH) in the 12 freshwater microalgae investigated. The values represent the means, and the standard deviation (n = 3) is shown in parentheses. Same letters represent means that did not show statistically significant differences among the microalgae (p-value < 0.05).

Microalgae	Chl a ($\mu g.mL^{-1}$)	Chl b, $c_{1\&2}$* ($\mu g.mL^{-1}$)	TC ($\mu g.mL^{-1}$)	Chl a/b	TPC ($mgEq.g^{-1}$)	DPPH ($\%_{inhibition}$)
C. emersonii	2.83(0.02)^{a}	1.42(0.05)$^{a\ b}$	0.83(0.00)^{a}	2.00(0.06)^{abc}	7.03(0.17)^{bcd}	28.70(1.15)^{bcd}
C. obovata	1.04(0.04)^{d}	0.90 (0,02)	—	—	11.01(0.37)^{a}	23.14(3.95)^{cde}
D. brasiliensis	1.14(0.30)^{d}	0.84(0.21)^{cd}	0.28(0.02)^{d}	1.44(0.28)^{d}	6.85(0.19)^{bcd}	19.41(2.31)^{de}
Dimorphococcus sp.	1.55(0.14)^{c}	1.08(0.12)^{bc}	0.36(0.02)^{c}	1.44(0.04)^{d}	7.63(0.25)^{bc}	18.73(0.87)^{e}
Ophiocytium sp.	0.96(0,04)^{de}	0.83 (0.03)	—	—	5.88(0.16)^{d}	25.03(4.90)^{cde}
Pediastrum sp.	2.92(0.04)^{a}	1.63(0.09)^{a}	0.83(0.00)^{a}	1.80(0.07)^{bcd}	8.07(0.43)^{b}	36.31(2.27)^{ab}
Raphidocelis sp.	1.08(0.04)^{d}	0.66(0.04)^{de}	0.3(0.00)^{cd}	1.64(0.05)$^{bcd\ ef}$	6.47(0.07)^{bc}	20.88(2.03)^{bc}
Radiococcus sp.	1.98(0.18)^{b}	1.35(0.09)^{ab}	0.57(0.04)^{b}	1.46(0.03)^{d}	7.85(0.08)^{cd}	31.22(2.62)^{de}
S. leptocladium	2.89(0.02)^{a}	1.24(0.02)^{b}	0.83(0.01)^{a}	2.33(0.02)^{a}	10.54(0.18)^{a}	42.68(1.04)^{a}
S. pantanale	0.69(0.04)^{ef}	0.41(0.01)^{ef}	0.26(0.01)^{d}	1.69(0.09)^{bcd}	7.39(0.34)^{bc}	33.99(2.67)^{b}
T. brasiliensis	1.19(0.07)^{d}	0.56(0.01)^{def}	0.34(0.03)$^{c\ d}$	2.13(0.15)^{ab}	6.69(0.94)^{bcd}	27.66(1.61)^{bcde}
W. botryoides	0.56(0.05)^{f}	0.29(0.01)^{f}	0.18(0.02)^{e}	1.96(0.14)^{abc}	3.43(0.03)^{e}	27.47(0.88)^{bcde}

* *C. obovata* is a Cryptophyceae and have Chlorophyll c_2 and *Ophiocytium* sp. is an Xanthophyceae and have Chlorophyll $c_{1\&2}$.

In terms of photosynthetic pigments, Chlorophyta and Charophyta followed the same production pattern, with higher concentrations of Chl a followed by Chl b. The microalgae *C. emersonii*, *Pediastrum* sp., and *S. leptocladium* had the highest values of Chl a, Chl b, and carotenoids. The others did not show any difference in pigment content. Regarding the ratio Chl a/b, the highest values were observed for *S. leptocladium*, *T. brasiliensis*, *C. emersonii*, and *W. botryoides*. *C. obovata* and *Ophiocytium* sp. showed similar amounts of Chl c.

Among the antioxidant potential of all the evaluated microalgae, the highest antioxidant activity values were observed in *S. leptocladium*, with 43% DPPH radical inhibition, followed by the microalga *Pediastrum* sp., which showed 36% inhibition. *Raphidocelis* sp. had significant activity, similar to that of *Pediastrum* sp., and also showed a similar polyphenol content. Regarding the total polyphenol content, the microalgae *C. obovata* and *S. leptocladium* stood out. However, unlike *S. leptocladium*, a greater reducing capacity did not translate into greater antioxidant activity for *C. obovata*, which had 23% DPPH radical inhibition. The other algae showed polyphenol content in the range of 3 to 8 $mgEq.g^{-1}$.

3.5. Principal component analysis of main biomolecules and antioxidants

Considering growth rate, biomolecules (proteins, carbohydrates, and lipids), pigments (Chl a and carotenoids), and antioxidant compounds, a principal component analysis (PCA) plot was generated (Figure 3).

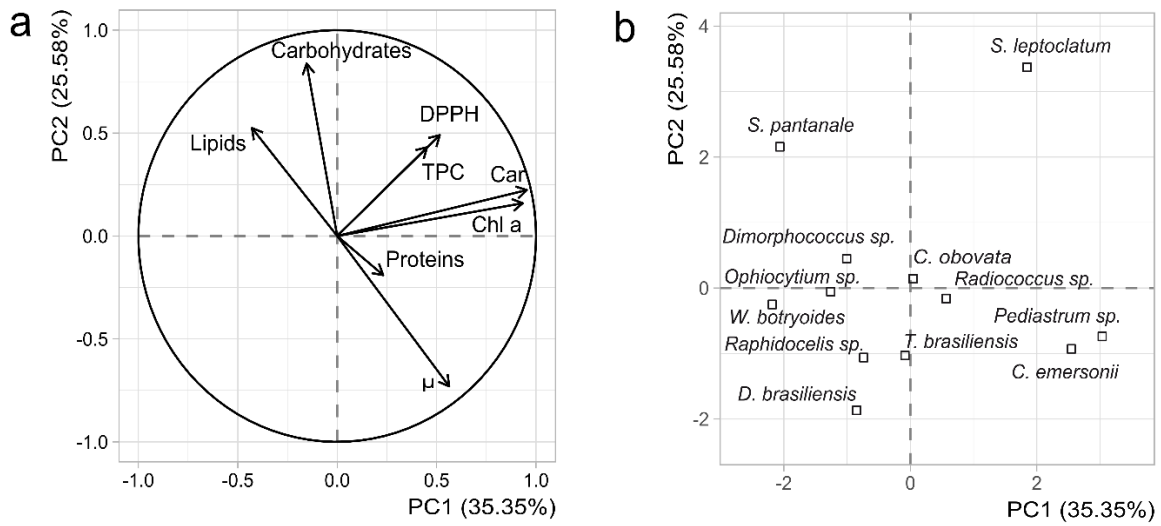

Figure 3. Principal component analysis of key biomolecules (lipids, proteins and carbohydrates), Chlorophyll a (Chl a) and carotenoids (Car), antioxidants, and growth rate (μ) for the 12 different microalgae species, considering: a) variables and b) individuals. The individual plot represents the mean point of triplicates (n=3).

For *C. obovata* and *Ophiocytium* sp. the values of carotenoids were not considered using the R-package missMDA to correct the missing values (AUDIGIER; HUSSON; JOSSE, 2016). PC1 (Figure 3a) explained 35.35% of the variation and was positively correlated with most variables except for carbohydrates and lipids. PC2 explained 25.58% of the variation, showing positive correlations only with lipids and carbohydrates. Together, these two components accounted for more than 60% of the variation in the observed variables. Some patterns can be mentioned, including a correlation between the growth rate and protein content, although it is not a strong correlation. A correlation was observed between Chlorophyll a, carotenoids and antioxidant activity (DPPH), as well as with total polyphenol content, showing almost a direct correlation. Lipids and carbohydrates also exhibited a correlation. In Figure 3b, PC1 clearly associates *C. emersonii* and *Pediastrum* sp., with higher growth rates, protein content, and pigment

production. *S. leptocladium* showed potential for producing antioxidant compounds, particularly polyphenols. PC2 highlighted the potential for lipid and carbohydrate production, with *Staurastrum* species standing out for these biomolecules, along with *Dimorphococcus* sp.

4. Discussion

The results obtained in the present research related to growth rates and biomolecules (lipids, proteins, and carbohydrates) are within the expected range reported in the literature for eukaryotic microalgae (FINKEL et al., 2016). The variation in growth rates, a species-specific variable that depends on nutritional factors, was expected due to both the different species and phenotypic factors, as observed in the relationship between cell volume and lower growth rate values (REITAN et al., 2021; TANG, 1996). The growth rate may also be associated with variations in the molecular composition of microalgae. The analysis of biomolecules by PCA showed a positive correlation between the growth rate and protein content. In their review, Finkel et al. (2016) highlighted that higher growth rates are associated with higher protein content. This likely occurs due to the significant need for protein synthesis and expression in microalgae with higher division rates. Rees and Raven (2021) observed an association between growth rate and a higher proportional RNA content among photosynthetic eukaryotes. The species that had the most significant influence on these variables were the microalgae *C. emersonii* and *Pediastrum* sp.

The *Chlorella* genus is commonly used as food source for humans and animals (BECKER, 2007), which is due to its ease of growth and accumulation of proteins of high nutritional value (AHMAD et al., 2020). In this study, both the growth rate (0.91 d^{-1}) and protein content (63%) in *C. emersonii* are consistent with the literature. Ma et al. (2021) obtained up to 54% proteins in *Chlorella sorokiniana* in batch cultivation using the modified BG11 medium. Silva et al. (2023) obtained, for *Chlorella fusca*, levels of up to 32% in the exponential growth

in Bold-basal medium (BBM). Illman et al. (2000) obtained 32% proteins in the stationary phase for *Chlorella emersonii* in Watanabe medium. The protein values reported in both Silva et al. (2023) and Illman et al. (2000) were around half of those obtained in this work, with cultures in the exponential growth phase.

In the present research, although not a commercially exploited species, *Pediastrum* sp. presented growth rate and protein values comparable to *C. emersonii*. Investigating *Pediastrum* sp., Sassi et al. (2019) obtained a growth rate of 0.63 d^{-1} in Zarrouk medium and 0.81 d^{-1} in WC medium, and in WC, the authors obtained a maximum protein content of 35% at the beginning of the stationary growth phase. However, in the present research, unlike *C. emersonii*, whose antioxidant capacity was 28.7%, *Pediastrum* sp. had 36% of antioxidant capacity and more than double the content of polyunsaturated fatty acids. The higher polyunsaturated fatty acids content can be related to the presence of linolenic acid, which made up almost half of the fatty acids in this alga, contributing to a favorable ω6:3 ratio (0.17). The ratio between these groups is important from a nutritional point of view, as ideally, the recommended intake varies from 4:1 to 1:1. Diets with higher proportions of omega-6 influence the onset of inflammation-related diseases and chronic illnesses (SIMOPOULOS, 2002). This makes *Pediastrum* sp. interesting for future studies of nutritional applications, as an alga that produces large amounts of antioxidants and PUFAs that are of interest for human and animal nutrition (MAVROMMATIS et al., 2023; SANTIN et al., 2022; SIDRA ZAMAN et al., 2023).

W. botryoides stood out in the production of PUFAs as it is the only species that presented above 80% and 20% DW as lipids, more significant to human health. Moreover, it is rich in alpha-linolenic (55%) and linoleic (27%) acids, essential for dietary consumption (CASTRO; TOCHER; MONROIG, 2016). In general, Chlorophyceae microalgae have been reported as good producers of ALA. Guedes et al. (2011) evaluated several groups of

microalgae and observed that the Chlorophyceae had, in general, a higher concentration of PUFAs than other groups. Matos et al. (2016) observed that *Chlorella vulgaris* had a composition of 40% PUFAs of the total fatty acids, which was higher than the other groups they evaluated (below 2%). Evaluating the fatty acid profile of 14 Chlorophyta, SANTHAKUMARAN; KOOKAL; RAY (2018) found that algae in the same family as *W. botryoides* had PUFA levels exceeding 50%, and ALA was the major fatty acid for *Scenedesmus obliquus*, *Scenedesmus acuminatus*, and *Pseudotetradesmus quaternarius*.

Ophyocytium sp. was the only microalgae species in the 12 investigated ones in the present research that could produce ARA, EPA, and DHA. This may be characteristic of the Xanthophyceae group to which *Ophyocytium* sp. belongs. Lang et al. (2011) evaluated the lipid composition of over 2,000 microalgae strains belonging to various groups and observed that among the Xanthophyceae, almost half of them had arachidonic acid, while just 14% was reported for the Chlorophyceae. However, even though half of the Xanthophyceae they investigated presented arachidonic acid, less than a quarter of that presented contents above 5%.

The other eight microalgae species studied in the present research produced higher amounts of MUFAs and SFAs than the afore mentioned four species. SFAs and MUFAs are fatty acids desirable for applications related to bioenergy, such as biodiesel. According to the literature, saturated acids such as palmitic acid and monounsaturated acids such as oleic acid are desirable for bioenergy (KNOTHE, 2008, 2014). For such applications, it is also recommended that PUFA values do not exceed 17% (BREUER et al., 2012). Considering these premises, the microalgae *Dimorphococcus* sp. proved to be a suitable strain for the bioenergy sector. *Dimorphococcus* sp. showed the highest production of lipids (28%) in exponentially growing cells, with 49% MUFAs and 41% SFAs, in addition to high protein levels (>50% DW). These variables, lipids and proteins, were antagonistic in the PCA, thus *Dimorphococcus* sp.

can be considered an exception among the strains. The growth rate also showed an inverse relationship with lipid content, where carbohydrates were the only factor that correlated with higher lipid percentages. This may be related to the fact that both play a fundamental role in various structural processes and act as carbon storage (BOROWITZKA et al., 2016).

Sánchez-Bayo et al. (2020) observed a negative correlation between protein accumulation and carbohydrate content in their evaluation of microalgae and cyanobacteria. Reitan et al. (2021) also noted that conditions favoring lower growth rates led to increased carbohydrates and lipids in marine microalgae. Considering the individual variables in PCA, those that stood out the most in carbohydrate and lipid content were the microalgae of the genus *Staurastrum*. *S. pantanale* presented 23% lipids and was notable as it produces a significant amount of carbohydrates (40% DW), while *S. leptocladium* had lower levels of carbohydrates (32% DW) and 20% lipids. For both species, these values are higher than most eukaryotic microalgae, which typically contain around 11 to 17% carbohydrates and 14 to 18% lipids (FINKEL et al., 2016). This could possibly be a characteristic of this genus, as Giroldo et al. (2005) observed significant carbohydrate production by this genus, and it was also reported to have the potential for lipid accumulation (STAMENKOVIĆ et al., 2019). However, biochemical studies of this group are still scarce in the literature.

The pigments, chlorophyll a and b, and carotenoids (produced by the species we studied) followed the pattern reported in Azaman et al. (2017), in which *Chlorella sorokiniana* and *Chlorella zofingiensis* presented a higher content of Chl a, followed by Chl b and carotenoids. The PCA analysis confirmed a correlation in between chlorophyll a and carotenoids. This is the expected pattern under photoautotrophic conditions for microalgae in exponential growth and healthy cells, as chlorophyll a are the main photosynthetic pigment, dominating in photosystems I and II (BOROWITZKA et al., 2016). Usually, there are around 7 or 8 Chl a to

5 Chl b per photosystem, and the Chl a/b ratio is close to 1.4 (EGGINK; PARK; HOOBER, 2001). In our study, ratios higher than 1.4 were detected, which, as expected, indicates physiological health. Additionally, we also observed that the algae that achieved higher growth rates, except for *D. brasiliensis*, exhibited higher Chl a/b ratios, which may indicate better light utilization (Friedland et al. 2019). According to COGNE et al. (2011) and FRIEDLAND et al. (2019) the higher content of Chl a in relation to Chl b can be associated with better photosynthetic performance, greater biomass accumulation and higher growth rates, thus healthier cells. *C. obovata* and *Ophiocytium* sp. do not produce chlorophyll b. *C. obovata* contains chlorophyll a and c_2, while *Ophiocytium* sp. chlorophylls $c_{1\&2}$ (Guiry, 1997). The chlorophyll c content values did not differ between the two species, and the calculated values for chlorophyll a were close to those observed for other Chlorophyta.

Carotenoids, although in smaller quantities, play a complementary role in light absorption and act as free radical inhibitors (Cirulis et al. 2013). In this study, an association was observed between higher carotenoid content and a greater antioxidant response. However, this correlation was not stronger because polyphenol content affects antioxidant activity due to its natural ability to stabilize free radicals, either by donating protons or electrons (Leopoldini et al. 2011). This was observed in the PCA analysis, which showed a direct correlation between increased antioxidant potential and polyphenol content for the 12 microalgae studied. The main contributor was the microalga *S. leptocladium*, which presented the highest antioxidant activity and total polyphenols compared to most of the other 11 microalgae investigated. Another alga with antioxidant potential was *Pediastrum* sp., which also showed significant inhibition of the DPPH radical. Corrêa et al. (2022) achieved 39.8% inhibition of the ABTS radical, demonstrating its capacity as a producer of antioxidant compounds. The authors obtained a lower polyphenol concentration (1.95 $mgEq.g^{-1}$) compared to the value obtained in the present study. Santiago-Díaz et al. (2021) obtained DPPH radical inhibition values of up to 30% by

evaluating methanolic extracts of three Chlorophyceae, similar to the results for most microalgae examined here. Banskota et al. (2019) observed up to 45% activity in *Tetraselmis chuii* and around 21% in *Chlorella sorokiniana*. For total polyphenols, they obtained 9.78 and 6.32 $mgEq.g^{-1}$, comparable to most of the microalgae assessed in this study. Using various solvent mixtures and extraction methods, Monteiro et al. (2020) achieved a maximum of 6 $mgEq.g^{-1}$ in different groups of macro and microalgae. In this research, only *Ophiocytium* sp. and *W. botryoides* were below that threshold.

5. Conclusion

As conclusion, the prospection of the 12 microalgae for biomolecules, growth rates, and biomass highlights their promising potential in various areas of biotechnology. *C. emersonii* and *Pediastrum* sp. stand out due to their high growth rates and production of biomass, proteins, and pigments. Specifically, *Pediastrum* sp. showed one of the highest antioxidant activities, in addition to producing more essential polyunsaturated fatty acids than *C. emersonii*. *Dimorphococcus* sp., emerges as a protein producer, with the potential for biofuel production due to the concentration and composition of its lipids. Microalgae of the genus *Staurastrum* and *W. botryoides* are rich in carbohydrates and essential polyunsaturated lipids, while *Ophiocytium* sp. excels in the production of uncommon essential fatty acids, such as DHA, EPA, and ARA.

The results of this study demonstrate the potential of microalgae from understudied taxonomic groups as sources of industrially relevant biomolecules. The unique and advantageous characteristics of these microalgae make them promising candidates for the development of novel products and processes in various biotechnology fields.

6. References

AHMAD, M. T. et al. Applications of microalga Chlorella vulgarisin aquaculture. **Reviews in Aquaculture**, v. 12, n. 1, p. 328–346, 19 fev. 2020.

ALBALASMEH, A. A.; BERHE, A. A.; GHEZZEHEI, T. A. A new method for rapid determination of carbohydrate and total carbon concentrations using UV spectrophotometry. **Carbohydrate Polymers**, v. 97, n. 2, p. 253–261, 2013.

AUDIGIER, V.; HUSSON, F.; JOSSE, J. A principal component method to impute missing values for mixed data. **Advances in Data Analysis and Classification**, v. 10, n. 1, p. 5–26, 24 mar. 2016.

AZAMAN, S. N. A. et al. A comparison of the morphological and biochemical characteristics of Chlorella sorokiniana and Chlorella zofingiensis cultured under photoautotrophic and mixotrophic conditions. **PeerJ**, v. 5, p. e3473, 8 set. 2017.

BANSKOTA, A. H. et al. Antioxidant properties and lipid composition of selected microalgae. **Journal of Applied Phycology**, v. 31, n. 1, p. 309–318, 31 fev. 2019.

BARBOSA, M. J. et al. Hypes, hopes, and the way forward for microalgal biotechnology. **Trends in Biotechnology**, v. 41, n. 3, p. 452–471, mar. 2023.

BEARDALL, J.; RAVEN, J. A. Carbon Acquisition by Microalgae. **The Physiology of Microalgae**. Springer International Publishing, 2016. p. 89–99.

BECKER, E. W. Micro-algae as a source of protein. **Biotechnology Advances**, v. 25, n. 2, p. 207–210, mar. 2007.

BOROWITZKA, M. A. High-value products from microalgae—their development and commercialization. **Journal of Applied Phycology**, v. 25, n. 3, p. 743–756, 29 jun. 2013.

BOROWITZKA, M. A. et al. **The Physiology of Microalgae**. Springer International Publishing, 2016. v. 6

BRAND-WILLIAMS, W.; CUVELIER, M.-E.; BERSET, C. Use of a free radical method to evaluate antioxidant activity. **LWT-Food science and Technology**, v. 28, n. 1, p. 25–30, 1995.

BREUER, G. et al. The impact of nitrogen starvation on the dynamics of triacylglycerol accumulation in nine microalgae strains. **Bioresource Technology**, v. 124, p. 217–226, nov. 2012.

CASTRO, L. F. C.; TOCHER, D. R.; MONROIG, O. Long-chain polyunsaturated fatty acid biosynthesis in chordates: Insights into the evolution of Fads and Elovl gene repertoire. **Progress in Lipid Research Elsevier Ltd**, 1 abr. 2016.

CIRULIS, J. T.; SCOTT, J. A.; ROSS, G. M. Management of oxidative stress by microalgae. **Canadian journal of physiology and pharmacology**, v. 91, n. 1, p. 15–21, 2013.

COGNE, G. et al. A model-based method for investigating bioenergetic processes in autotrophically growing eukaryotic microalgae: Application to the green algae Chlamydomonas reinhardtii. **Biotechnology Progress**, v. 27, n. 3, p. 631–640, 2011.

CORRÊA DA SILVA, M. G. et al. Phenolic compounds and antioxidant capacity of Pediastrum boryanum (Chlorococcales) biomass. **International Journal of Environmental Health Research,** v. 32, n. 1, p. 168–180, 2 jan. 2022.

DUMAY, J.; MORANÇAIS, M. Proteins and Pigments. **Seaweed in Health and Disease Prevention.** Elsevier, 2016. p. 275–318.

EGGINK, L. L.; PARK, H.; HOOBER, J. K. The role of chlorophyll b in photosynthesis: Hypothesis. **BMC Plant Biology**, v. 1, n. 1, p. 2, 2001.

FERNÁNDEZ, F. G. A. et al. The role of microalgae in the bioeconomy. **New Biotechnology**, v. 61, p. 99–107, mar. 2021.

FINKEL, Z. V. et al. Phylogenetic diversity in the macromolecular composition of microalgae. **PLoS ONE**, v. 11, n. 5, p. 1–16, 2016.

FOLCH, J.; LEES, M.; STANLEY, G. H. S. A simple method for the isolation and purification of total lipides from animal tissues. **Journal of Biological Chemistry**, v. 226, n. 1, p. 497–509, maio 1957.

FRIEDLAND, N. et al. Fine-tuning the photosynthetic light harvesting apparatus for improved photosynthetic efficiency and biomass yield. **Scientific Reports**, v. 9, n. 1, p. 13028, 10 set. 2019.

FU, Y. et al. The potentials and challenges of using microalgae as an ingredient to produce meat analogues. **Trends in Food Science & Technology**, v. 112, p. 188–200, jun. 2021.

GIROLDO, D.; VIEIRA, A. A. H. Polymeric and free sugars released by three phytoplanktonic species from a freshwater tropical eutrophic reservoir. **Journal of Plankton Research**, v. 27, n. 7, p. 695–705, 1 jul. 2005.

GOSWAMI, R. K.; AGRAWAL, K.; VERMA, P. An Overview of Microalgal Carotenoids: Advances in the Production and Its Impact on Sustainable Development. **Bioenergy Research**. Wiley, 2021. p. 105–128.

GRIFFITHS, M. J.; HARRISON, S. T. L. Lipid productivity as a key characteristic for choosing algal species for biodiesel production. **Journal of Applied Phycology**, v. 21, n. 5, p. 493–507, 6 out. 2009.

GUEDES, A. C. et al. Fatty acid composition of several wild microalgae and cyanobacteria, with a focus on eicosapentaenoic, docosahexaenoic and α-linolenic acids for eventual dietary uses. **Food Research International**, v. 44, n. 9, p. 2721–2729, nov. 2011.

GUILLARD, R. R. L. Culture of Phytoplankton for Feeding Marine Invertebrates. Boston, MA: Springer US, 1975. p. 29–60

ILLMAN, A. M.; SCRAGG, A. H.; SHALES, S. W. Increase in Chlorella strains calorific values when grown in low nitrogen medium. **Enzyme and Microbial Technology**, v. 27, n. 8, p. 631–635, 2000.

JANSSEN, M.; WIJFFELS, R. H.; BARBOSA, M. J. Microalgae based production of single-cell protein. **Current Opinion in Biotechnology**, v. 75, p. 102705, jun. 2022.

KNOTHE, G. " Designer " Biodiesel : Optimizing Fatty Ester Composition to Improve Fuel Properties. **Energy & Fuels**. p. 1358–1364, 2008.

KNOTHE, G. A comprehensive evaluation of the cetane numbers of fatty acid methyl esters. **FUEL**, v. 119, n. x, p. 6–13, 2014.

LAFARGA, T.; CLEMENTE, I.; GARCIA-VAQUERO, M. Carotenoids from microalgae. **Carotenoids: Properties, Processing and Applications**. Elsevier, 2020. p. 149–187.

LANG, I. et al. Fatty acid profiles and their distribution patterns in microalgae: a comprehensive analysis of more than 2000 strains from the SAG culture collection. **BMC Plant Biology**, v. 11, n. 1, p. 124, 6 dez. 2011.

LEOPOLDINI, M.; RUSSO, N.; TOSCANO, M. The molecular basis of working mechanism of natural polyphenolic antioxidants. **Food Chemistry**, v. 125, n. 2, p. 288–306, mar. 2011.

LI-BEISSON, Y. et al. The lipid biochemistry of eukaryotic algae. **Progress in Lipid Research**, v. 74, p. 31–68, abr. 2019.

MA, R. et al. Enhancement of co-production of lutein and protein in Chlorella sorokiniana FZU60 using different bioprocess operation strategies. **Bioresources and Bioprocessing**, v. 8, n. 1, p. 82, 30 dez. 2021.

MATOS, Â. P. et al. Chemical Characterization of Six Microalgae with Potential Utility for Food Application. **JAOCS, Journal of the American Oil Chemists' Society**, v. 93, n. 7, p. 963–972, 2016.

MAVROMMATIS, A. et al. Microalgae as a Sustainable Source of Antioxidants in Animal Nutrition, Health and Livestock Development. **Antioxidants**, v. 12, n. 10, p. 1882, 19 out. 2023.

MONTEIRO, M. et al. Effect of extraction method and solvent system on the phenolic content and antioxidant activity of selected macro- and microalgae extracts. **Journal of Applied Phycology**, v. 32, n. 1, p. 349–362, 28 fev. 2020.

MORALES, M.; AFLALO, C.; BERNARD, O. Microalgal lipids: A review of lipids potential and quantification for 95 phytoplankton species. **Biomass and Bioenergy**, v. 150, p. 106108, jul. 2021.

PARRISH, C. C. Determination of Total Lipid, Lipid Classes, and Fatty Acids in Aquatic Samples. **Lipids in Freshwater Ecosystems**. New York, NY: Springer New York, 1999. p. 4–20.

PRICE, C. A. A membrane method for determination of total protein in dilute algal suspensions. **Analytical Biochemistry**, v. 12, n. 2, p. 213–218, ago. 1965.

REES, T. A. V.; RAVEN, J. A. The maximum growth rate hypothesis is correct for eukaryotic photosynthetic organisms, but not cyanobacteria. **New Phytologist**, v. 230, n. 2, p. 601–611, 24 abr. 2021.

REITAN, K. I. et al. Chemical composition of selected marine microalgae, with emphasis on lipid and carbohydrate production for potential use as feed resources. **Journal of Applied Phycology**, v. 33, n. 6, p. 3831–3842, 14 dez. 2021.

RICHMOND, A.; HU, Q. **Handbook of Microalgal Culture**. Oxford, UK: John Wiley & Sons, Ltd, 2013.

RITCHIE, R. J.; SMA-AIR, S.; DUMMEE, V. DMSO formula for chlorophyll determination in dinoflagellates (Chl a + c2). **Journal of Applied Phycology**, v. 34, n. 1, p. 335–341, 26 fev. 2022.

RITCHIE, R. J.; SMA-AIR, S.; PHONGPHATTARAWAT, S. Using DMSO for chlorophyll spectroscopy. **Journal of Applied Phycology**, v. 33, n. 4, p. 2047–2055, 12 ago. 2021.

SÁNCHEZ-BAYO, A. et al. Cultivation of Microalgae and Cyanobacteria: Effect of Operating Conditions on Growth and Biomass Composition. **Molecules**, v. 25, n. 12, p. 2834, 19 jun. 2020.

SANTHAKUMARAN, P.; KOOKAL, S. K.; RAY, J. G. Biomass yield and biochemical profile of fourteen species of fast-growing green algae from eutrophic bloomed freshwaters of Kerala, South India. **Biomass and Bioenergy**, v. 119, n. March, p. 155–165, 2018.

SANTIAGO-DÍAZ, P. et al. Characterization of Novel Selected Microalgae for Antioxidant Activity and Polyphenols, Amino Acids, and Carbohydrates. **Marine Drugs**, v. 20, n. 1, p. 40, 30 dez. 2021.

SANTIN, A. et al. Microalgae-Based PUFAs for Food and Feed: Current Applications, Future Possibilities, and Constraints. **Journal of Marine Science and Engineering**, v. 10, n. 7, p. 844, 21 jun. 2022.

SASSI, K. K. B. et al. Metabolites of interest for food technology produced by microalgae from the Northeast Brazil. **Revista Ciencia Agronomica**, v. 50, n. 1, p. 54–65, 2019.

SHOAF, W. T.; LIUM, B. W. Improved extraction of chlorophyll a and b from algae using dimethyl sulfoxide. **Limnology and Oceanography**, v. 21, n. 6, p. 926–928, 1976.

SIDRA ZAMAN, M. M. et al. Supplementation of PUFA extracted from microalgae for the development of chicken patties. **PeerJ**, v. 11, p. e15355, 24 maio 2023.

SILVA, J. C. et al. Biomass, photosynthetic activity, and biomolecule composition in Chlorella fusca (Chlorophyta) cultured in a raceway pond operated under greenhouse conditions. **Journal of Biotechnology**, v. 367, p. 98–105, abr. 2023.

SIMOPOULOS, A. P. The importance of the ratio of omega-6/omega-3 essential fatty acids. **Biomedicine & Pharmacotherapy**, v. 56, n. 8, p. 365–379, out. 2002.

SLOCOMBE, S. P. et al. A rapid and general method for measurement of protein in micro-algal biomass. **Bioresource Technology**, v. 129, p. 51–57, 2013.

SOARES, A. T. et al. Comparative Analysis of the Fatty Acid Composition of Microalgae Obtained by Different Oil Extraction Methods and Direct Biomass Transesterification. **BioEnergy Research**, v. 7, n. 3, p. 1035–1044, 23 set. 2014.

STAMENKOVIĆ, M. et al. Desmids (Zygnematophyceae, Streptophyta) as a promising freshwater microalgal group for the fatty acid production: results of a screening study. **Journal of Applied Phycology**, v. 31, n. 2, p. 1021–1034, 11 abr. 2019.

STANIER, R. Y. et al. Generic Assignments, Strain Histories and Properties of Pure Cultures of Cyanobacteria. **Microbiology**, v. 111, n. 1, p. 1–61, 1 mar. 1979.

TANG, E. P. Y. WHY DO DINOFLAGELLATES HAVE LOWER GROWTH RATES? 1. **Journal of Phycology**, v. 32, n. 1, p. 80–84, 28 fev. 1996.

TOCHER, D. R. Omega-3 long-chain polyunsaturated fatty acids and aquaculture in perspective. **Aquaculture**, v. 449, p. 94–107, dez. 2015.

WANG, B. et al. CO2 bio-mitigation using microalgae. **Applied Microbiology and Biotechnology**, v. 79, n. 5, p. 707–718, 1 jul. 2008.

WELLBURN, A. R. The Spectral Determination of Chlorophylls a and b, as well as Total Carotenoids, Using Various Solvents with Spectrophotometers of Different Resolution. **Journal of Plant Physiology**, v. 144, n. 3, p. 307–313, 1994.

YAP, J. K. et al. Advancement of green technologies: A comprehensive review on the potential application of microalgae biomass. **Chemosphere**, v. 281, p. 130886, out. 2021.

ZHANG, Q. et al. A Simple 96-Well Microplate Method for Estimation of Total Polyphenol Content in Seaweeds. **Journal of Applied Phycology**, v. 18, n. 3–5, p. 445–450, 2006.

Chapter 2: Exploring the Antimicrobial Potential of Metabolites Produced by 26 Eukaryotic Microalgae Against Medically Relevant Bacteria.

Abstract

Antibiotic resistance is a global issue identified by the World Health Organization as one of the top ten health challenges. By 2050, it is estimated to cause nearly 40 million cumulative deaths, with an annual toll of almost 2 million. Therefore, exploring new sources of antimicrobials, such as microalgae, is crucial for discovering novel compounds. This study aimed to identify antimicrobial compounds from eukaryotic microalgae, analyze their metabolic profiles, and highlight promising metabolites. Twenty-six microalgae species were tested using biomass extracted with two solvents: dichloromethane/methanol and methanol. Antimicrobial activity was assessed against six bacteria: Gram-positive *Staphylococcus aureus*, *Streptococcus mutans*, *Enterococcus faecalis*, and Gram-negative *Escherichia coli*, *Pseudomonas aeruginosa*, *Klebsiella pneumoniae*. Microalgae extracts showing activity were fractionated and retested, and their metabolic profiles were analyzed using mass spectrometry and the GNPS workflow. Among the algae, *Chlorella emersonii* and *Selenastrum bibraianum* inhibited most Gram-positive bacteria, but no significant effect was detected in the Gram-negative ones. After fractionation, *C. emersonii* showed enhanced activity, with fractions B and C inhibiting *S. aureus* at concentrations as low as 50 µg.mL^{-1} and *S. mutans* at 25 µg.mL^{-1}. Metabolic analysis revealed significant levels of polyunsaturated fatty acids, including linolenic acid and its derivatives, as well as terpenes in active extracts. This study highlights *C. emersonii* as a promising source of antibiotic compounds, though further research is needed to identify the specific compounds responsible for the antimicrobial activity.

1. Introduction

The emergence in the number of antibiotic-resistant bacteria cases has led the World Health Organization to classify this issue as one of the top ten global health challenges (WHO, 2019). The reliance on these drugs to treat infections has worsened hospital-acquired infections caused by resistant pathogens. This has resulted in more annual deaths and increased healthcare costs due to more complex therapies (PULINGAM et al., 2022). By 2050, a cumulative total of almost 40 million deaths is estimated and an annual forecast of almost 2 million deaths (NAGHAVI et al., 2024).

The search for antibiotics has historically been successful when based on natural products. The golden age of antibiotics began in 1940 and extended to 1960, with various initiatives leading to the discovery of new molecules and mechanisms of action (HUTCHINGS; TRUMAN; WILKINSON, 2019). Newman and Cragg (2020) reviewed the drugs approved from 1981 to 2019, noting that approximately 48% of antimicrobials are classified as natural or natural-derived. Since the emergence of sulfonamides and penicillin, new antimicrobials have been discovered, such as darobactin, identified in *Photorhabdus* (IMAI et al., 2019), and clovibactin, extracted from a *Streptomyces* strain, which shows activity mainly against Gram-positive bacteria (SHUKLA et al., 2023).

One of the advantages of searching for antimicrobials based on natural products is that these compounds have been selected through evolutionary mechanisms. This has endowed them with advantageous biological properties, such as the ability to cross membranes more easily and interact with proteins and enzymes, making them more bioavailable than fully synthetic antibiotics (SCHNEIDER, 2021). However, one challenge in this context is the rediscovery of antimicrobials from terrestrial sources. On the other hand, compounds from marine organisms may represent a promising source. Due to the high dilution that occurs in aquatic environments, antibiotics from these sources tend to be more potent than those derived from terrestrial organisms (KONG; JIANG; ZHANG, 2010). Additionally, many of these compounds exhibit chemical novelty, making them promising candidates for the development of innovative metabolites (KONG; JIANG; ZHANG, 2010).

A still underexplored source of chemical diversity is eukaryotic microalgae. These cosmopolitan microorganisms exhibit a rich chemical, biochemical, and morphological diversity (RUANE; SONNINO; AGOSTINI, 2010). Initially, their use was focused on fuels, but later, applications for food and as a new potential source of proteins, carbohydrates, and

lipids gained attention (BARBOSA et al., 2023). Microalgae have gained prominence in pharmaceutical applications, serving as a source of bioactive compounds such as carotenoids, omega-3, antioxidants, and anti-inflammatory agents (SILVA et al., 2022). These properties have drawn attention to algae as sources of compounds with antimicrobial activity. The first report of an antimicrobial derived from a microalga was chlorellin, a lipid consortium derived from microalgae of the genus *Chlorella* sp. (PRATT et al., 1944). Since then, antimicrobial activity has been described for various genera of microalgae, including *Chlorella* (IBRAHIM et al., 2015; JAFARI et al., 2018; ÖRDÖG et al., 2004), *Dunaliella* (KILIC; ERDEM; DONMEZ, 2019; MAADANE et al., 2017) and *Scenedesmus* (DANTAS et al., 2019; PATIL; KALIWAL, 2019), which exhibit activity against *Escherichia coli*, *Staphylococcus aureus*, and other microorganisms of human and veterinary relevance.

Thus, the search for antimicrobials from new sources, especially within a diverse group of microalgae, emerges as a promising alternative for the discovery of new antimicrobial compounds.

2. Objectives

This study aimed to identify antimicrobial activity from eukaryotic microalgae extracts. It also sought to evaluate their metabolic profiles and identify promising metabolites as potential antimicrobials.

3. Material and Methods

3.1. Cultivation of algae

The strains used were obtained from the Freshwater Microalgae Culture Collection of the Federal University of São Carlos (CCMA-UFSCar) and the Freshwater Microalgae Culture Collection of the Institute of Biological Sciences of the Federal University of Rio Grande (FURG). In total, 26 strains were evaluated. They were cultivated in BG11 medium (Stanier et al., 1979) or WC medium (Guillard, 1975) in 1L Houx-type flasks (267 mm x 122 mm x 56 mm), containing the appropriate medium for each species. The cultures were maintained under constant aeration with filtered (0.22 µm) atmospheric air and a 12h/12h light/dark photoperiod up to the 8th day of the culture stationary phase. Afterward, the biomass was recovered, centrifuged (Heraeus Multifuge X3R Thermo Fisher Scientific, USA) at 4000 rpm, 4 °C for 10

min, the supernatant was discarded, and the pellet was frozen (-20 ºC), and then lyophilized. The dry biomass was kept under -80 ºC until extractions.

3.2. Preparation of extracts and fractions

The dried biomass was extracted with two solvents: dichloromethane/methanol (DCM:MeOH) in a ratio of 1:1 once, then it was filtered and the biomass extracted 3 times with methanol (MeOH) and the 3 MeOH extracts were combined. This procedure resulted in a total of 52 extracts, numbered from 1 to 52. Then they were concentrated in rotary evaporator (IKA, Staufen, Germany) and dried in a vacuum centrifuge (SpeedVac SPD210, ThermoScientific, USA). After, they were dissolved in DMSO at the concentration of 4 $mg.mL^{-1}$.

3.3. Test organism and culture media

Six bacterial strains were used, the Gram positive *Staphylococcus aureus* (ATCC 29213), *Streptococcus mutans* (ATCC 25175) and *Enterococcus faecalis* (ATCC 29212), and the Gram negative *Escherichia coli* (ATCC 25922), *Pseudomonas aeruginosa* (ATCC 27853) and *Klebsiella pneumoniae* (ATCC 700603). The strains were maintained in Trypticase soy agar (TSA) and for antimicrobial assays Müller-Hinton Broth (MHB) was used, except for *S. mutans* that was kept in Brain heart infusion (BHI) agar for maintenance and broth BHI.

3.4. Antimicrobial assay

Antimicrobial assays were conducted in triplicate with two independent trials, thus 6 replicates for each extract, however, only 3 replicates were used for the fractions due to volume limitation. The bacteria were prepared by collecting a single colony, transferring it to liquid medium, and incubating for 24 hours at 37 °C in an incubator (502/2-C Fanem, Brazil). After the respective incubation times, all strains were centrifuged and resuspended in a concentration within 0.5-1 in McFarland scale or 1 to 3×10^8 $cells.mL^{-1}$, which was confirmed through absorbance (600 nm). Subsequently, the cells were diluted in phosphate-buffered saline medium (PBS) to a concentration of 10^6 $cells.mL^{-1}$ (COCKERILL, 2012). 5 µL of each extract (4 $mg.mL^{-1}$) were added to the microplate wells containing 85 µL of Muller-Hinton broth and homogenized, followed by the addition of 10 µL of the cell suspension, resulting in a final concentration of 1 to 3×10^5 $cells.mL^{-1}$ and an extract concentration of 250 $\mu g.mL^{-1}$. Chlorhexidine at 5 mM was used as a positive control, while 5% DMSO was used as a negative control. Controls containing the medium and the microorganism, as well as a sterility control of the medium without the addition of the microorganism, were also performed. Subsequently,

the plates were incubated for 24 hours, and then 10 µL of Resazurin at 0.44 mM was added and incubated for an additional 30 minutes. After incubation, absorbance determinations were taken using a microplate reader (Epoch - Biotech, USA) at the wavelengths of 570 and 600 nm (WIKLER, 2006). For the fractions, a minimum inhibitory concentration (MIC) assay was conducted, which involved serial dilutions of each fraction from 100 to 12.5 $\mu g.mL^{-1}$. The parameters used for controls, incubation times, and readings were same as those described for the extracts. The MIC was defined as the concentration that inhibited 70% of microbial growth.

3.5. Automated fractionation by HPLC

The extracts that showed promising activity were fractionated using RP-HPLC (Waters Alliance e2695 Separations Module), equipped with a photodiode array detector (Waters 2998 PDA) and an automatic fraction collector III (Waters, Milford, MA, USA). Crude extracts (40 $mg.mL^{-1}$ e.g., 500 µL in a 1 mL loop) were injected and separated on an ACE10 C8 column (50×10 mm, ACE, Reading, UK) using a water (H_2O)/acetonitrile (MeCN) gradient. The collection times, gradient details, and chromatography settings are described in Table 1. Fractions were collected in 48 deep well plates and dried using a vacuum concentrator (CentriVap Concentrator, LabConco, Kansas City, MO, USA). After drying, the fractions were dissolved in DMSO at a final concentration of 4 $mg.mL^{-1}$ (FERREIRA et al., 2021).

Table 1. Parameters for HPLC, including run time, flow rate, elution proportions, and collection times of the fractions.

Time (min)	Flow ($mL \cdot min^{-1}$)	MeCN (%)	H_2O (%)	Collection Time (min)	Fraction
0	3	10	90	1.00–2.30	A
2.0	3	80	20	2.30–3.60	B
3.0	3	80	20	3.60–4.90	C
4.0	3	100	0	4.90–6.20	D
8.9	3	100	0	6.20–7.50	E
9.2	3.5	100	0	7.50–8.80	F
12.0	3.5	100	0	8.80–10.36	G
12.3	3	100	0	10.36–11.50	H
14.0	3	100	0	—	—
15.0	3	10	90	—	—
18.0	3	10	90	—	—

3.6. Metabolite profiling

The fractions were dried, resuspended in MeOH (1 $mg.mL^{-1}$) and analyzed using liquid chromatography-high resolution electrospray ionization tandem mass spectrometry (LC-HRESIMS/MS). A Dionex Ultimate 3000 HPLC, connected to a qExactive focus mass spectrometer, controlled by XCalibur 4.1 software (Thermo Fisher Scientific, Waltham, MA, USA) were used. Chromatography was performed on an ACE UltraCore 2.5 Super C18 column (75 mm×2.1 mm). Two mobile phases (A and B) were used. The mobile phase A was composed of 95% water, 5% methanol, 0.1% formic acid, and mobile phase B of 95% isopropanol, 5% methanol, 0.1% formic acid. Ten uL of each fraction was injected and the separation gradient began at 65% phase B, increasing to 100% over 8 minutes, followed by column cleaning at 100% phase B for 0.5 minutes and reconditioning to the starting conditions for 1.5 minutes; flow rate was maintained at 0.45 $mL.min^{-1}$ with 12 min. total run time. The sample manager was kept at 10 °C. Mass detection was accomplished in positive ion mode (ESI^+). The ESI source parameters configuration was: capillary voltage 3.2 kV, cone voltage 42 V, source temperature 125 °C, desolvation temperature 450 °C, nitrogen gas flow rate 800 $L.h^{-1}$, and a cone gas flow rate of 50 $L.h^{-1}$. Leucine enkephalin served as a Lockspray reference (Ribeiro et al., 2020).

The Raw data obtained were converted to mzML format with the software MSConvert using the Global Natural Products Social Molecular Networking (GNPS) recommended parameters, except the cosine score that was used the value of 0.85 (WANG et al., 2016). For Ion Identity Molecular Networking the feature quantification table and edges MSanotation was obtained using a software MZmine 3, the batch mode code used as parameters is described in appendix 1 (SCHMID et al., 2023). The parameters used for molecular networking are described in appendix 2 with the link to access the molecular network described in this work. To enhance chemical structural information within the molecular network, information from *in silico* structure annotations from GNPS Library Search, Network Annotation Propagation were incorporated into the network using the GNPS MolNetEnhancer workflow (https://ccms-ucsd.github.io/GNPSDocumentation/molnetenhancer/). The similarity scoring was improved using the function Spec2Vec in GNPS (HUBER et al., 2021). For the dereplication step, we the main chemical pathways associated with the mass spectra and the chemical classes were classified. The MS^2Query algorithm for predicting analogous structures was used following the recommended parameters (https://github.com/iomega/ms2query) (HUBER et al., 2021).

4. Results

4.1. Microalgae used

The microalgae used are shown in Table 2. The name, culture collection abbreviation and code, and identification code of the extracts (extract id) for each microalgae.

Table 2. Microalgae bank code, name and Extract id's used for antimicrobial assay.

Bank Code	Microalgae	Extract id	
		DCM:MeOH	MeOH
CCMA 323	*Chlorella emersonii*	1	27
CCMA 477	*Chlorolobion braunii*	2	28
CCMA 148	*Cryptomonas obovatum*	3	29
CCMA 262	*Desmodesmus brasiliensis*	4	30
CCMA 571	*Dimorphococcus* sp.	5	31
CCMA 493	*Hariotina reticulata*	6	32
CCMA 024	*Monoraphidium arcuatum*	7	33
CCMA 140	*Monoraphidium griffithii*	8	34
CCMA 549	*Monoraphidium indicum*	9	35
CCMA 325	*Monoraphidium pseudobraunii*	10	36
CCMA 553	*Ophiocytium* sp.	11	37
CH007	*Pediastrum* sp.	12	38
CCMA 655	*Radiococcus sp*	13	39
CCMA 498	*Raphidocelis piracicabana*	14	40
CCMA 005	*Selenastrum gracile*	15	41
CCMA 500	*Chlorolobion lunatum*	16	42
CCMA 350	*Curvastrum pantanale*	17	43
CCMA 663	*Dictyosphaerium* sp.	18	44
CCMA 062	*Desmodesmus spinosus*	19	45
CCMA 498	*Pseudokirchneriella elongata*	20	46
CCMA 125	*Selenastrum bibraianum*	21	47
FWAC 276	*Scenedesmus quadricauda*	22	48
CCMA 307	*Tetranephris brasiliensis*	23	49
CCMA 311	*Westella botryoides*	24	50
CCMA 204	*Staurastrum leptoclatum*	25	51
CCMA 382	*Staurastrum pantanale*	26	52

4.2. Antimicrobial assay of the extracts

The antimicrobial activity assay was conducted with 3 Gram-positive and 3 Gram-negative bacteria. Figure 1 shows the effect of the extracts on cell viability (cellular inhibition).

Extracts that significantly differed from the control with 5% DMSO are indicated by asterisks (p-value < 0.05).

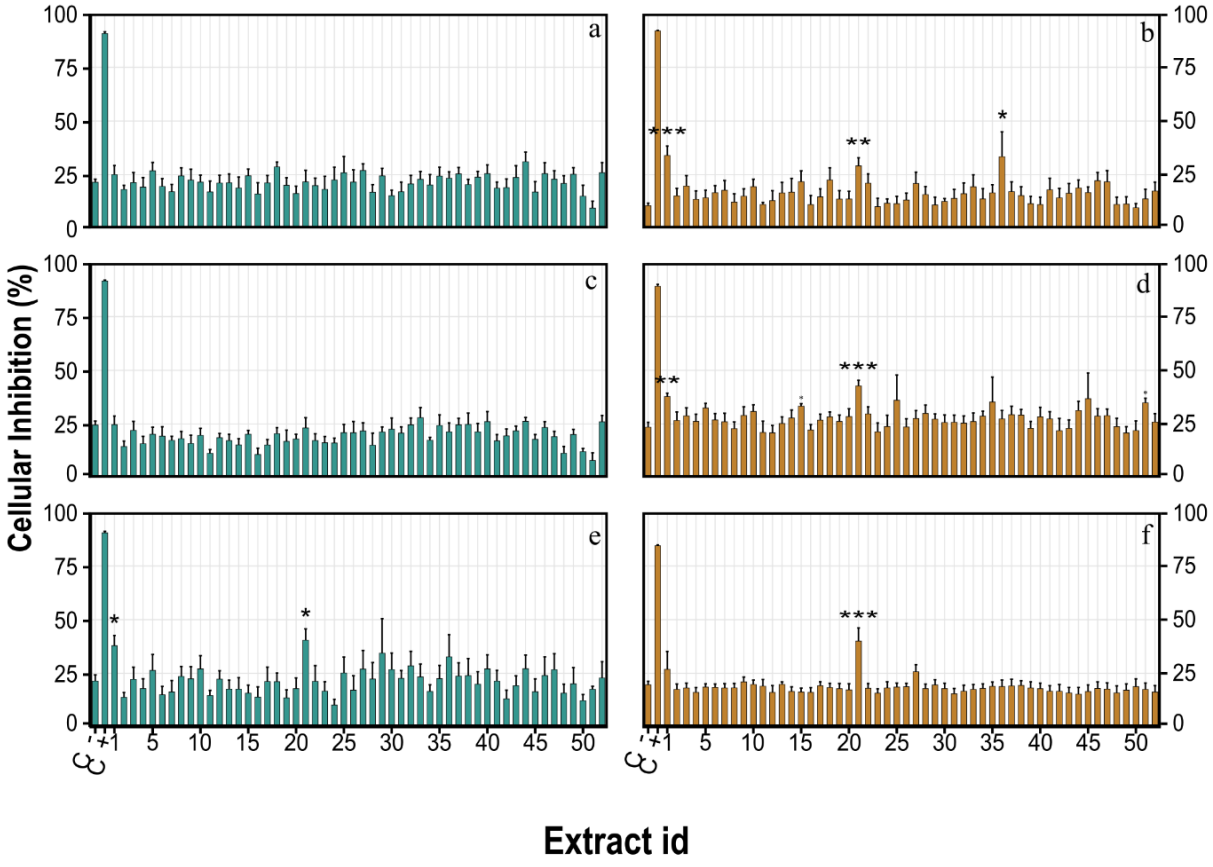

Figure 1. Inhibition of cell growth (%) for the DCM:MeOH extracts (IDs: 1-26) and MeOH extracts (IDs: 27-52) at 250 µg.mL^{-1}. Positive control (C+): Chlorhexidine 5mM and Negative control (C-): DMSO 5%. Gram-negative bacteria are represented in green: a) *E. coli*, c) *K. pneumoniae*, and e) *P. aeruginosa*. Gram-positive bacteria are represented in orange: b) *S. aureus*, d) *E. faecalis*, and f) *S. mutans*. The assays were conducted in triplicate with two independent experiments, totaling six replicates (n=6). Asterisks indicate significant differences compared to the negative control (C-), where *: p-value < 0.05; **: p-value < 0.01; ***: p-value < 0.001.

Considering the extracts, none were able to reduce microbial growth by more than 50%. However, a significant difference was observed compared to the control in 2 of them in 4 of the 6 tested bacteria. The microalgae *C. emersonii* and *S. bibraianum* were able to inhibit approximately 40% of the viability of the bacteria *E. faecalis*, *S. aureus*, and *P. aeruginosa*. Additionally, *S. bibraianum* also inhibited *S. mutans* at a concentration of 250 µg.mL^{-1}. Based

on these results, it was decided to fractionate these extracts (so refered to as fractions) and retest them for antimicrobial activity.

4.3. Antimicrobial assay for fractions

Considering the fractions, activity was observed only for the fractions of *C. emersonii*. Tables 3 and 4 present the MIC at which a 70% reduction in microbial growth was observed.

Table 3. Minimum inhibitory concentration (μg.mL^{-1}) for 70% reduction in viability for the fractions of the microalga *C. emersonii*. Values are presented as means (n = 3).

Fraction	Tested Organism					
	E. coli	*K. pneumoniae*	*P. aeruginosa*	*S. aureus*	*E. faecalis*	*S. mutans*
A	>100	>100	>100	>100	>100	>100
B	>100	>100	>100	50	100	50
C	>100	>100	>100	>100	>100	25
D	>100	>100	>100	>100	>100	>100
E	>100	>100	>100	>100	>100	>100
F	>100	>100	>100	>100	>100	>100
G	>100	>100	>100	>100	>100	>100
H	>100	>100	>100	>100	>100	>100

Table 4. Minimum inhibitory concentration (μg.mL^{-1}) for 70% reduction in viability for the fractions of the microalga *S. bibraianum*. Values are presented as means (n = 3).

Fraction	Tested Organism					
	E. coli	*K. pneumoniae*	*P. aeruginosa*	*S. aureus*	*E. faecalis*	*S. mutans*
A	>100	>100	>100	>100	>100	>100
B	>100	>100	>100	>100	>100	>100
C	>100	>100	>100	>100	>100	>100
D	>100	>100	>100	>100	>100	>100
E	>100	>100	>100	>100	>100	>100
F	>100	>100	>100	>100	>100	>100
G	>100	>100	>100	>100	>100	>100
H	>100	>100	>100	>100	>100	>100

Considering all fractions, no antibacterial activity was detected (100 μg.mL^{-1}) for *S. bibraianum*, indicating that such activity may have resulted from the combination of various

metabolites or that they are not active at concentrations lower than 100 µg.mL^{-1}. In contrast, for *C. emersonii*, antimicrobial activity was predominantly observed in fraction B, with inhibition at up to 50 µg.mL^{-1} for *S. aureus*, capable of inhibiting approximately 98% of microbial growth. Activity was observed for fractions B and C against *S. mutans*, with the highest activity noted in fraction C at 25 µg.mL^{-1}.

4.4. Molecular Network Analysis of the Fractions

Based on the observed activity results, a molecular network was constructed using the MS/MS values, incorporating both the fractions of *C. emersonii* and *S. bibraianum*. For the analysis, only the clusters predominantly present in the most active fractions (fractions B and C of *C. emersonii*) were considered. Figure 2 shows the complete molecular network, while Figure 3 highlights the nodes of greatest interest along with their annotations according to GNPS.

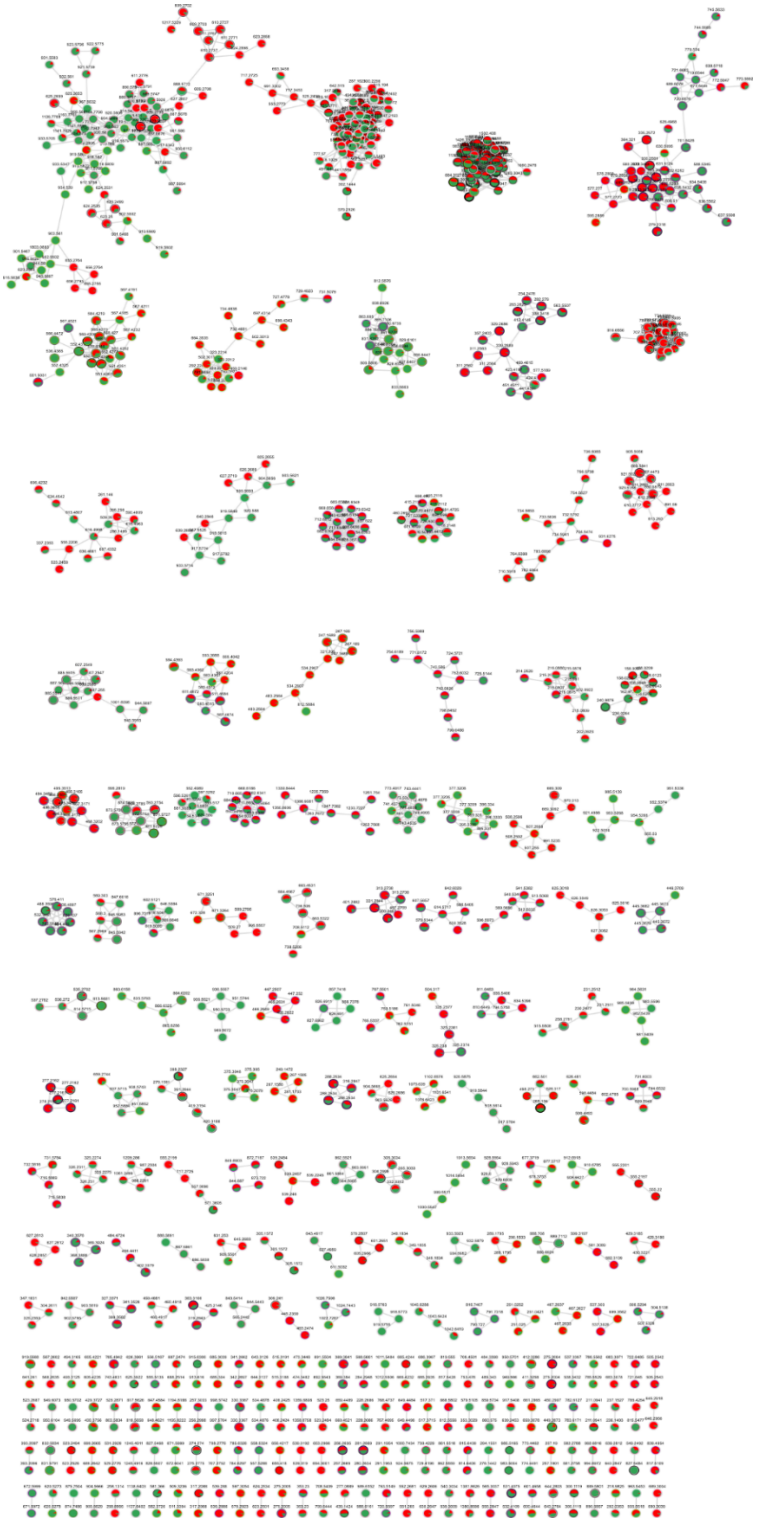

Figure 2. Complete molecular network with nodes corresponding to fractions A-H of *C. emersonii* and *S. bibraianum*, where the active fractions are highlighted in red and the inactive fractions in green.

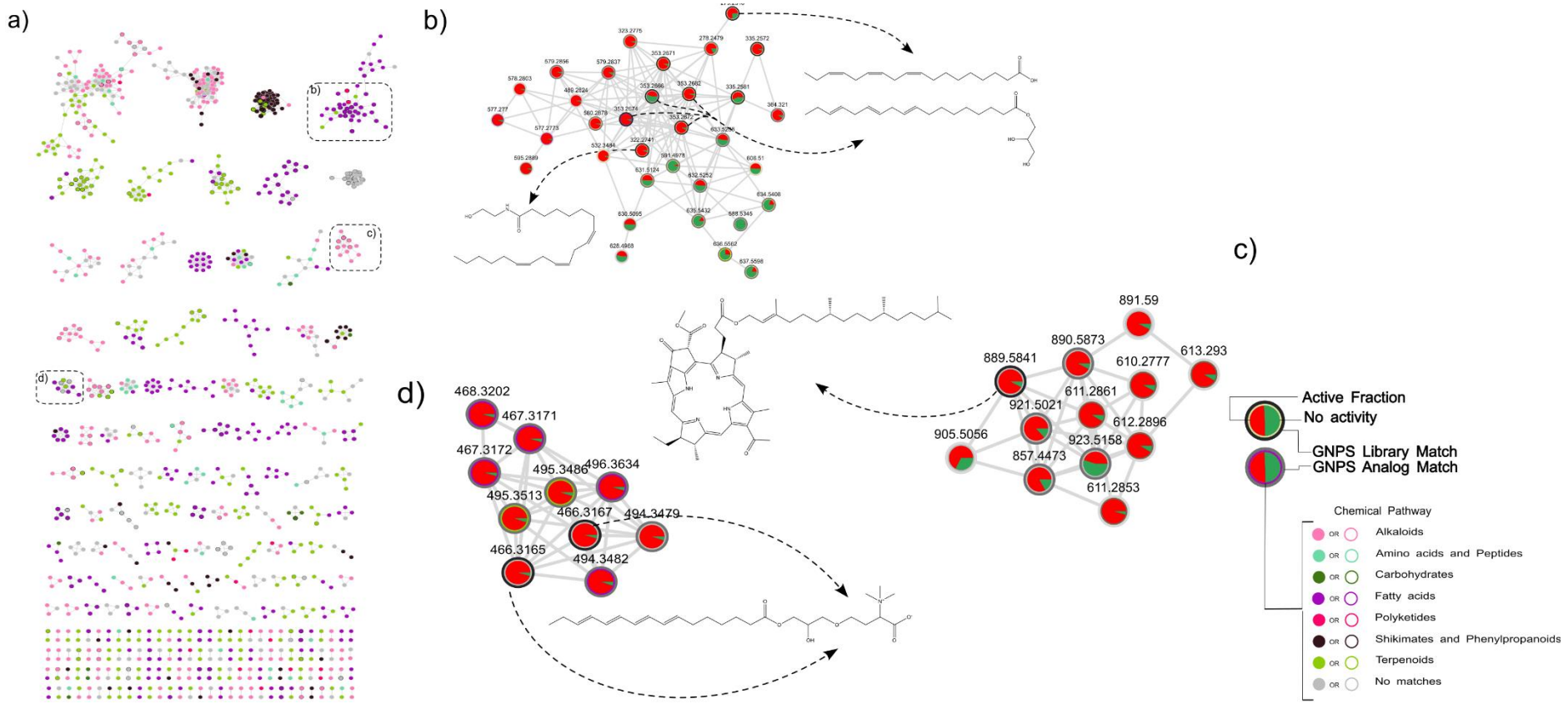

Figure 3. Highlights the main clusters predominantly composed of the most frequent metabolites in the active fractions (in red). The black outline indicates a match based on the GNPS database library. The gray outline indicates the identification of an analog with a similar structure. The colors of the molecular network (a) and the colors of the cluster rings (b-d) indicate the pathway associated with the synthesis of these compounds.

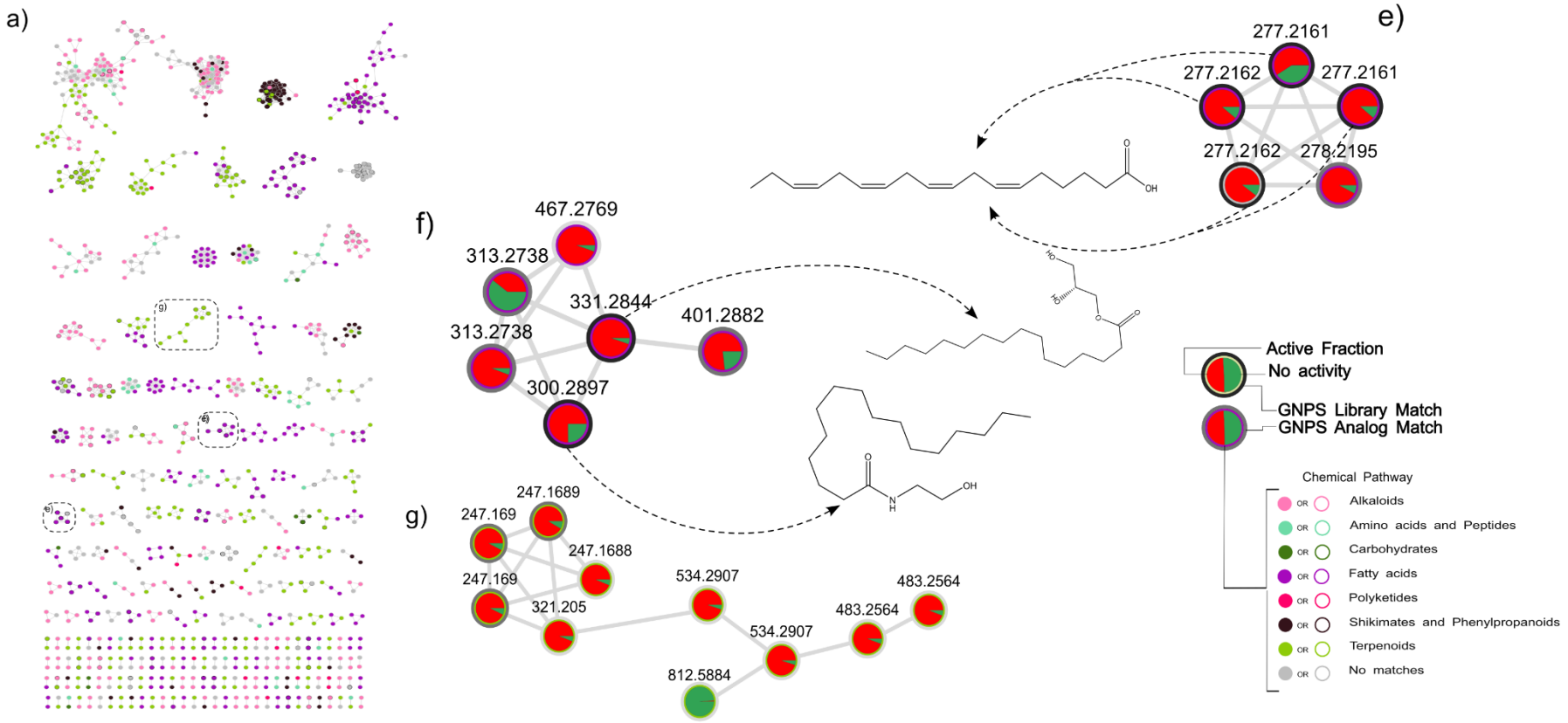

Figure 3. Cont. Highlights the main clusters predominantly composed of the most frequent metabolites in the active fractions (in red). The black outline indicates a match based on the GNPS database library. The gray outline indicates the identification of an analog with a similar structure. The colors of the molecular network (a) and the colors of the cluster rings (b-d) indicate the pathway associated with the synthesis of these compounds.

Six main clusters were observed, in which most of the metabolites were present in the active fractions and associated with fatty acids and derived compounds, such as polyunsaturated fatty acids and ethanolamines (Figures 3b, d-f). In Figure 3b, compounds derived from linoleic acid were annotated, including monolinolein (*m/z* 353.2682 $[M+H]^+$ ppm = 2.72), alpha-linolenic acid (*m/z* 279.2318 $[M+H]^+$ ppm = 2.15), and linolenoyl ethanolamide (*m/z* 322.2741 $[M+H]^+$ ppm = 1.49). In Figure 3d, two nodes were annotated as LysoDGTS 16:4 (a glycolipid associated with a Lyso group and hexadecatetraenoic acid) (*m/z* 466.3165 $[M+H]^+$ppm = 0.64). Figure 3e revealed a cluster exclusively composed of stearidonic acid (*m/z* 277.2161 $[M+H]^+$ ppm = 1.81). Figure 3f presented compounds containing molecules associated with hexadecanoic acid, including 1-Hexadecanoylglycerol (*m/z* 331.2844 $[M+H]^+$ ppm = 1.21) and palmitoyl ethanolamide (*m/z* 300.2879 $[M+H]^+$ ppm = 1.67). Figure 3c was not classified into any chemical class, and only one compound was annotated, namely bacteriopheophytin (*m/z* 888.5763 $[M+H]^+$ ppm = 0.20), where the presence of chlorophyll analogs was noted in this cluster. In Figure 3g, no annotated compounds were observed; however, it was classified as compounds associated with the terpenoid metabolic pathway. Two nodes were classified as analogs of canangalia H and 2-naphthalenemethanol, 7-(acetyloxy)decahydro-alpha,alpha,4a-trimethyl-8-methylene.

5. Discussion

Among the 52 eukaryotic microalgal extracts evaluated, only the dichloromethane extracts of *C. emersonii* and *S. bibraianum* exhibited inhibitory potential against the majority of the tested microorganisms. Microalgae from the genus *Chlorella* have been extensively reported for their ability to inhibit microbial growth. PRATT et al. (1944) were among the first to report this effect, with extracts from this alga shown to inhibit the growth of *S. aureus*. Ördög et al. (2004) observed significant antimicrobial activity in extracts of *C. minutissima* and *Chlorella* sp. against *S. aureus*, *E. faecalis*, and *P. aeruginosa*. In this study, similar activity against these bacteria was also observed, though Ördög et al. (2004) reported higher activity, with inhibition at concentrations as low as 10 $\mu g.mL^{-1}$. This difference could be attributed to the chlorophyll removal step they performed, which may have enhanced the antimicrobial activity. Another study evaluating different extraction solvents observed activity against *S. aureus*, *P. aeruginosa*, and *E. coli* in most *C. emersonii* extracts, assessed via the disk diffusion method (SAWANT; KELKAR MANE, 2018).

Shaima et al. (2022) identified inhibition at concentrations as low as 390 μg.mL^{-1} for *Chlorella* sp. extracts against methicillin-resistant *S. aureus* (MRSA). These authors also noted higher activity at higher concentrations for the microalga *Scenedesmus* sp.

Regarding *Selenastrum bibraianum*, studies on this genus remain scarce. Balouch (2020) observed activity from a related alga, *Monoraphidium* sp., where its methanolic extracts inhibited the growth of *Klebsiella pneumoniae*, a Gram-negative and super-resistant bacteria. Their experiments were performed through the disk diffusion method.

In an effort to reduce the chemical complexity of the extracts, the most bioactive extracts were fractionated. In the case of *S. bibraianum*, the fractions lost their activity, indicating that the observed effect was likely the result from interactions between the various metabolites, possibly working synergistically. However, for *C. emersonii*, the highest activity was found in fractions B and C, suggesting greater activity in less polar compounds. The fractions were exclusively active against Gram-positive microorganisms, which are more sensitive to antimicrobial agents than Gram-negative ones. This increased sensitivity is due to the lack of an outer lipid bilayer, making their cell walls more vulnerable to the entry and action of potentially active compounds (TETTEH; MATTHÄUS; HERNANDEZ-VARGAS, 2020). This results in the fact that Gram-positive bacteria also require lower amounts of the compound to exhibit significant antimicrobial activity (SCHNEIDER, 2021).

Molecular network analysis indicated that most compounds were associated with alkaloid and fatty acid pathways. The alkaloid pathway was likely assigned due to the categorization of most chlorophyll-derived compounds within this pathway. This may be due to the presence of the porphyrin ring, which, because of its structure, can be confused and associated with the alkaloid pathway (LICHMAN, 2021). Fatty acids were frequently associated with antimicrobial activity. Cepas et al. (2019) observed the effect of short-chain and polyunsaturated fatty acids on the inhibition of microbial biofilms. Later, Cepas et al. (2021) isolated the compounds responsible, identifying alpha-linolenic acid (ALA) as the primary agent responsible for antimicrobial activity against *S. aureus* at concentrations as low as 15.6 μg.mL^{-1}. They also noted a synergistic effect between ALA and lysophosphatidylcholine, which enhanced the inhibitory effect on the biofilms of *P. aeruginosa* and *K. pneumoniae*. In the present study, ALA was found in the active fractions,

along with derivative compounds such as monolinolein and ALA-ethanolamide. Although lysophosphatidylcholine was not identified, LysoDGTS 16:4, a structurally similar compound differing only in the presence of a glycerol group, was detected. Hexadecatetraenoic acid (C16:4) derivatives were also associated with antimicrobial activity. In the study by Findlay and Patil (1984), this fatty acid and stearic acid, which were also identified in the active fractions, were linked to antimicrobial activity against *Staphylococcus aureus*, *Staphylococcus epidermidis*, and other bacteria.

The antimicrobial potential of other polyunsaturated fatty acids has also been reported, such as docosahexaenoic acid and eicosapentaenoic acid, which inhibited the growth of periodontopathogenic bacteria at concentrations as low as 12 $\mu g.mL^{-1}$ (SUN et al., 2016). A similar result was found by Desbois et al. (2008), who observed activity not only for eicosapentaenoic acid but also for palmitoleic acid and (6Z, 9Z, 12Z)-hexadecatrienoic acid against the multidrug-resistant *Staphylococcus aureus*. Several authors describe possible metabolic pathways that could lead to the antimicrobial effect of these compounds, including mechanisms that involve DNA synthesis inhibition, cell wall disruption, or interference with bacterial lipid metabolism (CASILLAS-VARGAS et al., 2021).

Regarding the identification of bacteriopheophytin (*m/z* 889.5763 $[M+H]^+$, ppm = 0.20), despite the similar mass, the presence of this molecule is non-existent in eukaryotic microalgae (DEN; MANN; HANS MARTIN JAHNS, 1995). However, even though the fragmentation pattern is similar, other chlorophyll derivatives could generate a similar spectrum, such as 3-phorbinepropanoic acid (*m/z* 889.5843 $[M+H]^+$, ppm = 0.31), among other compounds. However, pheophorbide derivatives have not been reported to exhibit antimicrobial effects unless associated with photodynamic therapy (HA et al., 2023; KUSTOV et al., 2018; PIETROWSKA et al., 2022).

For the last evaluated cluster, although no matches were identified, the compounds were annotated as analogs of 2-naphthalenemethanol, 7-(acetyloxy)decahydro-alpha,alpha,4a-trimethyl-8-methylene, and Canangalia H. These compounds were classified as terpenoids, and the nodes were also classified as terpenoids according to the MS2Query annotation. Many terpenoids are known for their antimicrobial activity, often acting by disrupting the cell membrane, similar to the mechanisms observed for lipids (GUIMARÃES et al., 2019; YAMAGUCHI, 2022).

6. Conclusion

We conclude that 2 out of the 26 eukaryotic microalgae evaluated exhibited antimicrobial activity. Further fractionation confirmed activity only in *C. emersonii*, which demonstrated promising activity in two fractions of the 01 extract. These fractions were found to be rich in polyunsaturated lipids and their derived metabolites. This study highlights the promising potential of the lipids present in *C. emersonii*, warranting further investigation to deepen our understanding of its antimicrobial potential and to identify the key metabolites associated with this activity.

7. References

BALOUCH, H. Isolation, identification, and antimicrobial activity of psychrophilic freshwater microalgae Monoraphidium sp. from Almaty region. **International Journal of Biology and Chemistry**, v. 13, n. 1, p. 14–23, 15 ago. 2020.

BARBOSA, M. J. et al. Hypes, hopes, and the way forward for microalgal biotechnology. **Trends in Biotechnology**, v. 41, n. 3, p. 452–471, mar. 2023.

CASILLAS-VARGAS, G. et al. Antibacterial fatty acids: An update of possible mechanisms of action and implications in the development of the next-generation of antibacterial agents. **Progress in Lipid Research**, v. 82, p. 101093, abr. 2021.

CEPAS, V. et al. Inhibition of Bacterial and Fungal Biofilm Formation by 675 Extracts from Microalgae and Cyanobacteria. **Antibiotics**, v. 8, n. 2, p. 77, 12 jun. 2019.

COCKERILL, F. R. et al. Methods for Dilution Antimicrobial Susceptibility Tests for Bacteria That Grow Aerobically ; Approved Standard — Ninth Edition. **Methods for Dilution Antimicrobial Susceptibility Tests for Bacteria That Grow Aerobically; Approved Standar-Ninth Edition**, v. 32, n. 2, p. 18, 2012.

DANTAS, D. M. DE M. et al. Evaluation of antioxidant and antibacterial capacity of green microalgae Scenedesmus subspicatus. **Food Science and Technology International**, v. 25, n. 4, p. 318–326, 2019.

DE SOUZA, M. P. et al. Potential of microalgal bioproducts: general perspectives and main challenges. **Waste and Biomass Valorization**, v. 10, n. 8, p. 2139–2156, 8 ago. 2019.

DEN, V.; MANN, D. G.; HANS MARTIN JAHNS. **Algae. (Algen). An introduction to phycology.** Cambridge - New York - Oakleigh: Cambridge Univ. P, 1995.

DESBOIS, A. P. et al. Isolation and structural characterisation of two antibacterial free fatty acids from the marine diatom, Phaeodactylum tricornutum. **Applied Microbiology and Biotechnology**, v. 81, n. 4, p. 755–764, 1 dez. 2008.

FERREIRA, L. et al. Uncovering the Bioactive Potential of a Cyanobacterial Natural Products Library Aided by Untargeted Metabolomics. **Marine Drugs**, v. 19, n. 11, p. 633, 12 nov. 2021.

FINDLAY, J. A.; PATIL, A. D. Antibacterial Constituents of the Diatom Navicula delognei. **Journal of Natural Products**, v. 47, n. 5, p. 815–818, 1 set. 1984.

GUIMARÃES, A. C. et al. Antibacterial Activity of Terpenes and Terpenoids Present in Essential Oils. **Molecules**, v. 24, n. 13, p. 2471, 5 jul. 2019.

HA, N. M. et al. Antimicrobial photodynamic therapy with Ligularia fischeri against methicillin-resistant Staphylococcus aureus infection in Caenorhabditis elegans model. **Applied Biological Chemistry**, v. 66, n. 1, p. 19, 13 mar. 2023.

HUBER, F. et al. Spec2Vec: Improved mass spectral similarity scoring through learning of structural relationships. **PLOS Computational Biology**, v. 17, n. 2, p. e1008724, 16 fev. 2021.

HUTCHINGS, M. I.; TRUMAN, A. W.; WILKINSON, B. Antibiotics: past, present and future. **Current Opinion in Microbiology**, v. 51, p. 72–80, out. 2019.

IBRAHIM, K. et al. Antimicrobial property of water and ethanol extract Chlorella vulgaris: a value-added advantage for a new wound dressing material. **International Medical Journal**, v. 22, n. 5, p. 399–401, 2015.

IMAI, Y. et al. A new antibiotic selectively kills Gram-negative pathogens. **Nature**, v. 576, n. 7787, p. 459–464, 19 dez. 2019.

JAFARI, S. et al. Antibacterial potential of Chlorella vulgaris and Dunaliella salina extracts against Streptococcus mutans. **Jundishapur Journal of Natural Pharmaceutical Products**, v. 13, n. 2, 2018.

KILIC, N. K.; ERDEM, K.; DONMEZ, G. Bioactive Compounds Produced by Dunaliella species, Antimicrobial Effects and Optimization of the Efficiency. **Turkish Journal of Fisheries and Aquatic Sciences**, v. 19, n. 11, p. 923–933, 2019.

KONG, D.-X.; JIANG, Y.-Y.; ZHANG, H.-Y. Marine natural products as sources of novel scaffolds: achievement and concern. **Drug Discovery Today**, v. 15, n. 21–22, p. 884–886, nov. 2010.

KUSTOV, A. V. et al. Synthesis and investigation of water-soluble chlorophyll pigments for antimicrobial photodynamic therapy. **Dyes and Pigments**, v. 149, p. 553–559, fev. 2018.

LICHMAN, B. R. The scaffold-forming steps of plant alkaloid biosynthesis. **Natural Product Reports**, v. 38, n. 1, p. 103–129, 2021.

MAADANE, A. et al. ANTIMICROBIAL ACTIVITY OF MARINE MICROALGAE ISOLATED FROM MOROCCAN COASTLINES. **The Journal of Microbiology, Biotechnology and Food Sciences**, v. 6, n. 6, p. 1257, 2017.

NAGHAVI, M. et al. Global burden of bacterial antimicrobial resistance 1990–2021: a systematic analysis with forecasts to 2050. **The Lancet**, set. 2024.

NEWMAN, D. J.; CRAGG, G. M. Natural Products as Sources of New Drugs over the Nearly Four Decades from 01/1981 to 09/2019. **Journal of Natural Products**, v. 83, n. 3, p. 770–803, 2020.

NOTHIAS, L.-F. et al. Feature-based molecular networking in the GNPS analysis environment. **Nature Methods**, v. 17, n. 9, p. 905–908, 24 set. 2020.

ÖRDÖG, V. et al. Screening microalgae for some potentially useful agricultural and pharmaceutical secondary metabolites. **Journal of applied phycology**, v. 16, n. 4, p. 309–314, 2004.

PATIL, L.; KALIWAL, B. B. Microalga Scenedesmus bajacalifornicus BBKLP-07, a new source of bioactive compounds with in vitro pharmacological applications. **Bioprocess and biosystems engineering**, v. 42, n. 6, p. 979–994, 2019.

PIETROWSKA, A. et al. The Enhancement of Antimicrobial Photodynamic Therapy of Escherichia Coli by a Functionalized Combination of Photosensitizers: In Vitro Examination of Single Cells by Quantitative Phase Imaging. **International Journal of Molecular Sciences**, v. 23, n. 11, p. 6137, 30 maio 2022.

PRATT, R. et al. Chlorellin, an Antibacterial Substance from Chlorella. **Science**, v. 99, n. 2574, p. 351–352, 28 abr. 1944.

PULINGAM, T. et al. Antimicrobial resistance: Prevalence, economic burden, mechanisms of resistance and strategies to overcome. **European Journal of Pharmaceutical Sciences**, v. 170, p. 106103, mar. 2022.

RIBEIRO, I. et al. Diversity and Bioactive Potential of Actinobacteria Isolated from a Coastal Marine Sediment in Northern Portugal. **Microorganisms**, v. 8, n. 11, p. 1691, 30 out. 2020.

RUANE, J.; SONNINO, A.; AGOSTINI, A. Bioenergy and the potential contribution of agricultural biotechnologies in developing countries. **Biomass and Bioenergy**, v. 34, n. 10, p. 1427–1439, 2010.

SAWANT, S. S.; KELKAR MANE, V. NUTRITIONAL PROFILE, ANTIOXIDANT, ANTIMICROBIAL POTENTIAL, AND BIOACTIVES PROFILE OF CHLORELLA EMERSONII KJ725233. **Asian Journal of Pharmaceutical and Clinical Research**, v. 11, n. 3, p. 220, 1 mar. 2018.

SCHMID, R. et al. Integrative analysis of multimodal mass spectrometry data in MZmine 3. **Nature Biotechnology**, v. 41, n. 4, p. 447–449, 1 abr. 2023.

SCHNEIDER, Y. K. Bacterial Natural Product Drug Discovery for New Antibiotics: Strategies for Tackling the Problem of Antibiotic Resistance by Efficient Bioprospecting. **Antibiotics**, v. 10, n. 7, p. 842, 10 jul. 2021.

SHAIMA, A. F. et al. Unveiling antimicrobial activity of microalgae Chlorella sorokiniana (UKM2), Chlorella sp. (UKM8) and Scenedesmus sp. (UKM9). **Saudi Journal of Biological Sciences**, v. 29, n. 2, p. 1043–1052, 2022.

SHUKLA, R. et al. An antibiotic from an uncultured bacterium binds to an immutable target. **Cell**, v. 186, n. 19, p. 4059- 4073.e27, set. 2023.

SILVA, M. et al. Microalgae as Potential Sources of Bioactive Compounds for Functional Foods and Pharmaceuticals. **Applied Sciences (Switzerland)**, v. 12, n. 12, 1 jun. 2022.

SUN, M. et al. Antibacterial and antibiofilm activities of docosahexaenoic acid (DHA) and eicosapentaenoic acid (EPA) against periodontopathic bacteria. **Microbial Pathogenesis**, v. 99, p. 196–203, out. 2016.

TETTEH, J. N. A.; MATTHÄUS, F.; HERNANDEZ-VARGAS, E. A. A survey of within-host and between-hosts modelling for antibiotic resistance. **Biosystems**, v. 196, p. 104182, out. 2020.

WANG, M. et al. Sharing and community curation of mass spectrometry data with Global Natural Products Social Molecular Networking. **Nature Biotechnology**, v. 34, n. 8, p. 828–837, 9 ago. 2016.

WIKLER, M. A. Methods for dilution antimicrobial susceptibility tests for bacteria that grow aerobically: approved standard. **Clsi (Nccls)**, v. 26, p. M7--A7, 2006.

WORLD HEALTH ORGANIZATION. **Ten threats to global health in 2019**. Disponível em: <https://www.who.int/news-room/spotlight/ten-threats-to-global-health-in-2019>.

YAMAGUCHI, T. Antibacterial effect of the combination of terpenoids. **Archives of Microbiology**, v. 204, n. 8, p. 520, 25 ago. 2022.

Chapter 3 - Novel anti obesity effects of eukaryotic microalgae: lipid reducing, appetite suppressant and anti-inflammatory activity.

Abstract

Obesity is a disease characterized by the excessive accumulation of fat, with a body mass index (BMI) exceeding 30. Pharmacological therapy can be an effective approach for the treatment and nature offers a source of inspiration for the development of new drugs. Natural resources present an interesting potential for novel bioactivities, in particular microalgae due to the limited exploration of their chemical diversity. In this context, the objective of this study was to identify bioactivities from Dichloromethane (DCM) and Methanol (MeOH) extracts of freshwater microalgae for lipid and appetite reduction, as well as anti-inflammatory. A total of 26 different species of eukaryotic microalgae, encompassing 4 distinct phyla and 16 different genera, were evaluated. The dry biomass was extracted using two solvents: DCM:MeOH (1:1) and MeOH. The lipid-reducing capacity and appetite inhibition were assessed using zebrafish embryos, while the anti-inflammatory activity and cytotoxicity of the extracts were analyzed in cellular cultures. For the extracts, no toxicity or malformations were observed in zebrafish, in agreement with the absence of cytotoxicity in cellular assays. Six extracts exhibited lipid-reducing activity, with reductions exceeding 40%. These extracts were fractionated, and fraction C of *S. bibraianum* showed the highest activity, achieving a 50% reduction in lipid content. Metabolite profiling identified potential metabolites strongly associated with bioactivity, such as chlorophyll derivatives, including pheophorbide a and chlorin. Chlorophyll derivatives have been reported in the literature as potential lipid reducers and possess anti-obesity properties. For appetite inhibition, three microalgae stood out, showing more than 50% reduction in food intake, with fraction D of Dictyosphaerium sp. achieving a 70% reduction. Metabolomic analysis reported the presence of polar lipids, mainly fatty acids associated with ethanolamine and phosphocholine, which could be strongly linked to the observed biological activity. Ethanolamine has also been reported as an appetite-reducing compound. For anti-inflammatory activity, three microalgae had more than 40% of activity, and after the fractionation the C fraction of *Dictyosphaerium* sp. demonstrated a 95% reduction in inflammation. Metabolomic analysis indicated compounds strongly associated with this activity, such as 10-methyl-hydroxyphaeophorbide and sulfoquinovosyldiacylglycerol (SQGD) (16:0/18:3), both of which have been reported in the literature with anti-inflammatory properties.

Thus, potential candidates for new compounds with lipid-reducing, appetite-inhibiting, and anti-inflammatory activities were identified. *S. bibraianum* and *Dictyosphaerium* sp. emerged as promising new sources for further studies aimed at isolating and characterizing the metabolites responsible for these activities. This work highlights the unexplored potential of eukaryotic microalgae as a source of new compounds for the treatment of chronic diseases.

Keywords: Zebrafish, Chlorophyll derivates, *S. bibraianum*, *Dictyosphaerium* sp.

1. Introduction

Obesity is a medical condition characterized by excessive accumulation of fat that can adversely affect health. It is defined as having a body mass index (BMI) greater than thirty (WHO, 2021). The prevalence of obesity has been on the rise globally, with about 12.5% of the world's population classified as obese in 2015, which is 80% higher than in 1980 (CHOOI; DING; MAGKOS, 2019). In Brazil, the proportion of obesity is higher than the global average, with 20% of the population classified as obese and 55% as overweight (MINISTÉRIO DA SAÚDE, 2018). It is estimated that by 2030, there will be at least one billion people with obesity (LOBSTEIN; BRINSDEN; NEVEUX, 2022). One of the most common comorbidities associated with obesity is metabolic syndrome, a condition that increases the risk of developing several other health complications such as chronic inflammation, insulin resistance, hepatic steatosis, and cancer (ROCHLANI et al., 2017).

The regulation of appetite plays a central role in the development and persistence of obesity. The appetite reduction system is linked to several complex hormonal and environmental mechanisms that control hunger and satiety (KUCKUCK et al., 2023). Alterations in these processes can lead to changes in energy balance, stimulating food consumption and worsening obesity (FARHADIPOUR; DEPOORTERE, 2021). Additionally, the increase in fat levels leads to chronic inflammatory processes, contributing to what is known as metabolic syndrome (ELLULU et al., 2017).

Measures to prevent and combat obesity and related diseases include regular physical exercise, a balanced diet, and treatment options such as drug therapy and bariatric surgery (CASTRO et al., 2016). However, drug therapies can cause considerable adverse effects, such as hyperthermia, agranulocytosis, heart problems, and neurotoxicity (SRIVASTAVA; APOVIAN, 2018). Therefore, there is a growing tendency in the pharmaceutical industry to search for new substances of natural origin with fewer adverse effects. Newman and Cragg (2020) compiled a list of drugs approved for use by the FDA, which revealed that natural products, specifically molecules of low molecular weight, make up a third of the drugs approved today. Additionally, 64% of all medicines released for human use between 1981 and 2019 are derived from or inspired by natural products, including synthetic molecules. For obesity, new compounds such as semaglutide and

liraglutide, agonists of the GLP-1 receptor, were initially discovered for diabetes treatment, but they were quickly found to have appetite-suppressing and anti-obesity effects (BLUNDELL et al., 2017; KNUDSEN; LAU, 2019)

According to the review by Castro et al. (2016) natural products with anti-obesity activity are mostly derived from plants, followed by seaweeds. Although fewer bioactive compounds are known from microalgae, these organisms may be a promising source of biomolecules that have yet to be explored. Olaizola (2003) observed few microalgal biomolecules compared to other organisms, due to the under exploitation of the diversity of microalgae worldwide. Estimates suggest that there may be up to 800,000 species of microalgae, with only 40,000 to 50,000 recorded. Therefore, exploring this biodiversity is an important step in finding and developing new pharmaceuticals and/or nutraceuticals (MORANÇAIS; MOUGET; DUMAY, 2018).

Several studies have highlighted the potential of microalgae for addressing obesity, appetite suppression, and anti-inflammatory effects, whether through the ingestion of dried powder, extracts, or derived compounds. Zeinalian et al. (2017) observed that a daily supplementation of 1g of *Arthrospira platensis* in humans promoted appetite suppression, weight loss, and a decrease in total serum cholesterol levels. Another study, using a daily supplementation of 500 mg of *Arthrospira platensis* in humans, reported reductions in body weight, body fat, and triglyceride levels(YOUSEFI; MOTTAGHI; SAIDPOUR, 2018). Regarding eukaryotic microalgae, few trials have been conducted in humans, but promising results have been observed in cellular and animal models. In male mice, dietary supplementation with *Euglena gracilis* biomass reduced visceral fat levels and improved inflammation markers (SAKANOI et al., 2018). For *Chlorella* sp., the ingestion of polyunsaturated lipids by mice led to reductions in body weight, fat, and blood sugar levels (YANG et al., 2022).

2. Objectives

Screening of 52 extracts from 26 microalgae species for their lipid reduction, appetite suppressing and anti-inflammatory activities. Furthermore, identify some of the bioactive compounds from those extracts of tropical freshwater microalgae.

3. Material and Methods

3.1. Cultivation of algae and preparation of extracts

The cultivation and extract preparation followed the same protocol as described in chapter 2 topics 3.1 and 3.2. After drying, the extracts were resuspended in DMSO at a concentration of 1 $mg.mL^{-1}$. The identification codes for the extracts and algae are described in Chapter 2, Table 2.

3.2. Automated fractionation by HPLC

The extracts that showed promising activity were fractionated using RP-HPLC with a Waters Alliance e2695 Separations Module. The fractionation protocol was carried out as described in chapter 2, topic 3.5. After drying, the fractions were dissolved in DMSO to a concentration of 10 $mg.mL^{-1}$.

3.3. Zebrafish larvae preparation

Lipid-reducing and appetite assays were conducted on zebrafish (*Danio rerio*) embryos. Adult male and female zebrafish were placed in a reproduction chamber under appropriate light conditions to stimulate female ovulation. Up to Six hours post-fertilization, the eggs were collected and maintained in artificial sea salt medium. The eggs were cleaned, and viable ones were separated and transferred to petri dishes containing E3 media, supplemented with methylene blue (1 mg.L-1) as a fungicide. The eggs were incubated at 28°C throughout the incubation and development periods. On the first day post-fertilization (1 DPF), the media was replaced and supplemented with 1-phenyl-2-thiourea (PTU) to suppress pigmentation. (URBATZKA et al., 2018). For these trials, approval by an ethics committee was not required as they were not considered animal testing in accordance with EU directive 86/609/EEC for animal experimentation considering the legislation of Portugal, where this chapter was developed.

3.4. Lipid-reducing assay

On the third day post-fertilization (3 DPF), zebrafish embryos were transferred to a 96-well plate, with 3 embryos per well in E3 media. For the exposure, 2 µL of 1 $mg.mL^{-1}$ extract was added to 200 µL of E3 media, resulting in a final concentration of 10 $\mu g.mL^{-1}$. As a negative control, 0.1%

DMSO was used, and resveratrol at 50 µM was used as a positive control. On the fourth day post-fertilization (4 DPF), neutral lipid staining was performed by adding 5 µL of a 500 $ng.mL^{-1}$ Nile Red solution, resulting in a final concentration of 10 $ng.mL^{-1}$ for 15 hours. Finally, on the fifth day post-fertilization (5 DPF), the media was replaced with fresh E3 media, and the embryos were anesthetized with 0.03% tricaine (MS–222, Sigma-Aldrich). Images of the stained zebrafish embryos were captured using a digital microscope plate reader (BioTek Cytation 5, Agilent, USA) with an excitation wavelength of 552 nm and emission at 636 nm. The images were then analyzed using ImageJ software (ImageJ©1.53a) to quantify the mean fluorescence per area. The zone labeled by the fluorescent dye was selected in the software, and the mean fluorescence intensity within the labeled area was recorded (REGUEIRAS et al., 2021). The assay was made in triplicate in two independent assays totalizing 6 biological replicates (n = 6).

3.5. Appetite inhibition assay

For the appetite assay, fish at 6 DPF were transferred to a 96-well plate and exposed to the extracts under the same conditions as the lipid-reducing assay. Fluoxetine (Fluo) at 10 µM was used as a positive control, and 0.1% DMSO as a negative control. After 24 hours, the medium containing the extract was replaced with a 0.62% liposome solution. This solution was prepared by dissolving 1 mL of egg yolk in 19 mL of E3 medium, followed by filtration through a 55-mesh filter. The solution was then sonicated using a probe sonicator for 25 cycles (each cycle consisting of a 25W pulse for 1 second followed by 5 seconds of rest). The egg liposome was stained with BODIPY at a final concentration of 6.4 µM, and diluted eight times with E3 media. This solution replaced the medium for 2 hours to allow the larvae to feed. After feeding, the wells were washed with E3 media until the liposomes were completely removed. The larvae were anesthetized, and the readings were taken using a fluorescence microplate reader (BioTek, Cytation 5) with excitation at 475 nm and emission at 509 nm. The quantification of stained liposomes in the zebrafish intestine was performed using the ImageJ protocol. The assay was carried out in triplicate across two independent experiments, totaling six biological replicates (n = 6). This assay was based on protocols described by (WEE et al., 2019).

3.6. Cellular toxicity

The cellular toxicity was made using HepG2 (human hepatoma-derived) cells cultured in modified Dulbecco's Eagle's medium (DMEM) supplemented with fetal bovine serum and the addition of penicillin and streptomycin (1% v/v). The cell cultures were maintained at 37 ºC in a humidified atmosphere containing 5% CO_2.

The HepG2 were seeded in a 96-well microtiter plate at a concentration of 3.3×10^4 cell.mL-1 with 200 µL per well. After 24 hours, the cells were exposed to the extracts at a concentration of 25 $\mu g.mL^{-1}$ and incubated for 48 hours in a CO_2 incubator. After this period, 40 µL of a solution of MTT (3-(4,5-dimethylthiazol-2-yl)-2,5-diphenyltetrazolium bromide) at 1 $mg.mL^{-1}$ in phosphate-buffered saline was added. The plate was again incubated for 4 hours. After this period and visualization of crystal formation, the medium was replaced by 200 µL of DMSO and the plate was shaken for 10 minutes. The reading was performed in microplate reader at 570 nm (GREEN; READE; WARE, 1984).

3.7. Anti-inflammatory assay

The anti-inflammatory activity was made using RAW 264.7 (murine macrophage cell line) cultured in DMEM in the same condition as HepG2 cells. The production of nitric oxide (NO) was quantified in macrophages after stimulation with lipopolysaccharide (LPS). The cell culture, pre-incubated with the extracts at 25 $\mu g.mL^{-1}$ for 2 hours, had the addition of LPS at a final concentration of 1 $\mu g.mL^{-1}$ and was incubated for 22 hours. The supernatant from the cultures was collected, and the same volume of Griess reagent (1% sulfanilamide and 0.1% N-(1-naphthyl) ethylenediamine in 2% H_3PO_4) was added and incubated for 10 minutes. Subsequently, it was read at 562 nm (Agilent BioTek Cytation 5). Controls were conducted using cultures with DMSO and cultures with/without LPS stimulation. The activity was calculated by the ratio between the sample absorbance and the control absorbance, and normalized by the control and the result was expressed as a percentage of NO production (%NO) (BARBOSA et al., 2017).

The cytotoxicity of the fractions also was monitored through the 3-(4,5-dimethylthiazole-2-yl)-2,5-diphenyltetrazolium bromide (MTT) assay. The MTT solution was freshly prepared at 0.5 $mg.mL^{-1}$, in DMEM media. Them after collection of supernatant 100 uL of MTT solution was

added in each week and incubated at 37 ºC for 45 min. The viable cell´s will reduce the MTT reagent and generate insoluble crystals, after the incubation the supernatant was removed, and the crystals were dissolved in 100 uL DMSO and shaken for 10 min. The absorbance was read in 515 nm and expressed as percentage of cell viably in comparison to the solvent control. Both assays were made in triplicate in two independent assay totalizing 6 replicates.

3.8. Metabolite profiling

The fractions which demonstrated activity were dried and resuspended in methanol at a concentration of 1 $mg.mL^{-1}$ and analyzed using liquid chromatography-high resolution electrospray ionization tandem mass spectrometry (LC-HRESIMS/MS). The system was a Dionex Ultimate 3000 HPLC, connected to a qExactive focus mass spectrometer, controlled by XCalibur 4.1 software (Thermo Fisher Scientific, Waltham, MA, USA). The Chromatographic separation was performed using an ACE UltraCore 2.5 Super C18 column (75 mm × 2.1 mm). Was used two mobile phase, mobile phase A: mixture 95% water, 5% methanol, 0.1% formic acid and mobile phase B was 95% isopropanol, 5% methanol, 0.1% formic acid. 10 uL of each fraction was injected and the separation gradient, detection and MS parameter was described by Ribeiro et al., (2020)

The Raw data obtained were converted to mzML format using the software MSConvert using Global Natural Products Social Molecular Networking (GNPS) recommended parameters (WANG et al., 2016). For feature based molecular networking the feature quantification table was obtained using a software MZmine 3, The Batch Mode code used as parameters is described in appendix 1. (SCHMID et al., 2023). The feature based molecular networking workflow were used to generate the molecular networking for all fractions of each extract (NOTHIAS et al., 2020). The parameters used are described in appendix 3 with the link to access all molecular networks described in this work. To enhance chemical structural information within the molecular network, information from in silico structure annotations from GNPS Library Search, Network Annotation Propagation were incorporated into the network using the GNPS MolNetEnhancer workflow (https://ccms-ucsd.github.io/GNPSDocumentation/molnetenhancer/). The correlation with the bioactivity was made using the protocol described by Nothias et al. (2018) to obtain a bioactive based molecular networking.

For the dereplication step, Cytoscape 3.10.0 (SHANNON et al., 2003) was used, highlighting the nodes with significant correlation (Correlation > 0.63 and p-value < 0.05) and prioritize the nodes with the highest correlation. The *m/z* of high correlations nodes were manually checked in the Xcalibur software (version 4.1, Thermo Scientific Exactive Series 2.9) and searched for isotopes and Na^+ adducts. The annotated compounds was checked by GNPS database and search the exact mass (±0.005 *m/z* and a deviation of <5 ppm) in Dictionary of Marine Natural Products database (https://dmnp.chemnetbase.com/) and Natural Products Atlas (VAN SANTEN et al., 2019).

4. Results

4.1. Lipid-reducing assay

The reduction of lipid accumulation was evaluated in Zebrafish embryos. The figure 1 shows the differences between the DMSO and the positive control, REV, evidencing the reduction of neutral lipids in the yolk sac/intestine region.

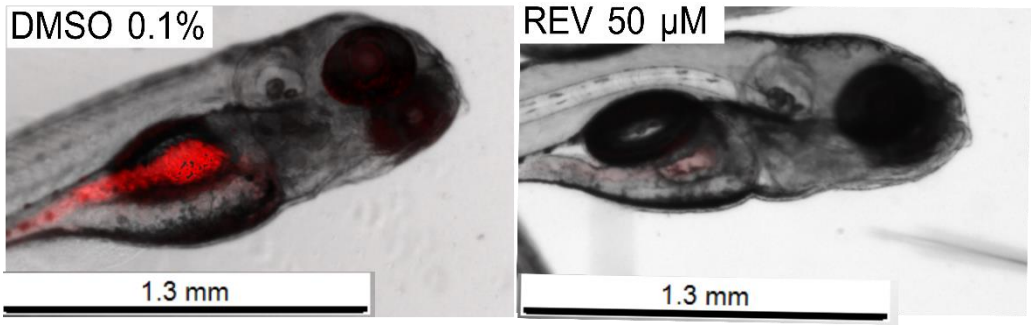

Figure 1. The lipid-reducing Nile Red assay. The difference between DMSO 0.1%, negative control and Rev 50 µM, positive control.

Out of the fifty-two tested extracts, 6 showed more than 40% lipid-reducing activity, namely the DCM:MeOH extracts from the microalgae *Chlorella emersonii*, *Chlorobium braunii*, *Ophiocytium* sp., *Radiococcus* sp., *Selenastrum bibraianum* and the MeOH extract from the microalga *Westella botryoides* (fig.2).

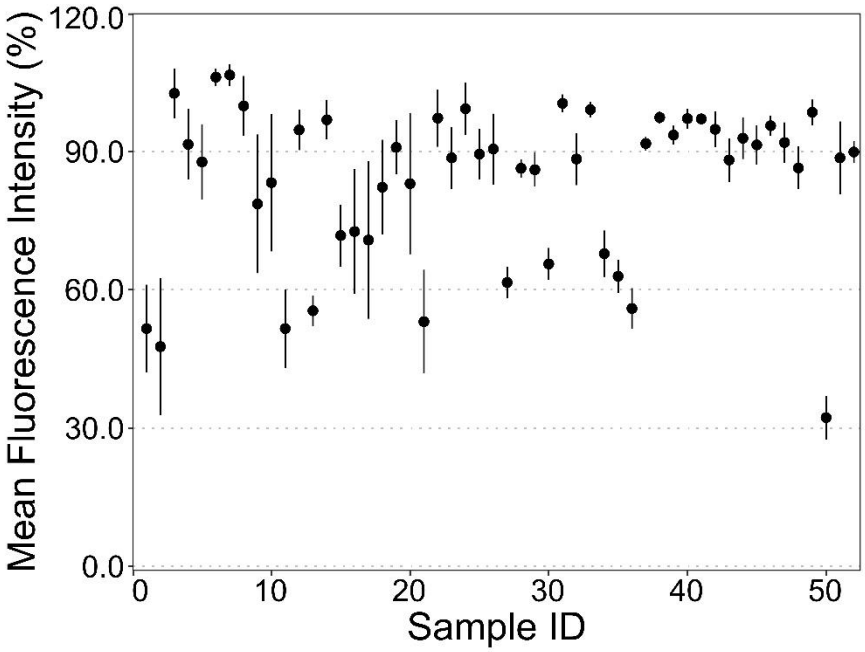

Figure 2. Screening of 52 microalgae extracts for Nile-red lipid reducing assay. Data are presented as mean fluorescence activity relative to the solvent control. The node shows the mean value, and the line the variation between individuals (n=6).

The next step for the selected algae was to confirm the activity and determine the effective concentration at 50% (EC_{50}) of the fluorescence. This assay was performed with extracts at varying concentrations from 1.25 to 20.0 $\mu g.mL^{-1}$. The EC_{50} values for the algae were calculated using non-linear regressions in the GraphPad Prism software, and these values are expressed in table 1. The dose response curves for the EC_{50} assays are attached in the appendix 4.

Table 1. EC_{50} values for the 8 selected algae with lipid-reducing activity.

Microalgae	EC_{50} (µg.mL^{-1})
Selenastrum bibraianum	9.48
Chlorella emersonii	19.76
Westella botryoides	21.41
Radiococcus sp.	25.10
Chlorobium braunii	26.78
Ophiocytium sp.	986.8

Due to the biological variations expected in zebrafish embryos, all assays were performed for at least two independent experiments. Of the six selected algae, only *Ophiocytium* sp. showed almost no activity, while the strongest activity was observed for the microalgae *Selenastrum bibraianum* with an EC_{50} of 9.58 µg.mL^{-1}. The remaining algae had EC_{50} values around 20 µg.mL^{-1}. Then, the algae with the five lowest EC_{50} values were selected and fractionated. Lipid reduction was then analyzed for each of the fractions and the results are shown in figure 3.

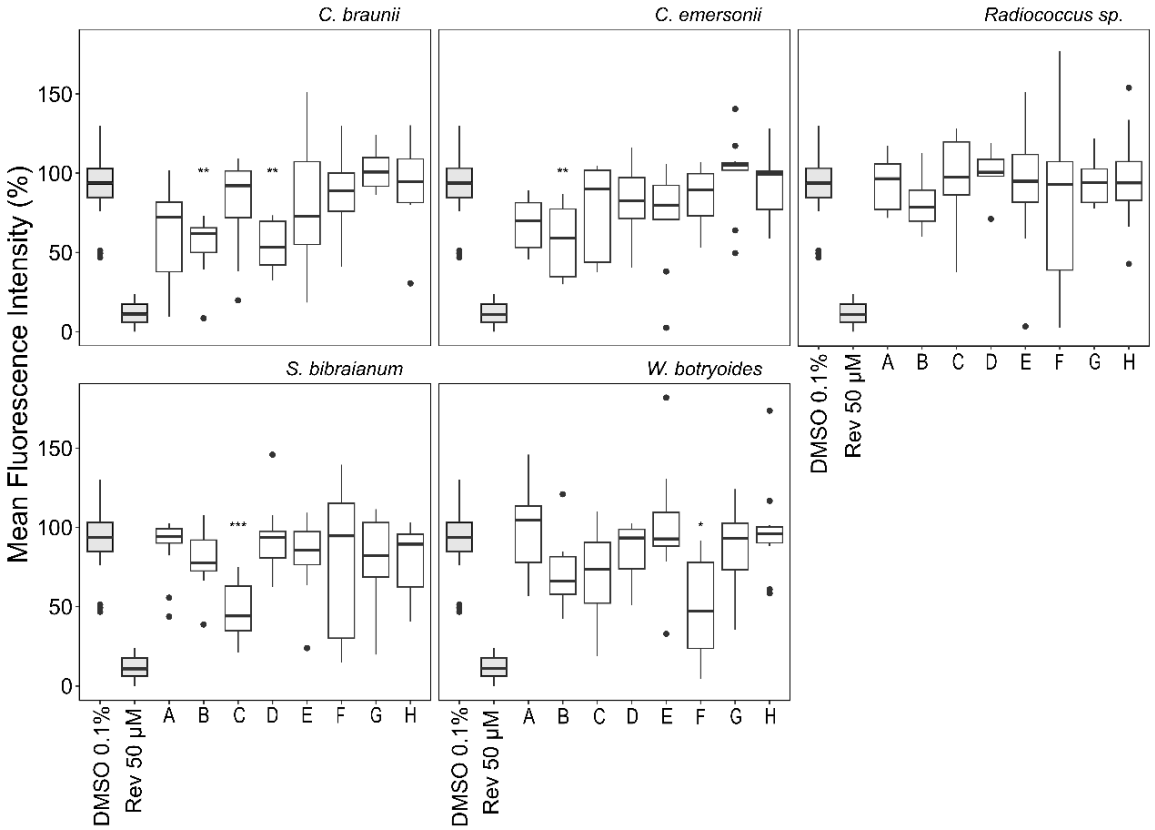

Figure 3. Lipid-reducing activity for the five fractionations of each of the six algae. Data are presented as mean fluorescence activity relative to the solvent control (DMSO 0.1%). Resveratrol 50 µM (Rev 50µM) was used as positive control. The box-and-whisker plots (5–95 percentile) represent the variation between the tests performed (n = 6). The dots represent outliers and were not considered for statistical analysis. Asterisks indicate statistically significant results (*p-value < 0.05; **p-value < 0.01; ***p-value < 0.001).

Most of the bioactivity was detected in fractions B and D, except for *W. botryoides*, whose activity was in fraction F. The fractionation process elutes low polarity compounds first, going toward high polarity compounds at the end, suggesting that active fractions have intermediate to lower polarity compounds. The highest activity was observed in *S. bibraianum* fraction C (p-value < 0.001). Subsequently, the *S. bibraianum* fractions were analyzed by LC-MS/MS, followed by bioactivity-based molecular networking that revealed highly correlated metabolites. Fig. 4 and 5 show the molecular networking for fractions A to H of *S. bibraianum* extracts. Figure 5 highlights

the main clusters. The visible nodes represent compounds that exhibited significant correlation (p-value < 0.05 or Cor > 0.63).

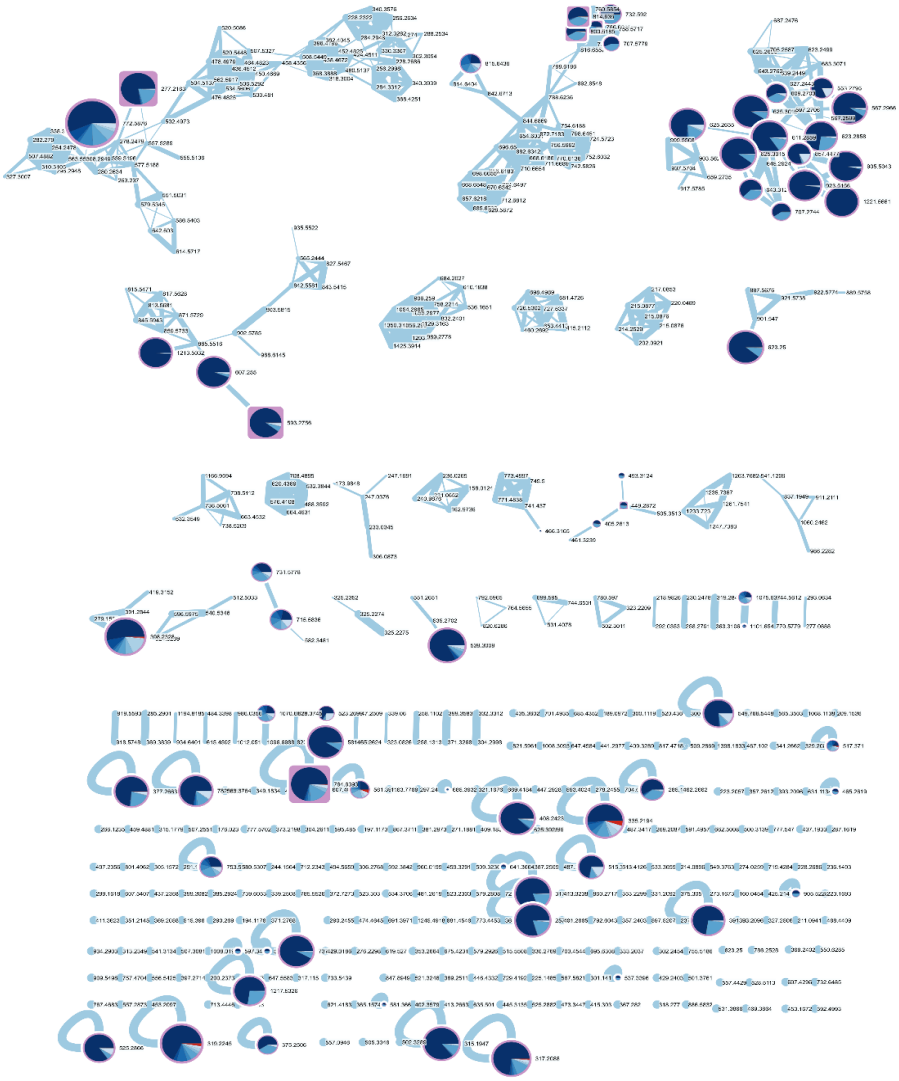

Figure 4. Molecular networks observed for fractions of the *S. bibraianum* extract. The nodes represent molecules observed in each fraction with their respective molecular mass indicated. The shape of the node indicates the compounds that have been identified in the GNPS database (squares) and that have not been identified (circle). The pie chart at each node represents the relative abundance in each fraction, with each color represents a fraction. The darker colors represent the greater the biological activity observed in fraction. The graph only shows nodes with significant correlation (p-value <0.05 or Cor>0.63) with bioactivity. The size of the circle is proportional to the correlation with bioactivity. The diameter of the lines connecting the nodes represent the similarity between the nodes, the larger the line the greater the correlation between nodes (0.7 to 1).

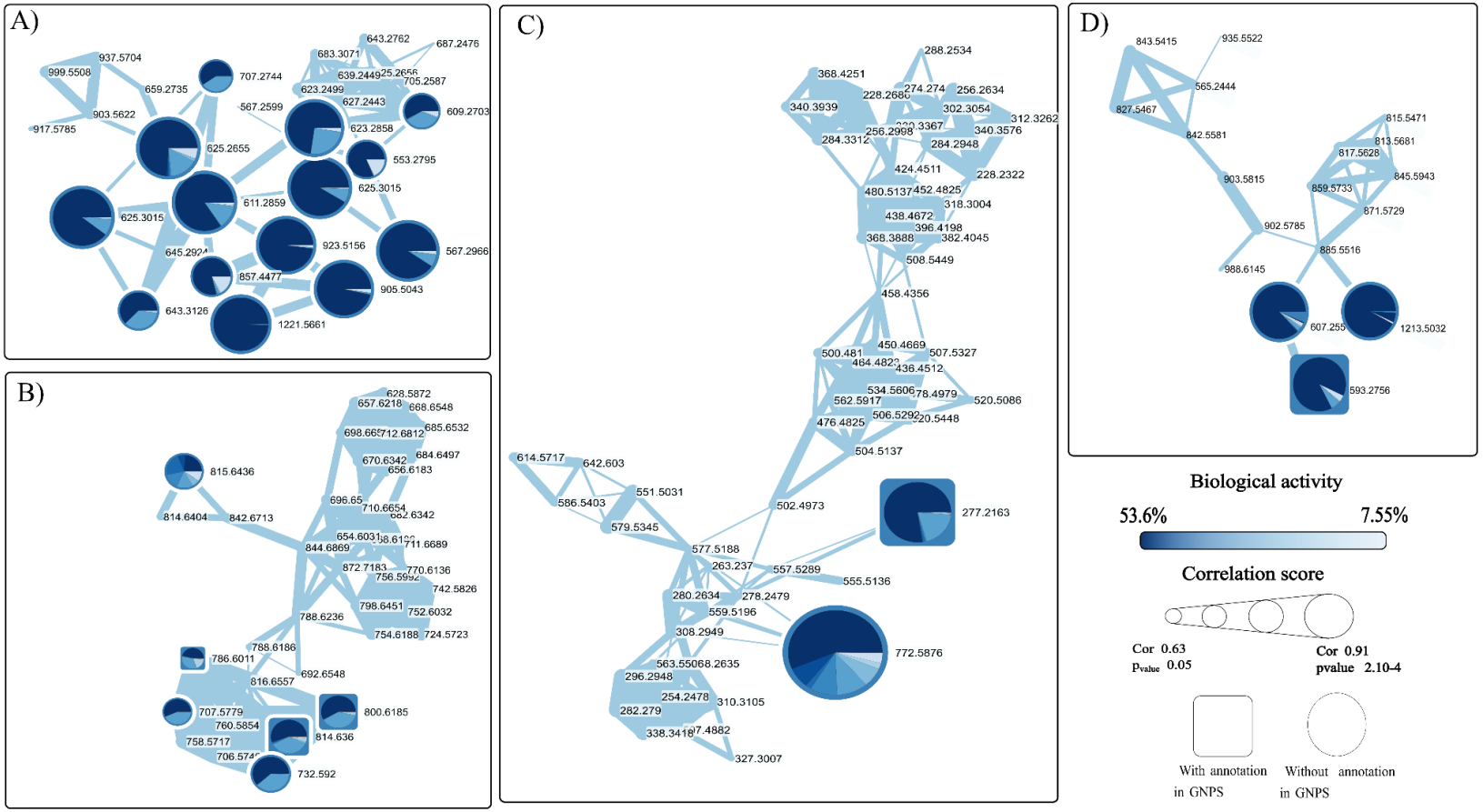

Figure 5a-d. Main molecular networks observed for lipid-reducing activity of the fractions of microalgae *S. bibraianum*. The nodes represent molecules observed in each fraction with their respective molecular mass indicated. The shape of the node indicates the compounds that have been identified in the GNPS database (squares) and that have not been identified (circle). The pie chart at each node represents the relative abundance in each fraction, with each color represents a fraction. The darker colors represent the greater the biological activity observed in fraction. The graph only shows nodes with significant correlation (p-value <0.05 or Cor>0.63) with bioactivity. The size of the circle is proportional to the correlation with bioactivity. The diameter of the lines connecting the nodes represent the similarity between the nodes, the larger the line the greater the correlation between nodes (0.7 to 1).

In the molecular network, 69 nodes out of 520 showed a significant correlation with lipid-reducing activity. Among these 69 nodes, 10 exhibited a strong correlation (Cor > 0.85). Among the observed clusters, the one with the highest number of nodes showing a strong correlation was the Figure 5A. No MS^2 annotation GNPS was observed for this cluster, however, using the analogue identification tool, some analog structures were identified for this network. The analogs indicated that it is a molecular network composed of compounds containing porphyrins. This was later observed by the annotations based on the values of *m/z*, compared with the NPA and DMNP database. Although the other clusters did not yield a substantial number of nodes with a strong correlation, it is possible to observe some groups of interesting compounds. The Figure 5D, according to the annotation provided by GNPS, three compounds were annotated as Pyropheophytin a (*m/z* 813.5681 $[M+H]^+$).), Pheophytin a (*m/z* 871.5729 $[M+H]^+$) and Pheophorbide a (*m/z* 593.2756 $[M+H]^+$), where only Pheophorbide A showed correlation with activity (cor: 0.84). Figure 5C showed compounds annotated as fatty acids and nodes with strong correlations, one of 0.85 that was classified as 13-Hydroxyoctadeca-9,11,15-trienoic acid (*m/z* 277.2163 $[M+H]^+$) and 0.91 that was not classified by the GNPS database, was also not associated with any compound by searching for *m/z* values. Among these nodes, 15 nodes belonging to the highlighted clusters with the highest correlations (0.91-0.80) were selected and putatively identified based on their *m/z* values. Table 2 shows the results obtained for these nodes along with their putative identifications.

Table 2. Putative identification of high correlation compounds indicated by bioactive based molecular networking on figure 5. Identifications were based on GNPS based on MS^2 fragmentation and on *m/z* values with a deviation of 0.005 against the database DMNP and NPA. Only identifications with mass error less than 5 ppm were considered. From the 15 compounds 11 were putatively identified. [M^+]: Observed mass; Rt: retention time (min); Cor: Correlation Score; ppm: Mass error; GNPS: Global Natural Products Social Molecular Networking; DMNP: Dictionary of Marine Natural Products; NPA: Natural product atlas.

[M^+]	Rt (min)	Cor	Putative Identification	ppm	Formula	Source
397.2250	10.13	0.87	Altercrasin D	0.76	$C_{24}H_{31}NO_4$	NPA/ DNP
			Altercrasin E			NPA
			Aspochalasin C; 17,18-Diketone	0.76	$C_{24}H_{31}NO_4$	DNP
538.2931	10.01	0.86	8-hydroxy-22-dehydroxymethylkijanolide	0.00	$C_{32}H_{42}O_7$	NPA/ DNP
293.2117	9.37	0.85	11-Keto-9(E),12(E)-octadecadienoic acid			GNPS
610.2781	9.35	0.85	Bacteriophaeophorbide a	1.60	$C_{35}H_{38}N_4O_6$	DNP
			Biliverdin; Di-Me ester			DNP
			3-Desvinyl-3-(α-hydroxyethyl) phaeophorbide a			DNP
624.2937	10.07	0.85	Asperphenalenone B and A	0.48	$C_{35}H_{44}O_{10}$	DNP
			Chlorin e6 - Di-Me ester	1.60	$C_{36}H_{40}N_4O_6$	NPA
624.2577	10.94	0.85	Cryptophycin - 17 or 19 or 28 or 29 or 49	4.00	$C_{34}H_{41}ClN_2O_7$	NPA/ DNP
566.2888	9.75	0.85	Arugosin P	1.41	$C_{33}H_{42}O_8$	NPA
			Corallistin B	0.88	$C_{34}H_{38}N_4O_4$	DNP

Table 2. Cont. Putative identification of high correlation compounds indicated by bioactive based molecular networking on figure 5. Identifications were based on GNPS based on MS^2 fragmentation and on *m/z* values with a deviation of 0.005 against the database DMNP and NPA. Only identifications with mass error less than 5 ppm were considered. From the 15 compounds 11 were putatively identified. [M^+]: Observed mass; Rt: retention time (min); Cor: Correlation Score; ppm: Mass error; GNPS: Global Natural Products Social Molecular Networking; DMNP: Dictionary of Marine Natural Products; NPA: Natural product atlas.

[M^+]	Rt (min)	Cor	Putative Identification	ppm	Formula	Source
606.2472	9.64	0.84	Microulin B;	1.15	$C_{34}H_{38}O_{10}$	DNP
			Pheophorbide b	0.99	$C_{35}H_{34}N_4O_6$	DNP
592.2678	11.25	0.84	Pheophorbide a	1.35	$C_{35}H_{36}N_4O_5$	GNPS
904.4965	11.72	0.84	Protochlorophyllide b; Phytyl ester	2.65	$C_{55}H_{68}MgN_4O_6$	DNP
622.2780	11.56	0.84	Methyl (10S)-hydroxypheophorbide a	1.77	$C_{36}H_{38}N_4O_6$	DNP
771.5798	12.57	0.91	-	-	-	-
610.7831	9.25	0.84	-	-	-	-
922.5078	11.41	0.84	-	-	-	-
856.4399	11.99	0.80	-	-	-	-

4.2. Appetite inhibition

In the appetite inhibition assay with zebrafish embryos, 52 extracts were screened, and Figure 6 show the difference between Control and Fluoxetin. Highlighting the difference between the controls.

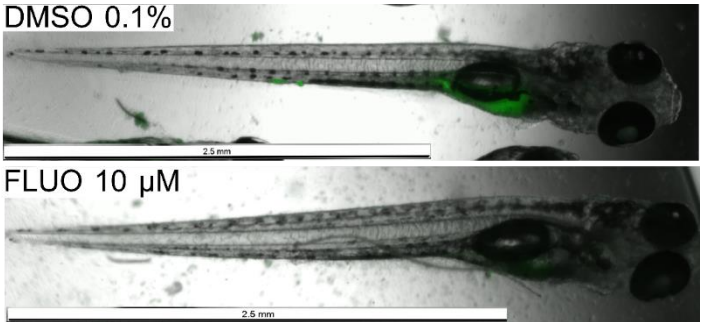

Figure 6. Zebrafish embryos in the appetite inhibition assay. Green fluorescence signal is derived from the intake of labelled liposomes. The difference between DMSO 0.1%, negative control and Fluoxetine (Fluo) 10 µM, positive control.

Figure 7 represents the distribution of appetite inhibition obtained from all examined 52 extracts. However, only the methanolic extracts (27 – 52) revealed bioactivity. The algae that showed more than 50% of appetite reduction were *C. obovata* (80.8% inhibition), *M. arcuatum* (67.0% inhibition), and *Dictyosphaerium* sp. (56.6% inhibition).

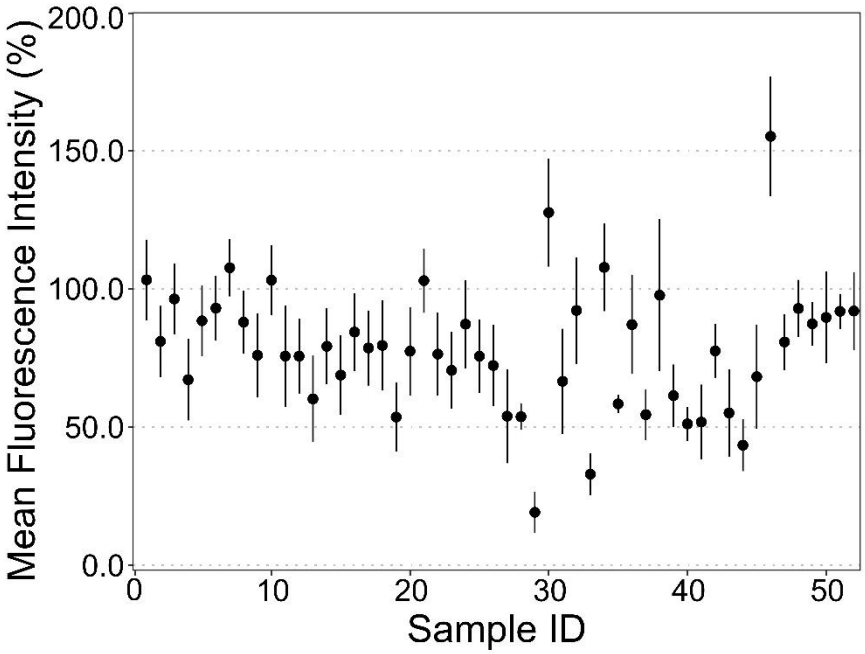

Figure 7. Screening of 52 microalgae extracts for appetite inhibition assay. Data are presented as mean fluorescence activity relative to the solvent control. The node shows the mean value, and the line the variation between individuals (n=6).

The effective concentration that reduced by 50% the fluorescence (EC_{50}) was evaluated using extracts concentrations between 2 and 50 µg.mL^{-1}. These results are shown in Table 3. The dose response curves for the EC_{50} assays are shown in appendix 5.

Table 3. EC_{50} for the 4 selected algae with appetite inhibition assay.

Microalgae	EC_{50} (µg. mL^{-1})
Dictyosphaerium sp.	10.32
M. arcuatum	25.25
C. obovata	39.88

The lowest EC_{50} value for appetite reduction was observed for the microalgae *Dictyosphaerium* sp. All three microalgae were selected for extracts fractionation and again for reassessment of the biological activity of the fractions. These results are shown in figure 8.

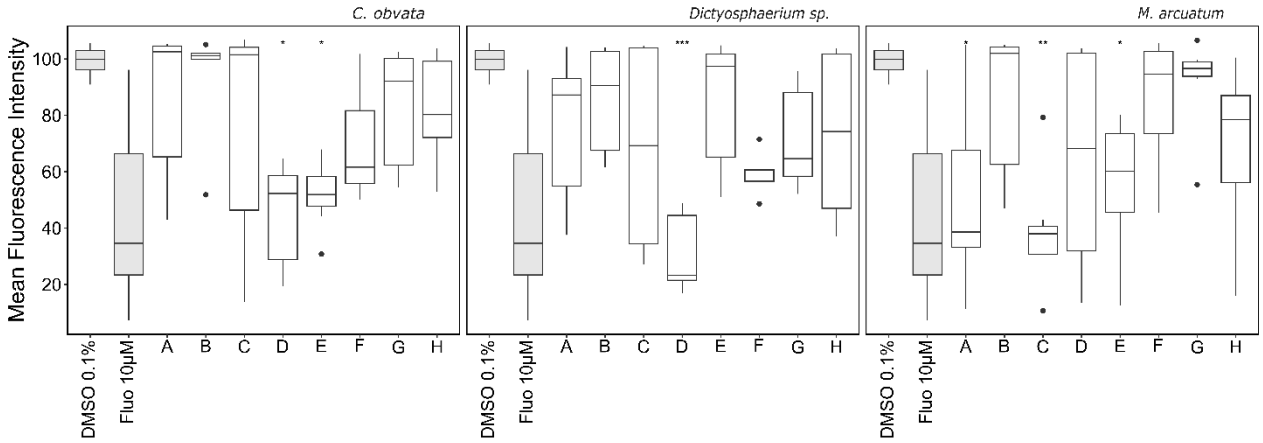

Figure 8. Appetite inhibition assay activity for the five fractions of each of the six algae. Data are presented as mean fluorescence activity relative to the solvent control in grey (DMSO 0.1%) and Fluoxetine 10 µM (Fluo 10 µM) was used as positive control. The box-and-whisker plots (5–95 percentile) represent the variation between the tests performed (n = 6). The dots represent outliers and were not considered for statistical analysis. Asterisks indicate statistically significant results (*: p-value < 0.05; **: p-value < 0.01; ***: p-value < 0.001).

The greatest effect was present in the microalgae *Dictyosphaerium* sp. fraction D (p-value < 0.001), with 69.0% of appetite inhibition compared to the control. Considering the promising effect, the fractions of this alga were sent for analysis by LC-MS/MS and the data processed. Figures 9 and 10 shows the observed molecular network of fractions A to H of *Dictyosphaerium* sp. extracts and figure 10 highlights the main observed clusters.

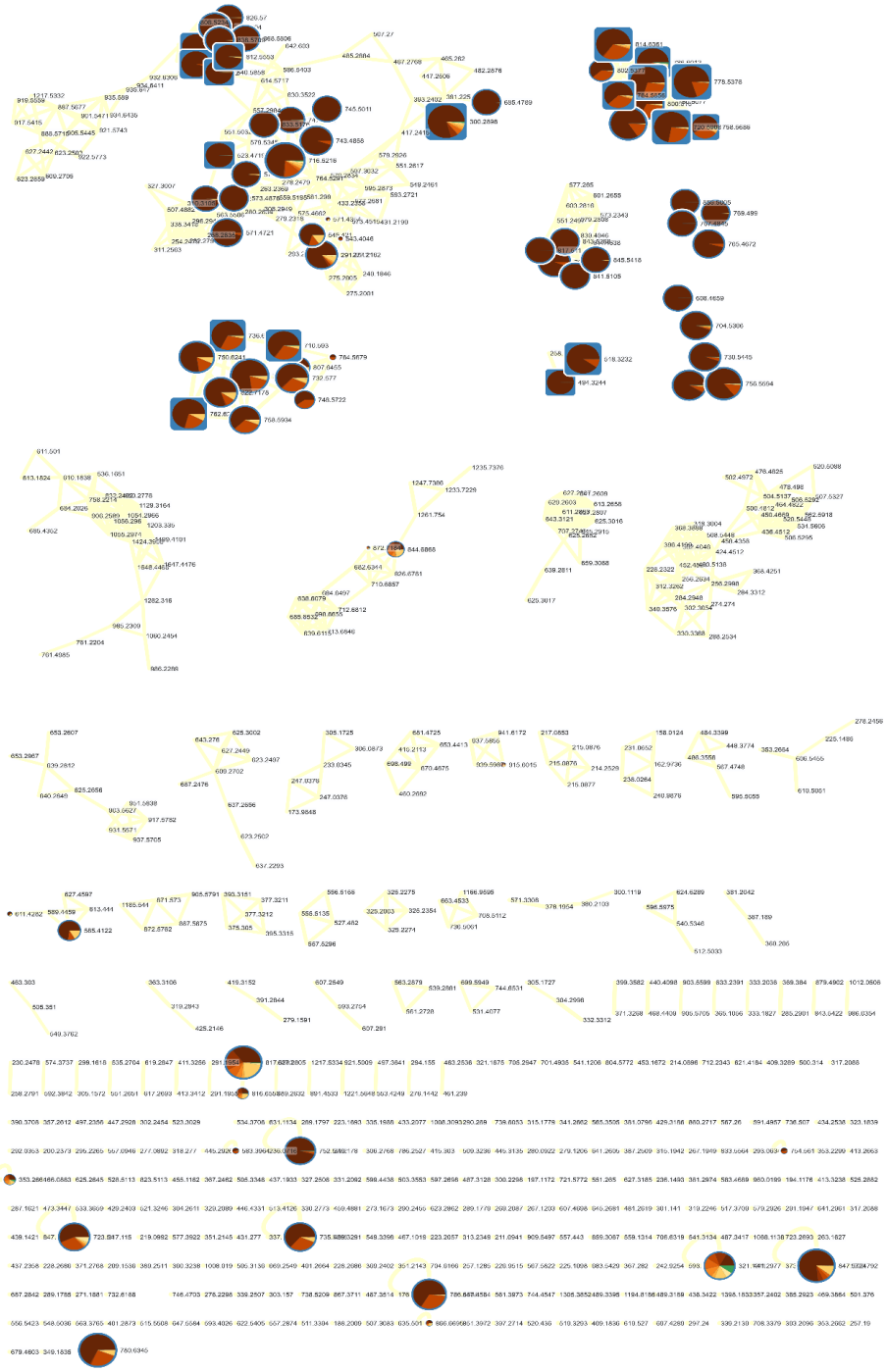

Figure 9. Molecular networks observed for appetite inhibition activity of the fractions A to H of *Dictyosphaerium sp*. extracts. The nodes represent molecules observed in each fraction with their respective molecular mass indicated. The shape of the node indicates the compounds that have been identified in the GNPS database (squares) and that have not been identified (circle). The pie chart at each node represents the relative abundance in each fraction, with each color represents a fraction. The darker colors represent the greater the biological activity observed in fraction. The graph only shows nodes with significant correlation (p-value <0.05 or Cor>0.63) with bioactivity. The size of the circle is proportional to the correlation with bioactivity. The diameter of the lines connecting the nodes represent the similarity between the nodes, the larger the line the greater the correlation between nodes (0.7 to 1).

d

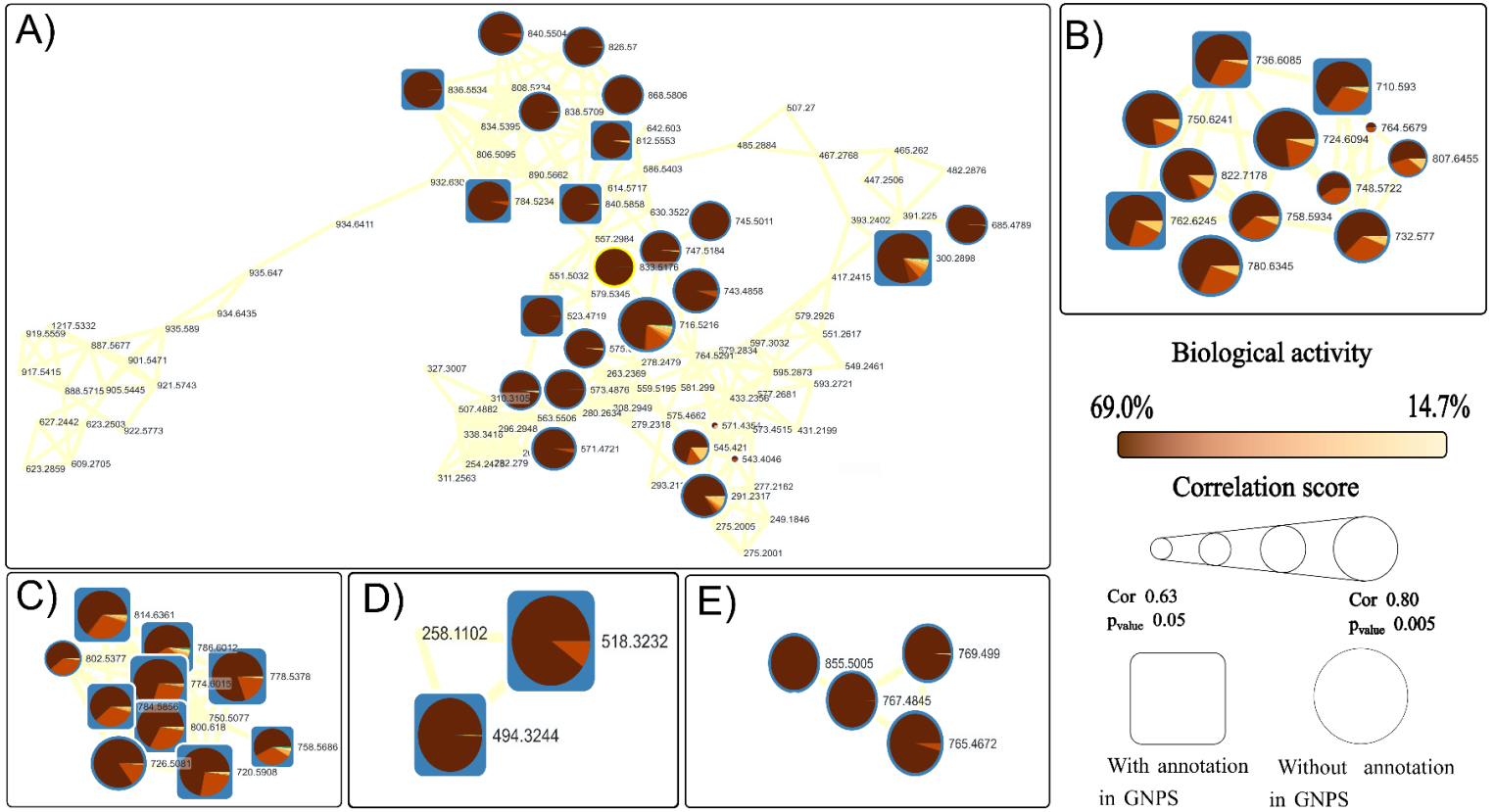

1

Figure 10a-e. Molecular networks observed for appetite inhibition activity of the microalgae *Dictyosphaerium sp*. The nodes represent molecules observed in each fraction with their respective molecular mass indicated. The shape of the node indicates the compounds that have been identified in the GNPS database (squares) and that have not been identified (circle). The pie chart at each node represents the relative abundance in each fraction, with each color represents a fraction. The darker colors represent the greater the biological activity observed in fraction. The graph only shows nodes with significant correlation (p-value <0.05 or Cor>0.63) with bioactivity. The size of the circle is proportional to the correlation with bioactivity. The diameter of the lines connecting the nodes represent the similarity between the nodes, the larger the line the greater the correlation between nodes (0.7 to 1).

2

For appetite inhibition activity, 66 nodes were observed with metabolites having a correlation greater than 0.75, and 79 with significant correlation (Cor > 0.63 e p-value <0.05). In figure 10C, several nodes showed a correlation greater than 0.75, and most of them were identified by the GNPS database. Those classifieds were categorized as lipids, being associated with phosphocholine. The most correlated compound (Cor = 0.80) was *m/z* 778.5378 $[M+H]^+$, which was annotated as 1,2-Di-(9Z,12Z,15Z-octadecatrienoyl)-sn-glycero-3-phosphocholine or L-Dilinolenoyl lecithin. In Figure 10D, the same compounds associated with phosphocholine were identified and annotated by the GNPS database as PC (18:3/0:0) 518.3232 $[M+H]^+$ and Lyso PC (16:1) 494.3244 $[M+H]^+$. Both showed a correlation between 0.77 and 0.78. In figure 10A, six nodes with Cor > 0.75 were annotated. Since the compounds of *m/z* 784.5234, 812.5553, 836.5534, and 840.5858 $[M+H]^+$ were all classified as sulfoquinovosyl diacylglycerol, the difference between them lies in the variations in the groups of carboxylic acids associated with the sulfoquinovosyl glycerol group. The compound with *m/z* 523.4719 $[M+H]^+$ was annotated as acyl glycerol (o-14:1/16:1), and the mass compound with *m/z* 300.2898 $[M+H]^+$ was identified as palmitoyl ethanolamide, with a correlation of 0.80. Another compound with correlation of 0.80 appeared in this cluster, had no annotation in GNPS, but was putatively annotated as 1-palmitoyl-2-linoleoyl-sn-glycero-3-phosphoethanolamine (ppm = 1.96) by DNP. In relation to Figure 10B, a cluster was observed with several correlated nodes (0.68-0.80), which were all annotated as betaine lipids (diacylglyceryltrimethylhomo-serine or DGTSA), in which the difference lies in the fatty acid chain. In this cluster the node with the highest correlation *m/z* 724.6094 $[M+H]^+$ was not recorded in any of the evaluated databases. In Figure 10E no GNPS database annotations was observed. Fifteen nodes from the highlighted clusters (figure 10), which had the highest correlations (0.80 to 0.79), were selected to proceed search in DMNP and NPatlas database. Table 4 shows the results obtained for these nodes along with their putative identifications.

Table 4. Putative identification of high correlation compounds indicated by bioactive based molecular networking on figure 10. Identifications were based on GNPS based on MS^2 fragmentation and on M+ values with a deviation of 0.005 against the database DMNP and NPA. Only identification with mass error less than 5 ppm were considered. From the 15 compounds 11 were putative identified. [M^+]: Observed mass; Rt: retention time (min); Cor: Correlation Score; ppm: Mass error; GNPS: Global Natural Products Social Molecular Networking; DMNP: Dictionary of Marine Natural Products; NPA: Natural product atlas.

[M^+]	Rt (min)	Cor	Putative Identification	ppm	Formula	Source
715.5138	12.43	0.80	1-palmitoyl-2-linoleoyl-sn-glycero-3-phosphoethanolamine	1.96	$C_{39}H_{74}NO_8P$	DNP
299.2820	10.90	0.80	Palmitoyl ethanolamide	1.34	$C_{18}H_{37}NO_2$	GNPS
777.5300	12.08	0.80	1,2-Di-(9Z,12Z,15Z-octadecatrienoyl)-sn-glycero-3-phosphocholine	1.09	$C_{44}H_{76}NO_8P$	GNPS
799.6102	12.67	0.79	PC (18:1/19:1)	1.38	$C_{45}H_{86}NO_8P$	GNPS
719.5830	12.53	0.79	PC (16:0/O-16:0)	0.15	$C_{40}H_{83}NO_7P$	GNPS
517.3154	9.43	0.79	(2-Hydroxy-3-octadeca-6,9,12-trienoyloxypropyl) 2-(trimethylazaniumyl)ethyl phosphate	2.71	$C_{26}H_{48}NO_7P$	GNPS
735.6007	12.42	0.79	DGTSA (16:1/18:1)	0.82	$C_{44}H_{81}NO_7$	GNPS
813.6283	12.81	0.79	PC (18:2/20:0)	4.42	$C_{46}H_{88}NO_8P$	GNPS
709.5852	12.37	0.79	DGTS/DGTA (32:1)	0.63	$C_{42}H_{79}NO_7$	GNPS
761.6167	12.49	0.79	DGTSA (18:1/18:2)	0.33	$C_{46}H_{84}NO_7$	GNPS
773.5937	12.66	0.79	PC (17:0/18:1)	0.31	$C_{43}H_{84}NO_8P$	GNPS
723.6016	12.46	0.80	-	-	-	-
725.5003	12.07	0.79	-	-	-	-
749.6163	12.51	0.79	-	-	-	-
779.6267	12.68	0.79	-	-	-	-

4.3. Cellular viability

Regarding cellular viability, none of the extracts demonstrated strong activity ($p < 0.05$). The lowest value observed was for the DCM:MeOH extract from the microalga *S. bibraianum*, with approximately 20% reduction of cellular viability (Figure 11). In comparison, the negative control (20% DMSO) showed around 70% reduction.

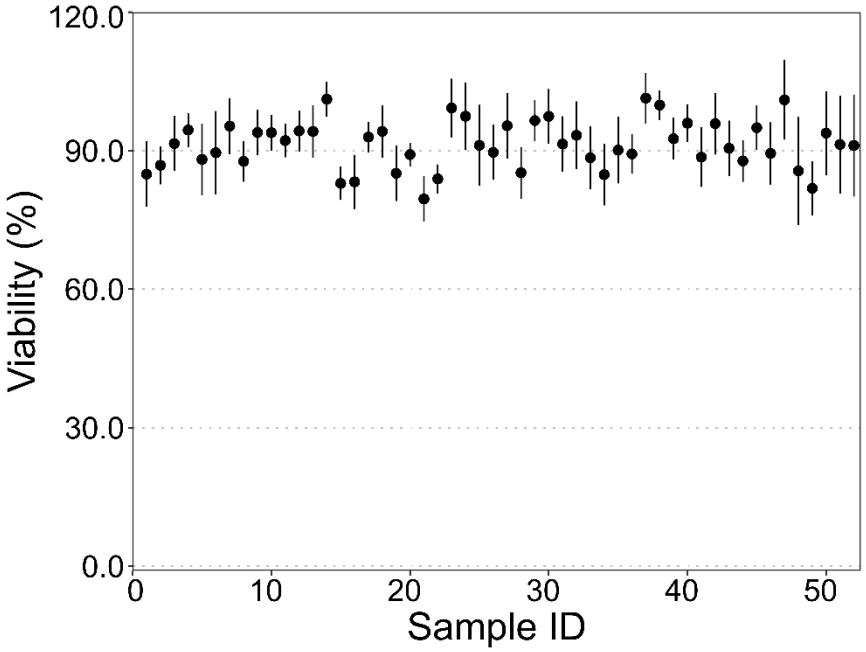

Figure 11. Screening of 52 microalgae extracts for viability assay. Data are presented as viability (%) relative to the solvent control. The node shows the mean value, and the line the variation between individuals (n=6).

4.4. Anti-inflammatory activity

Regarding the inflammation assay, three extracts were observed with more than 40% of inhibition (figure 12), namely DCM:MeOH extracts from *C. emersonii* (51.12% NO reduction), *Dictiosphaerum* sp. (43.11% NO reduction) and *S. bibraianum* (65.42% NO reduction). All of them showed no effect on cell viability. For the inflammation assay, the EC_{50} test was not performed because concentrations greater than 0.25% of DMSO interfered with the NO production by the macrophages.

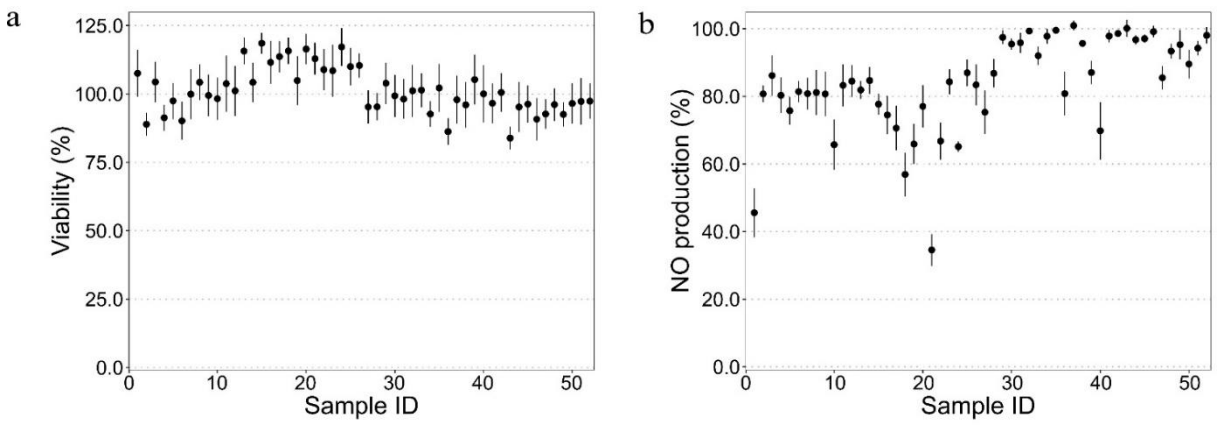

Figure 12. Screening of 52 microalgae extracts for anti-inflammatory assay. A: Cell viability by reaction with MTT, relative to control (DMSO 0.1%+LPS). B: Nitric Oxide production relative the control (DMSO 0.1%+LPS). The node shows the mean value, and the line the variation between individuals (n=6).

The activity and toxicity of the fractions are shown in figure 13. After fractionating the DCM:MeOH extracts that presented activity against inflammation (*S. bibraianum*, *Dictyosphaerium* sp. and *C. emersonii*), no toxicity was detected. For these 3 algae strains, fractions B and C demonstrated some degree of activity, but for *S. bibraianum* it was not statistically significant. *Dictyosphaerium* sp. displayed notable activity, with fraction B inhibiting 59.4% (p-value < 0.05) and fraction C inhibiting 95.0% (p-value < 0.0001).

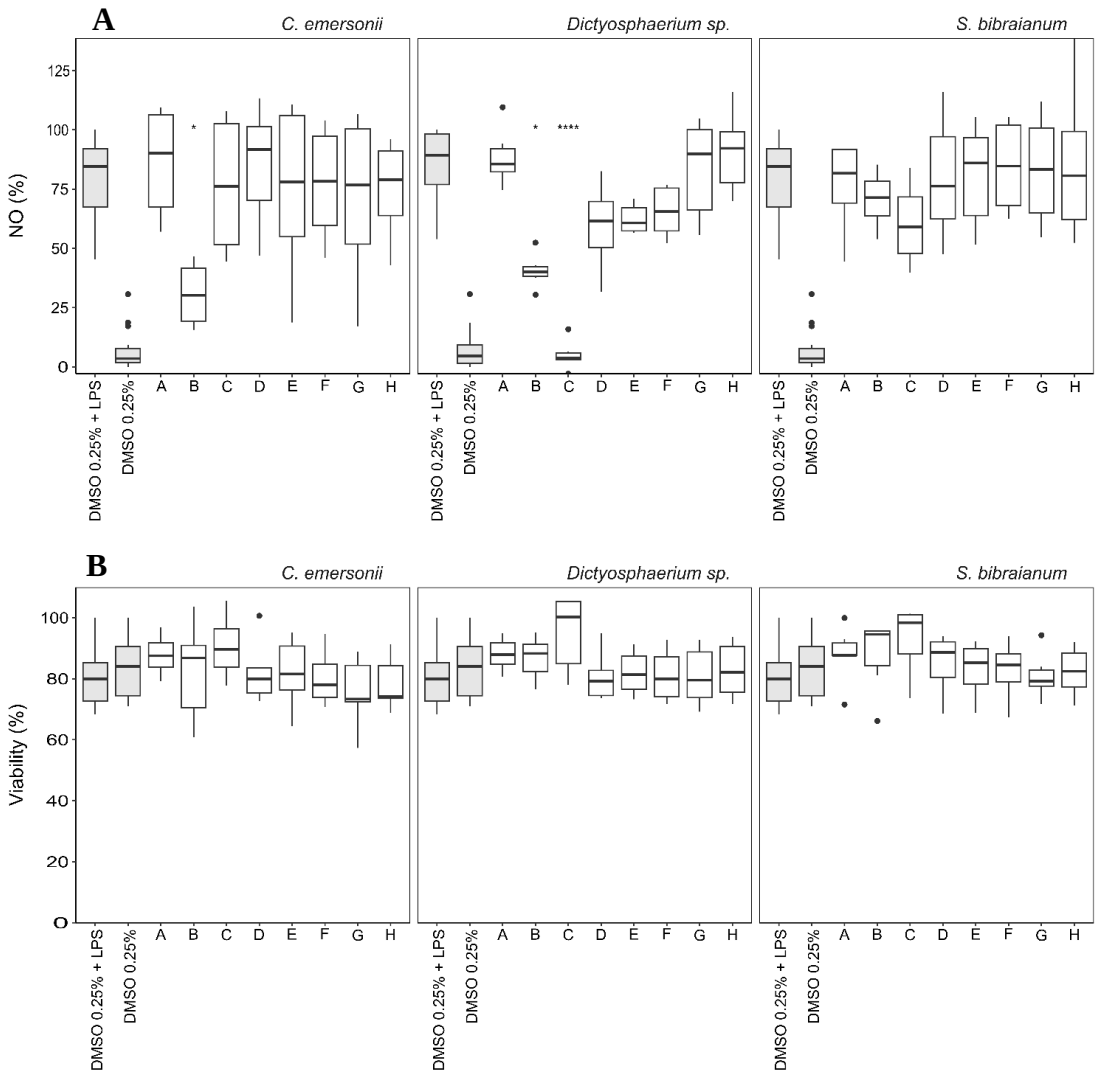

Figure 13. A: Relative production (%) of nitric oxide (NO) for each fraction. B: Cell viability (%) for each fraction. Data are presented relative to basal NO levels without stimulation with LPS (DMSO 0.25%) and with stimulation with LPS (DMSO + LPS), both used as controls (in gray). The box-and-whisker plots (5–95 percentile) represent the variation between the tests performed (n = 6). The dots represent outliers and were not considered for statistical analysis. Asterisks indicate statistically significant results (*p < 0.05; **p < 0.01; ***p < 0.001, ****p < 0.0001).

Nitric oxide (NO) production is associated with the inflammatory response of macrophages, and its reduction indicates a possible decrease in inflammatory response. Among the fractions tested, the fraction C of *Dictiosphaerum* sp. showed the highest activity (95.04% NO reduction). Thus, the fractions A to H of *Dictiosphaerum* sp. were used to construct a

molecular network represented in the figure below (figure 14) and the main clusters obtained are highlighted in figure 15.

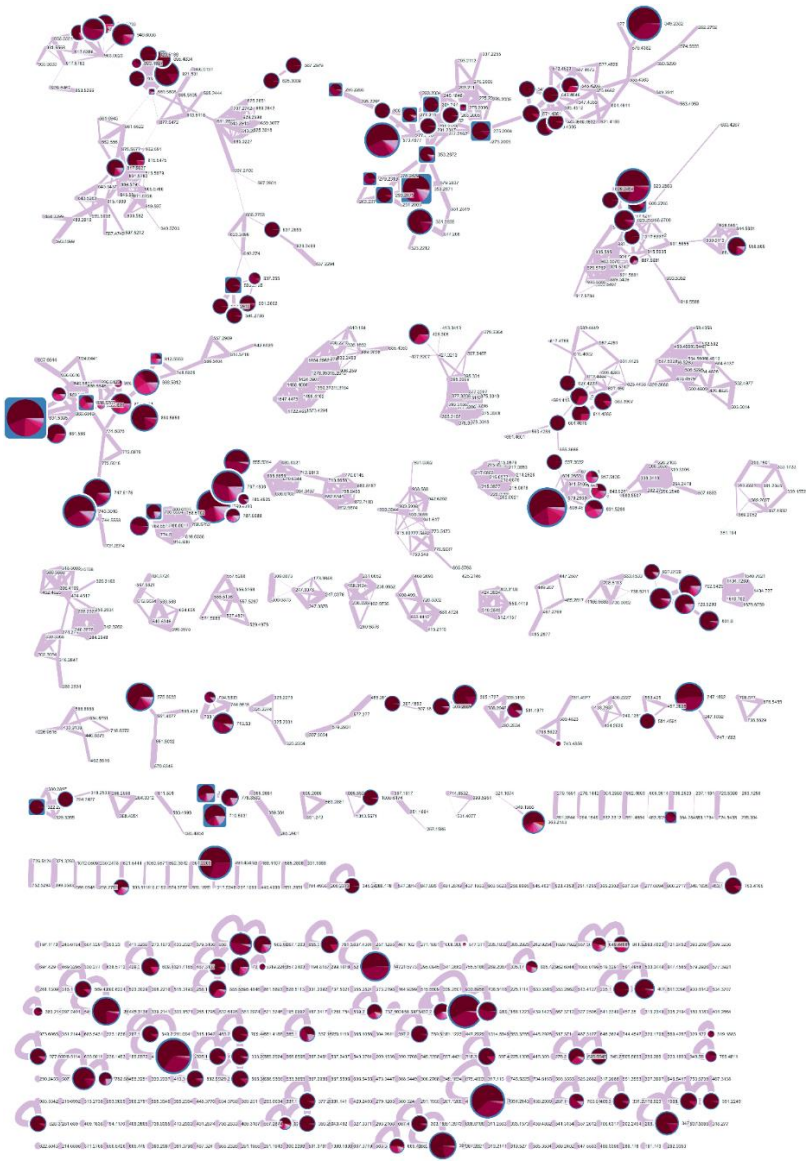

Figure 14. Molecular networks observed for anti-inflammatory activity of the fractions of *Dictyosphaerium sp.* extracts. The nodes represent molecules observed in each fraction with their respective molecular mass indicated. The shape of the node indicates the compounds that have been identified in the GNPS database (squares) and that have not been identified (circle). The pie chart at each node represents the relative abundance in each fraction, with each color represents a fraction. The darker colors represent the greater the biological activity observed in fraction. The graph only shows nodes with significant correlation (p-value <0.05 or Cor>0.63) with bioactivity. The size of the circle is proportional to the correlation with bioactivity. The diameter of the lines connecting the nodes represent the similarity between the nodes, the larger the line the greater the correlation between nodes (0.7 to 1).

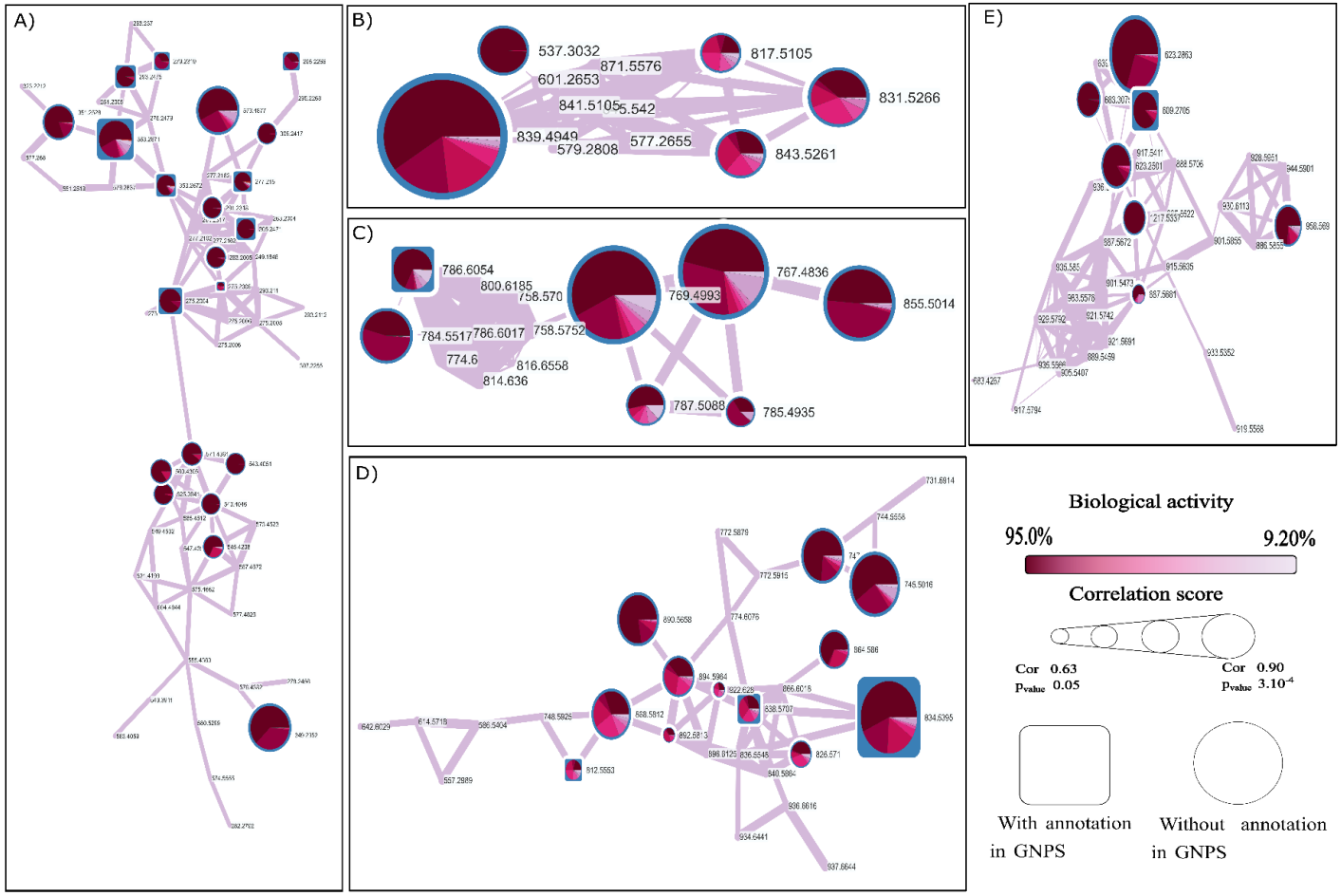

1 **Figure 15A-E.** Main molecular networks observed for anti-inflammatory activity (A-D) activity of the microalgae *Dictyosphaerium* sp. The nodes represent molecules observed in each fraction with their respective molecular mass indicated. The shape of the node indicates the compounds that have been identified in the GNPS database (squares) and that have not been identified (circle). The pie chart at each node represents the relative abundance in each fraction, with each color represents a fraction. The darker colors represent the greater the biological activity observed in fraction. The graph only shows nodes with significant correlation (p-value <0.05 or Cor>0.63) with bioactivity. The size of the circle is proportional to the correlation with bioactivity. The diameter of the lines connecting the nodes represent the similarity between the nodes, the larger the line the greater the correlation between nodes (0.7 to 1).

For the anti-inflammatory activity, 873 nodes were observed, and 179 exhibited a significant correlation with anti-inflammatory activity (Cor > 0.63 and p-value < 0.05), with 13 nodes correlating above 0.85, in which 5 clusters stood out (Figure 15 A-E). In Figure 15D, 3 clusters presented a strong correlation value (Cor > 0.85). The compound *m/z* 353.2671 $[M+H]^+$ (Cor = 0.85) was classified in GNPS database as monolinolenin, a monoacyl glycerol. Regarding the other compounds, the monoisotopic mass *m/z* 573.4877 [M+H] + (Cor = 0.88) was identified as octacosyl caffeate (ppm = 1.05) based on DMNP database. The third compound of *m/z* 349.2352 $[M+H]^+$ (Cor = 0.88) did not receive any annotation. In Figure 15A, the compounds *m/z* 834.5395 and 745.5016 $[M+H]^+$ showed a strong correlation, and the first compound correlating at 0.91, annotated as sulfoquinovosyl diacylglycerol (16:0/18:3). In Figure 15C, 2 metabolites with strong correlation were observed, *m/z* 769.4993 and 767.4836 $[M+H]^+$ (Cor: 0.87), but it was not recorded as any known compound in the GNPS and other databases. In figure 15E the compound *m/z* 623.2863 $[M+H]^+$ presented a correlation coefficient of 0.87 with bioactivity. In figure 15B, the compound *m/z* 839.4949 $[M+H]^+$ exhibited a correlation coefficient of 0.90, but as with *m/z* 623.2863 $[M+H]^+$ no known recorded compound in the GNPS and other databases were annotated. Among these nodes, 15 nodes belonging to the highlighted clusters with the highest correlations (0.81-0.90) were selected. Table 5 presents the results obtained for these nodes along with their putative identifications.

Table 5. Putative identification of high correlation compounds indicated by bioactive based molecular networking on figure 15. Identifications were based on GNPS based on MS^2 fragmentation and on *m/z* values with a deviation of 0.005 against the database DMNP and NPA. Only identification with mass error less than 5 ppm were considered. From the 15 compounds 11 were putative identified. [M^+]: Observed mass; Rt: retention time (min); Cor: Correlation Score; ppm: Parts per Million; GNPS: Global Natural Products Social Molecular Networking; DMNP: Dictionary of Marine Natural Products; NPA: Natural product atlas.

[M^+]	Rt (min)	Cor	Putative Identification	ppm	Formula	Source
816.5057	15.08	0.91	SQDG (16:0/18:3)	0.09	C46H75NO12	GNPS
572.4799	14.98	0.88	Octacosyl caffeate	1.05	C37H64O4	DNP
622.2785	11.38	0.88	Methyl 10-hydroxyphaeophorbide	1.12	C35H42O10	DNP
744.4941	15.00	0.87	Myxol; 2'-O-(3-O-Methyl-α-L-fucoside)	3.22	C47H68O7	DNP
352.2593	10.00	0.85	Monolinolenin	5.85	C21H36O4	GNPS
350.2450	8.64	0.83	Glycerol-1-octadecatetraenoate	2.00	C21H34O4	DNP
746.5098	15.44	0.85	Bistratene B	2.28	C42H70N2O9	DNP
838.4871	15.08	0.90	-	-	-	-
349.2352	9.44	0.88	-	-	-	-
768.4915	15.46	0.87	-	-	-	-
766.4758	14.99	0.87	-	-	-	-
889.5580	15.06	0.84	-	-	-	-
867.573	16.09	0.83	-	-	-	-
854.494	14.85	0.83	-	-	-	-
893.589	16.28	0.81	-	-	-	-

5. Discussion

Microalgae have long been a source of food for both humans and animals with numerous health benefits being discovered over time (BOROWITZKA, 2018). However, their potential health effects remain largely unexplored and may vary among different species. Of the 52 evaluated eukaryotic microalgae extracts, most yielded unprecedented results regarding secondary metabolites and their effects on lipid reduction, appetite regulation, and anti-inflammatory activity. Among the microalgae evaluated, 6 demonstrated promising activity in reducing lipid accumulation in zebrafish. EC_{50} assays confirmed this activity for all, except *Ophiocytium* sp. The microalgae *S. bibraianum* and *C. emersonii* had the most significant effects. Previous studies have highlighted the impact of *Chlorella* species on obesity in cell

culture. Chon et al. (2009) identified inhibition of triacylglycerol accumulation of *Chlorella* sp. MeOH extracts. Yang et al. (2022) observed that the unsaturated fatty acids from *Chlorella* powder, induced a reduction of body weight, blood fat and blood sugar levels on fat induced obese mice. In zebrafish, Regueiras et al. (2022) reported a reduction in lipid accumulation of up to 75% under heterotrophic culture conditions of *Chlorella vulgaris*. Notably, *S. bibraianum* (this research) has not been previously reported for its effects against obesity.

The fraction C of *S. bibraianum* exhibited the highest activity against obesity among all the tested fractions, and bioactivity-based molecular networking revealed metabolites that were strongly correlated with this biological activity. Some of the identified compounds were annotated as chlorophyll derivatives, including pheophorbide a, chlorin, and protochlorophyllide. Effects related to the stimulation of lipid consumption and inhibition of adipogenesis have already been reported for pheophorbide in mouse 3T3-L1 preadipocytes (PARK; KIM; HAN, 2022). Similarly, Liu et al. (2022) observed a reduction in lipid accumulation in 8-day differentiated adipocytes, which was attributed to pheophorbide a and pyropheophorbide. Freitas et al. (2019) identified 2 chlorophyll derivatives with lipid-reducing activity, 13^2-hydroxy-pheophytin a (*m/z* 887.5697 $[M+H]^+$) and 13^2-hydroxy-pheofarnesin a (*m/z* 817.4522 $[M+H]^+$), in a zebrafish model. Similarly, pheophorbide a was putatively identified in the bioactive fraction of *S. bibraianum* in this research and associated with a correlation score of 0.84. The high anti-obesity activity we obtained for *S. bibraianum* extracts was confirmed by the metabolomic study, however, some metabolites have not been identified and may be new structures.

Regarding the appetite inhibition activity of the evaluated extracts the 3 algae that showed significant activity (>50% inhibition), had the greatest appetite inhibition in fraction D compared to the negative control. Literature show that some algae do have appetite-reducing effects. Human consumption of *Spirulina platensis* promoted food intake reduction and a decrease in body weight (ZEINALIAN et al., 2017). Even though we obtained 69% appetite reduction and no strong correlation among clusters in the metabolic networking analysis, several metabolites moderately correlated with appetite inhibition and with lipid metabolism, including ethanolamine, sulfoquinovosyl glycerol, betaine, and phosphocholine were obtained. It is known that fatty acid ethanolamine derivatives have been associated with reduced food intake, particularly oleoylethanolamide, which has been linked to appetite reduction in both rats and humans (GAETANI; OVEISI; PIOMELLI, 2003; LALEH et al., 2018).

Laleh et al. (2018) observed that oleoylethanolamide intake was effective in reducing weight gain and increasing the expression of the proximal proliferator-activated receptor-α (PPAR-α) gene, which is associated with various metabolic processes, reduced hunger, decreased desire to eat, and increased satiety. In the present research, one of the compounds identified with a moderate correlation (cor = 0.80) was palmitoyl ethanolamide (*m/z* 300.2898 $[M+H]^+$, ppm = 1.34), which has already been associated with reduction of food intake in ovariectomized rats (MATTACE RASO et al., 2014). The effect of medium-chain triglycerides (MCT) and conjugated linoleic acid (CLA) has also been observed to increase satiety in a study with 19 patients, where a reduction in food intake over a day was reported (COLEMAN; QUINN; CLEGG, 2016). Although MCT and CLA were not identified in the present study, the possible presence of long-chain lipids and fatty acid derivatives that may influence appetite was observed.

Related to the toxicity of the extracts, the present results are in accordance with the results of Gürlek et al. (2020) and Silva et al. (2022). These studies observed some toxicity in microalgae extracts at concentrations of 100 $\mu g.mL^{-1}$. Gürlek et al. (2020) evaluated Chlorophyta microalgae, and even at higher concentrations, almost no effects on HepG2 cells were observed. The authors showed no toxicity in rat macrophage cells (RAW 264.7), and after exposure to lipopolyssacharides, some extracts significantly reduced the inflammatory response.

The extracts from *C. emersonii*, *Dictyosphaerium* sp., and *S. bibraianum* showed a reduction in the inflammatory response in zebrafish by more than 40%. *Chlorella* has previously shown potential anti-inflammatory activity; specifically, acetone extracts exhibited a significant reduction in inflammatory activity in RAW 264.7 cells in extracts with high lipid content (YANG et al., 2022). *Dictyosphaerium* sp. has also been identified as promising in this regard. Halaj et al. (2019) observed the immunomodulatory effects of polysaccharides from three species of *Dictyosphaerium*, noting an increased expression of pro-inflammatory cytokines in RAW 264.7 cells. However, studies investigating the effects of its extract in relation to inflammation remain limited.

Regarding the fractions and anti-inflammation, the microalgae *Dictyosphaerium* sp. fraction C showed 95% reduction in NO production. The presence of lipids in microalgae extracts has been linked to anti-inflammatory activity. Yang et al. (2022) observed a reduction in macrophage NO production in the lipid-rich fraction of *Chlorella* sp., associating this effect with the presence of linoleic acid and linolenic acid. Lauritano et al. (2020) reported that fractions of *Cylindrotheca closterium* successfully inhibited the release of tumor necrosis

factor-α (TNF-α) in human monocyte cultures. They identified the lipid-derived compound 1-palmitoyl-sn-glycero-3-phosphocholine, which was subsequently tested and confirmed to have anti-inflammatory activity. In this study, monolinolenin was putatively identified (*m/z* 353.2671 $[M+H]^+$, ppm = 5.85), which is a linolenic acid associated with a glycerol molecule with a high correlation (Cor = 0.85). Additionally, glycerol-1-octadecatetraenoate (*m/z* 351.2528 $[M+H]^+$, ppm = 2) was also identified with a correlation of 0.83. In the present research the metabolic analysis confirmed the lipid-derived metabolites in *Dictyosphaerium* sp. fraction C, such as monolinolenin, octadecatetraenoate, and monoterpenoids, supporting its anti-inflammatory activity.

Polar lipids were also detected in the fractions of *Dictyosphaerium* sp., and according to literature, they may have anti-inflammatory activity. In fact, investigating extracts of *Gloeothece* sp., da Costa et al. (2020) showed anti-inflammatory activity through the capacity to inhibit the enzyme COX-2. In this study, sulfoquinovosyldiacylglycerol (SQGD) (16:0/18:3) (*m/z* 817.5153 $[M+H]^+$, ppm = 0.09) exhibited a strong correlation (Cor: 0.91), confirming the potential to act as anti-inflammation agent. According to literature, this compound has anti-inflammatory effects as reported in Bruno et al. (2005). The authors studied mouse with croton-oil-induced ear edema. Another compound identified by the metabolic study in the present research that supports anti-inflammatory activity is octacosyl caffeate (*m/z* 573.4877 $[M+H]^+$, ppm = 1.05), a derivative of caffeic acid. Compounds such as octyl caffeate have been shown to inhibit inflammatory activity in rat aortic smooth muscle cells (RASMCs), where it was noted that longer chains might enhance the activity. We also identified methyl 10-hydroxyphaeophorbide (*m/z* 623.2863 $[M+H]^+$, ppm = 1.12), which may have anti-inflammatory activity, but there is no literature information regarding its action as anti-inflammatory. Nevertheless, Lauritano et al. (2020) showed that pheophorbide a has anti-inflammatory activity in human monocyte cultures, similar to the methyl 10-hydroxyphaeophorbide identified in the present investigation. Overall, in the present research the metabolic analysis confirmed the lipid-derived metabolites in *Dictyosphaerium* sp. fraction C, such as monolinolenin, octadecatetraenoate, and monoterpenoids, supporting its anti-inflammatory activity.

6. Conclusion

The present results suggest a promising effect of some microalgae in the treatment of obesity and inflammation. Specifically, *Dictyosphaerium sp.* and *S. bibraianum* demonstrated significant activity in lipid reduction, appetite suppression, and inhibition of inflammatory responses, all of which are factors related to the exacerbation of obesity. Additionally, metabolites with potential effects on these diseases were identified. For the reduction of lipids, appetite suppression, and anti-inflammatory purposes, various chlorophyll and lipid metabolism compounds were putatively identified, with evidences in the literature supporting their bioactivity. Several other compounds of unknown identification may have contributed to the observed bioactivity, since they were present in nodes of identified mass peaks. This research underscores the potential of eukaryotic microalgae as source of promising metabolites for disease treatments, highlighting their efficacy and potential for the discovery of new compounds.

7. References

BARBOSA, M. et al. Phlorotannin extracts from Fucales: Marine polyphenols as bioregulators engaged in inflammation-related mediators and enzymes. **Algal Research**, v. 28, n. April, p. 1–8, 2017.

BLUNDELL, J. et al. Effects of once-weekly semaglutide on appetite, energy intake, control of eating, food preference and body weight in subjects with obesity. **Diabetes, Obesity and Metabolism**, v. 19, n. 9, p. 1242–1251, 5 set. 2017.

BOROWITZKA, M. A. Chapter 3 - Biology of Microalgae. Em: LEVINE, I. A.; FLEURENCE, J. (Eds.). **Microalgae in Health and Disease Prevention.** Academic Press, 2018. p. 23–72.

BRUNO, A. et al. Selective in vivo anti-inflammatory action of the galactolipid monogalactosyldiacylglycerol. **European Journal of Pharmacology**, v. 524, n. 1–3, p. 159–168, nov. 2005.

CASTRO, M. et al. Obesity: The Metabolic Disease, Advances on Drug Discovery and Natural Product Research. **Current Topics in Medicinal Chemistry**, v. 16, n. 23, p. 2577–2604, 2016.

CHON, J. et al. Chlorella Methanol Extract Reduces Lipid Accumulation in and Increases the Number of Apoptotic 3T3-L1 Cells. **Annals of the New York Academy of Sciences**, v. 1171, n. 1, p. 183–189, 15 ago. 2009.

CHOOI, Y. C.; DING, C.; MAGKOS, F. The epidemiology of obesity. Metabolism, v. 92, p. 6–10, mar. 2019.

COLEMAN, H.; QUINN, P.; CLEGG, M. E. Medium-chain triglycerides and conjugated linoleic acids in beverage form increase satiety and reduce food intake in humans. **Nutrition Research**, v. 36, n. 6, p. 526–533, jun. 2016.

DA COSTA, E. et al. Screening for polar lipids, antioxidant, and anti-inflammatory activities of Gloeothece sp. lipid extracts pursuing new phytochemicals from cyanobacteria. **Journal of Applied Phycology**, v. 32, n. 5, p. 3015–3030, 26 out. 2020.

ELLULU, M. S. et al. Obesity and inflammation: the linking mechanism and the complications. **Archives of Medical Science**, v. 4, p. 851–863, 2017.

FARHADIPOUR, M.; DEPOORTERE, I. The Function of Gastrointestinal Hormones in Obesity—Implications for the Regulation of Energy Intake. **Nutrients**, v. 13, n. 6, p. 1839, 27 maio 2021.

FERREIRA, L. et al. Uncovering the Bioactive Potential of a Cyanobacterial Natural Products Library Aided by Untargeted Metabolomics. **Marine Drugs**, v. 19, n. 11, p. 633, 12 nov. 2021.

FREITAS, S. et al. Chlorophyll Derivatives from Marine Cyanobacteria with Lipid-Reducing Activities. **Marine Drugs**, v. 17, n. 4, p. 229, 17 abr. 2019.

GAETANI, S.; OVEISI, F.; PIOMELLI, D. Modulation of Meal Pattern in the Rat by the Anorexic Lipid Mediator Oleoylethanolamide. **Neuropsychopharmacology**, v. 28, n. 7, p. 1311–1316, 22 jul. 2003.

GREEN, L. M.; READE, J. L.; WARE, C. F. Rapid colormetric assay for cell viability: Application to the quantitation of cytotoxic and growth inhibitory lymphokines. **Journal of Immunological Methods**, v. 70, n. 2, p. 257–268, maio 1984.

GUILLARD, R. R. L. Culture of Phytoplankton for Feeding Marine Invertebrates. **Boston, MA: Springer US**, 1975. p. 29–60

GÜRLEK, C. et al. Screening of antioxidant and cytotoxic activities of several microalgal extracts with pharmaceutical potential. **Health and Technology**, 2020.

HALAJ, M. et al. Extracellular biopolymers produced by Dictyosphaerium family - Chemical and immunomodulative properties. **International Journal of Biological Macromolecule**s, v. 121, p. 1254–1263, jan. 2019.

KNUDSEN, L. B.; LAU, J. The Discovery and Development of Liraglutide and Semaglutide. **Frontiers in Endocrinology**, v. 10, 12 abr. 2019.

KUCKUCK, S. et al. Glucocorticoids, stress and eating: The mediating role of appetite-regulating hormones. **Obesity Reviews**, v. 24, n. 3, 8 mar. 2023.

LALEH, P. et al. Oleoylethanolamide increases the expression of PPAR-A and reduces appetite and body weight in obese people: A clinical trial. **Appetite**, v. 128, p. 44–49, set. 2018.

LAURITANO, C. et al. Lysophosphatidylcholines and Chlorophyll-Derived Molecules from the Diatom Cylindrotheca closterium with Anti-Inflammatory Activity. **Marine Drugs**, v. 18, n. 3, p. 166, 17 mar. 2020.

LIU, Y. et al. Anti-adipogenic activities of pheophorbide a and pyropheophorbide a isolated from wild bitter gourd (Momordica charantia L. var. abbreviata Seringe) in vitro. **Journal of the Science of Food and Agriculture**, v. 102, n. 14, p. 6771–6779, 17 nov. 2022.

LOBSTEIN, T.; BRINSDEN, H.; NEVEUX, M. World Obesity Atlas 2022. Disponível em: < https://s3-eu-west-1.amazonaws.com/wof-files/World_Obesity_Atlas_2022.pdf>. Acesso em: 4 abr. 2022.

MATTACE RASO, G. et al. Palmitoylethanolamide Prevents Metabolic Alterations and Restores Leptin Sensitivity in Ovariectomized Rats. **Endocrinology**, v. 155, n. 4, p. 1291–1301, 1 abr. 2014.

MINISTÉRIO DA SAÚDE. Vigilância de fatores de risco e proteção para doenças crônicas por inquérito telefônico. **Vigitel brasil**, 2018.

MORANÇAIS, M.; MOUGET, J.-L.; DUMAY, J. Proteins and Pigments. Em: BILLIE JEAN FERNANDEZ (Ed.). **Microalgae in Health and Disease Prevention**. United Kingdom: Elsevier, 2018. p. 145–175.

NEWMAN, D. J.; CRAGG, G. M. Natural Products as Sources of New Drugs over the Nearly Four Decades from 01/1981 to 09/2019. **Journal of Natural Products**, v. 83, n. 3, p. 770–803, 2020.

NOTHIAS, L.-F. et al. Bioactivity-Based Molecular Networking for the Discovery of Drug Leads in Natural Product Bioassay-Guided Fractionation. **Journal of Natural Products**, v. 81, n. 4, p. 758–767, 27 abr. 2018.

NOTHIAS, L.-F. et al. Feature-based molecular networking in the GNPS analysis environment. **Nature Methods**, v. 17, n. 9, p. 905–908, 24 set. 2020.

OLAIZOLA, M. Commercial development of microalgal biotechnology: From the test tube to the marketplace. **Biomolecular Engineering**, v. 20, n. 4–6, p. 459–466, 2003.

ORGANIZAÇÃO MUNDIAL DA SAÚDE. Obesity and overweight. Disponível em: <https://www.who.int/news-room/fact-sheets/detail/obesity-and-overweight>. Acesso em: 4 abr. 2022.

PARK, M. H.; KIM, H.-J.; HAN, J.-S. Pheophorbide A isolated from Gelidium amansii inhibits adipogenesis by regulating adipogenic transcription factors and AMPK in 3T3-L1 adipocytes. **Nutrition Research**, v. 107, p. 187–194, nov. 2022.

REGUEIRAS, A. et al. Potential Anti-Obesity, Anti-Steatosis, and Anti-Inflammatory Properties of Extracts from the Microalgae Chlorella vulgaris and Chlorococcum amblystomatis under Different Growth Conditions. **Marine Drugs**, v. 20, n. 1, p. 9, 22 dez. 2021.

RIBEIRO, I. et al. Diversity and Bioactive Potential of Actinobacteria Isolated from a Coastal Marine Sediment in Northern Portugal. **Microorganisms**, v. 8, n. 11, p. 1691, 30 out. 2020.

ROCHLANI, Y. et al. Metabolic syndrome: Pathophysiology, management, and modulation by natural compounds. **Therapeutic Advances in Cardiovascular Disease**, v. 11, n. 8, p. 215–225, 2017.

SAKANOI, Y. et al. Simultaneous Intake of Euglena Gracilis and Vegetables Synergistically Exerts an Anti-Inflammatory Effect and Attenuates Visceral Fat Accumulation by Affecting Gut Microbiota in Mice. **Nutrients**, v. 10, n. 10, p. 1417, 3 out. 2018.

SCHMID, R. et al. Integrative analysis of multimodal mass spectrometry data in MZmine 3. **Nature Biotechnology**, v. 41, n. 4, p. 447–449, 1 abr. 2023.

SHANNON, P. et al. Cytoscape: A Software Environment for Integrated Models of Biomolecular Interaction Networks. **Genome Research**, v. 13, n. 11, p. 2498–2504, nov. 2003.

SILVA, M. et al. Microalgae as Potential Sources of Bioactive Compounds for Functional Foods and Pharmaceuticals. **Applied Sciences (Switzerland)**, v. 12, n. 12, 1 jun. 2022.

SRIVASTAVA, G.; APOVIAN, C. M. Current pharmacotherapy for obesity. **Nature Reviews Endocrinology**, v. 14, n. 1, p. 12–24, 2018.

STANIER, R. Y. et al. Generic Assignments, Strain Histories and Properties of Pure Cultures of Cyanobacteria. **Microbiology**, v. 111, n. 1, p. 1–61, 1 mar. 1979.

URBATZKA, R. et al. Lipid reducing activity and toxicity profiles of a library of polyphenol derivatives. **European Journal of Medicinal Chemistry**, v. 151, p. 272–284, maio 2018.

VAN SANTEN, J. A. et al. The Natural Products Atlas: An Open Access Knowledge Base for Microbial Natural Products Discovery. **ACS Central Science**, v. 5, n. 11, p. 1824–1833, 27 nov. 2019.

WANG, M. et al. Sharing and community curation of mass spectrometry data with Global Natural Products Social Molecular Networking. **Nature Biotechnology**, v. 34, n. 8, p. 828–837, 9 ago. 2016.

WEE, C. L. et al. A bidirectional network for appetite control in larval zebrafish. **eLife**, v. 8, 18 out. 2019.

YANG, L. et al. Anti-Inflammatory Effect of Acetone Extracts from Microalgae Chlorella sp. WZ13 on RAW264.7 Cells and TPA-induced Ear Edema in Mice. **Frontiers in Marine Science**, v. 9, 5 jul. 2022a.

YANG, Y. et al. Chlorella unsaturated fatty acids suppress high-fat diet-induced obesity in C57/BL6J mice. **Journal of Food Science**, v. 87, n. 8, p. 3644–3658, 13 ago. 2022b.

YOUSEFI, R.; MOTTAGHI, A.; SAIDPOUR, A. Spirulina platensis effectively ameliorates anthropometric measurements and obesity-related metabolic disorders in obese or overweight

healthy individuals: A randomized controlled trial. **Complementary Therapies in Medicine**, v. 40, p. 106–112, out. 2018.

ZEINALIAN, R. et al. The effects of Spirulina Platensis on anthropometric indices, appetite, lipid profile and serum vascular endothelial growth factor (VEGF) in obese individuals: a randomized double blinded placebo controlled trial. **BMC Complementary and Alternative Medicine**, v. 17, n. 1, p. 225, 21 dez. 2017.

FEUNANG, Yannick Djoumbou et al. ClassyFire: Automated chemical classification with a comprehensive, computable taxonomy. **Journal of Cheminformatics**, v. 8, p. 61, 2016.

SILVA, Ricardo R. da et al. Propagating annotations of molecular networks using in silico fragmentation. **PLoS Computational Biology**, v. 14, p. e1006089, 2018.

WANDY, Joe et al. Ms2lda.org: web-based topic modelling for substructure discovery in mass spectrometry. **Bioinformatics**, v. 34, n. 2, p. 317-318, 2017.

Main conclusions

In this project, the biotechnological and bioactive potential of 26 eukaryotic freshwater microalgae was evaluated, with 12 of them undergoing physiological and biochemical composition analysis for proteins, carbohydrates, lipids, polyphenols, fatty acids profile and antioxidant potential. Among these, *Chlorella emersonii* and *Pediastrum sp.* emerged as promising nutritional sources, containing over 60% proteins and exhibiting rapid growth. *Pediastrum sp.* showed significant antioxidant potential, with high levels of total polyphenols, polyunsaturated fatty acids (omega-3), making it a candidate for future large-scale trials and economic feasibility studies for nutritional applications. In contrast, *Dimorphococcus sp.* was noted for its high lipid content rich in saturated fatty acids, indicating its potential as a biodiesel producer.

Biological activity assays revealed that the 26 analyzed microalgae exhibited relevant bioactive properties in their extracts. *Chlorella emersonii* inhibited the growth of 4 out of 6 bacteria, with activity confirmed by an decrease in minimum inhibitory concentration in two tested fractions. These fractions were rich in lipids, including compounds such as alpha-linolenic acid, known for their antimicrobial activity.

In assays related to obesity (lipid reduction, appetite inhibition, and anti-inflammatory activity), the dichloromethane:methanol extract of *Selenastrum bibraianum* exhibited the highest lipid-reducing activity. After fractionation of the extract, this activity persisted in one specific fraction (fraction C), where correlation analysis revealed the presence of compounds known for their lipid-reducing effects, such as pheophorbide a and other derivatives of lipid metabolism. For appetite inhibition, *Dictyosphaerium sp.* stood out in its fraction D, containing compounds such as ethanolamine that are frequently associated with lipid inhibition. Additionally, fraction C demonstrated strong anti-inflammatory activity, comprising several identified compounds related to lipid metabolism derivatives, such as polar fatty acids, glycerol lipids, and sulfoglycolipids.

It is concluded that 5 out of the 26 studied microalgae species were promising: *Pediastrum sp.* for studies as a functional food, *Dimorphococcus sp.* for investigation of its lipid-producing potential for biodiesel, and *S. bibraianum* as an interesting source of lipid-reducing compounds, with further research needed for compound isolation and identification of associated metabolites. The same applies to *Dictyosphaerium sp.*, which showed appetite-inhibiting activity and strong anti-inflammatory effects linked to two of its generated fractions.

Finally, *C. emersonii* stood out in various aspects, presenting an interesting protein content, growth rate and antimicrobial potential, alongside the ability to produce lipid-reducing and anti-inflammatory compounds. This species remained one of the most promising in the tests carried out.

In general, the present results emphasize the importance of studying and valuing Brazilian biodiversity, highlighting that through the investigation of a small (26), but diverse group of microalgae, it was possible to identify 5 species with potential alternative applications that can be added to those traditionally used.

APPENDIX 1 – Batch mode source code used in MZmine 3 for data processing the fractions and extracs for obtaining the feature based networking.

```
<?xml version="1.0" encoding="UTF-8"?><batch>
  <batchstep method="io.github.mzmine.modules.dataprocessing.featdet_massdetection.MassDetectionModule">
    <parameter name="Raw data files" type="GUI_SELECTED_FILES"/>
    <parameter name="Scans">
      <ms_level>1</ms_level>
      <scan_definition/>
    </parameter>
    <parameter name="Mass detector" selected="Centroid">
      <module name="Centroid">
        <parameter name="Noise level">1000000.0</parameter>
      </module>
      <module name="Exact mass">
        <parameter name="Noise level"/>
      </module>
      <module name="Local maxima">
        <parameter name="Noise level"/>
      </module>
      <module name="Recursive threshold">
        <parameter name="Noise level"/>
        <parameter name="Min m/z peak width"/>
        <parameter name="Max m/z peak width"/>
      </module>
      <module name="Wavelet transform">
        <parameter name="Noise level"/>
        <parameter name="Scale level"/>
        <parameter name="Wavelet window size (%)"/>
      </module>
    </parameter>
    <parameter name="Mass list name">masses</parameter>
    <parameter name="Output netCDF filename (optional)" selected="false"/>
  </batchstep>
  <batchstep method="io.github.mzmine.modules.dataprocessing.featdet_massdetection.MassDetectionModule">
    <parameter name="Raw data files" type="GUI_SELECTED_FILES"/>
    <parameter name="Scans">
      <ms_level>2</ms_level>
      <scan_definition/>
    </parameter>
    <parameter name="Mass detector" selected="Centroid">
      <module name="Centroid">
        <parameter name="Noise level">10.0</parameter>
      </module>
      <module name="Exact mass">
        <parameter name="Noise level"/>
      </module>
      <module name="Local maxima">
        <parameter name="Noise level"/>
      </module>
      <module name="Recursive threshold">
        <parameter name="Noise level"/>
        <parameter name="Min m/z peak width"/>
        <parameter name="Max m/z peak width"/>
      </module>
      <module name="Wavelet transform">
        <parameter name="Noise level"/>
        <parameter name="Scale level"/>
        <parameter name="Wavelet window size (%)"/>
      </module>
    </parameter>
    <parameter name="Mass list name">masses</parameter>
    <parameter name="Output netCDF filename (optional)" selected="false"/>
  </batchstep>
  <batchstep
method="io.github.mzmine.modules.dataprocessing.featdet_ADAPchromatogrambuilder.ADAPChromatogramBuilderModule">
    <parameter name="Raw data files" type="GUI_SELECTED_FILES"/>
    <parameter name="Scans">
      <ms_level>1</ms_level>
    </parameter>
    <parameter name="Mass list">masses</parameter>
    <parameter name="Min group size in # of scans">2</parameter>
    <parameter name="Group intensity threshold">1000000.0</parameter>
    <parameter name="Min highest intensity">1000000.0</parameter>
    <parameter name="m/z tolerance">
```

```
            <absolutetolerance>0.0</absolutetolerance>
            <ppmtolerance>10.0</ppmtolerance>
          </parameter>
          <parameter name="Suffix">chromatograms</parameter>
        </batchstep>
        <batchstep method="io.github.mzmine.modules.dataprocessing.featdet_chromatogramdeconvolution.DeconvolutionModule">
          <parameter name="Feature lists" type="BATCH_LAST_PEAKLISTS"/>
          <parameter name="Suffix">deconvoluted</parameter>
          <parameter name="Algorithm" selected="Wavelets (ADAP)">
            <module name="Baseline cut-off">
              <parameter name="Min peak height"/>
              <parameter name="Peak duration range (min)">
                <min>0.0</min>
                <max>10.0</max>
              </parameter>
              <parameter name="Baseline level"/>
            </module>
            <module name="Noise amplitude">
              <parameter name="Min peak height"/>
              <parameter name="Peak duration range (min)">
                <min>0.0</min>
                <max>10.0</max>
              </parameter>
              <parameter name="Amplitude of noise"/>
            </module>
            <module name="Savitzky-Golay">
              <parameter name="Min peak height"/>
              <parameter name="Peak duration range (min)">
                <min>0.0</min>
                <max>10.0</max>
              </parameter>
              <parameter name="Derivative threshold level"/>
            </module>
            <module name="Local minimum search">
              <parameter name="Chromatographic threshold"/>
              <parameter name="Search minimum in RT range (min)"/>
              <parameter name="Minimum relative height"/>
              <parameter name="Minimum absolute height"/>
              <parameter name="Min ratio of peak top/edge"/>
              <parameter name="Peak duration range (min)">
                <min>0.0</min>
                <max>10.0</max>
              </parameter>
            </module>
            <module name="Wavelets (XCMS)">
              <parameter name="S/N threshold">10.0</parameter>
              <parameter name="Wavelet scales">
                <min>0.25</min>
                <max>5.0</max>
              </parameter>
              <parameter name="Peak duration range">
                <min>0.0</min>
                <max>10.0</max>
              </parameter>
              <parameter name="Peak integration method">Use smoothed data</parameter>
              <parameter name="R engine">RCaller</parameter>
            </module>
            <module name="Wavelets (ADAP)">
              <parameter name="S/N threshold">10.0</parameter>
              <parameter name="S/N estimator" selected="Intensity window SN">
                <module name="Intensity window SN"/>
                <module name="Wavelet Coeff. SN">
                  <parameter name="Peak width mult.">3.0</parameter>
                  <parameter name="abs(wavelet coeffs.)">true</parameter>
                </module>
              </parameter>
              <parameter name="min feature height">1000.0</parameter>
              <parameter name="coefficient/area threshold">100.0</parameter>
              <parameter name="Peak duration range">
                <min>0.02</min>
                <max>1.0</max>
              </parameter>
              <parameter name="RT wavelet range">
                <min>0.02</min>
                <max>0.6</max>
              </parameter>
```

```
            </module>
        </parameter>
        <parameter measure="MEDIAN" name="m/z center calculation" weighting="NONE">CenterFunction</parameter>
        <parameter name="m/z range for MS2 scan pairing (Da)" selected="false"/>
        <parameter name="RT range for MS2 scan pairing (min)" selected="true">0.1</parameter>
        <parameter name="Remove original feature list">false</parameter>
    </batchstep>
    <batchstep method="io.github.mzmine.modules.dataprocessing.filter_deisotoper.IsotopeGrouperModule">
        <parameter name="Feature lists" type="BATCH_LAST_PEAKLISTS"/>
        <parameter name="Name suffix">deisotoped</parameter>
        <parameter name="m/z tolerance">
            <absolutetolerance>0.0</absolutetolerance>
            <ppmtolerance>10.0</ppmtolerance>
        </parameter>
        <parameter name="Retention time tolerance" type="absolute">0.3</parameter>
        <parameter name="Monotonic shape">false</parameter>
        <parameter name="Maximum charge">1</parameter>
        <parameter name="Representative isotope">Most intense</parameter>
        <parameter name="Remove original peaklist">false</parameter>
    </batchstep>
    <batchstep method="io.github.mzmine.modules.dataprocessing.align_ransac.RansacAlignerModule">
        <parameter name="Feature lists" type="BATCH_LAST_PEAKLISTS"/>
        <parameter name="Feature list name">Aligned feature list</parameter>
        <parameter name="m/z tolerance">
            <absolutetolerance>0.0</absolutetolerance>
            <ppmtolerance>10.0</ppmtolerance>
        </parameter>
        <parameter name="RT tolerance" type="absolute">0.3</parameter>
        <parameter name="RT tolerance after correction" type="absolute">0.5</parameter>
        <parameter name="RANSAC iterations">0</parameter>
        <parameter name="Minimum number of points">0.8</parameter>
        <parameter name="Threshold value">0.3</parameter>
        <parameter name="Linear model">false</parameter>
        <parameter name="Require same charge state">true</parameter>
    </batchstep>
    <batchstep method="io.github.mzmine.modules.dataprocessing.gapfill_peakfinder.PeakFinderModule">
        <parameter name="Feature lists" type="BATCH_LAST_PEAKLISTS"/>
        <parameter name="Name suffix">gap-filled</parameter>
        <parameter name="Intensity tolerance">0.1</parameter>
        <parameter name="m/z tolerance">
            <absolutetolerance>0.0</absolutetolerance>
            <ppmtolerance>10.0</ppmtolerance>
        </parameter>
        <parameter name="Retention time tolerance" type="absolute">0.3</parameter>
        <parameter name="RT correction">false</parameter>
        <parameter name="Parallel (never combined with RT correction)">false</parameter>
        <parameter name="Remove original feature list">false</parameter>
    </batchstep>
    <batchstep method="io.github.mzmine.modules.dataprocessing.filter_rowsfilter.RowsFilterModule">
        <parameter name="Feature lists" type="BATCH_LAST_PEAKLISTS"/>
        <parameter name="Name suffix">filtered</parameter>
        <parameter name="Minimum peaks in a row" selected="false"/>
        <parameter name="Minimum peaks in an isotope pattern" selected="false"/>
        <parameter name="m/z" selected="false"/>
        <parameter name="Retention time" selected="false"/>
        <parameter name="Peak duration range" selected="true">
            <min>0.0</min>
            <max>1.0</max>
        </parameter>
        <parameter name="Chromatographic FWHM" selected="false">
            <min>0.0</min>
            <max>1.0</max>
        </parameter>
        <parameter name="Charge" selected="false"/>
        <parameter name="Kendrick mass defect" selected="false">
            <parameter name="Kendrick mass defect">
                <min>0.0</min>
                <max>1.0</max>
            </parameter>
            <parameter name="Kendrick mass base"/>
            <parameter name="Shift">0.0</parameter>
            <parameter name="Charge">1</parameter>
            <parameter name="Divisor">1</parameter>
            <parameter name="Use Remainder of Kendrick mass">false</parameter>
        </parameter>
        <parameter name="Parameter">No parameters defined</parameter>
```

```
                    <parameter name="Only identified?">false</parameter>
                    <parameter name="Text in identity" selected="false"/>
                    <parameter name="Text in comment" selected="false"/>
                    <parameter name="Keep or remove rows">Keep rows that match all criteria</parameter>
                    <parameter name="Keep only peaks with MS2 scan (GNPS)">true</parameter>
                    <parameter name="Reset the peak number ID">true</parameter>
                    <parameter name="Remove source feature list after filtering">false</parameter>
                  </batchstep>
                  <batchstep method="io.github.mzmine.modules.dataprocessing.filter_duplicatefilter.DuplicateFilterModule">
                    <parameter name="Feature lists" type="BATCH_LAST_PEAKLISTS"/>
                    <parameter name="Name suffix">filtered</parameter>
                    <parameter name="Filter mode">NEW AVERAGE</parameter>
                    <parameter name="m/z tolerance">
                      <absolutetolerance>0.0</absolutetolerance>
                      <ppmtolerance>10.0</ppmtolerance>
                    </parameter>
                    <parameter name="RT tolerance" type="absolute">0.1</parameter>
                    <parameter name="Require same identification">false</parameter>
                    <parameter name="Remove original peaklist">false</parameter>
                  </batchstep>
                  <batchstep method="io.github.mzmine.modules.io.gnpsexport.fbmn.GnpsFbmnExportAndSubmitModule">
                    <parameter name="Feature lists" type="BATCH_LAST_PEAKLISTS"/>
                    <parameter name="Filename">
                      <current_file>G:\Meu
Drive\Doutorado\Projeto\CIIMAR\Resultados\LCMS\FBMN\FBMN_DCM_Lucas_quant.csv</current_file>
                    </parameter>
                    <parameter name="Mass list">masses</parameter>
                    <parameter name="Merge MS/MS (experimental)" selected="false">
                      <parameter name="Select spectra to merge">across samples</parameter>
                      <parameter name="m/z merge mode">weighted average (remove outliers)</parameter>
                      <parameter name="intensity merge mode">sum intensities</parameter>
                      <parameter name="Expected mass deviation">
                        <absolutetolerance>0.001</absolutetolerance>
                        <ppmtolerance>5.0</ppmtolerance>
                      </parameter>
                      <parameter name="Cosine threshold (%)">0.7</parameter>
                      <parameter name="Peak count threshold (%)">0.2</parameter>
                      <parameter name="Isolation window offset (m/z)">0.0</parameter>
                      <parameter name="Isolation window width (m/z)">3.0</parameter>
                    </parameter>
                    <parameter name="Filter rows">ONLY WITH MS2</parameter>
                    <parameter name="Submit to GNPS" selected="false">
                      <parameter name="Meta data file" selected="false"/>
                      <parameter name="Presets">HIGHRES</parameter>
                      <parameter name="Job title"/>
                      <parameter name="Email"/>
                      <parameter name="Username"/>
                      <parameter name="Password"/>
                      <parameter name="Open website">true</parameter>
                    </parameter>
                    <parameter name="Open folder">false</parameter>
                  </batchstep>
                </batch>
```

APPENDIX 2 – Parameter used for feature based networking with the public link to access the molecular networking job.

A molecular network was created with the Feature-Based Molecular Networking (FBMN) workflow on GNPS (https://gnps.ucsd.edu). The mass spectrometry data were first processed with MZMINE3 and the results were exported to GNPS for FBMN analysis. The data was filtered by removing all MS/MS fragment ions within +/- 17 Da of the precursor *m/z*. MS/MS spectra were window filtered by choosing only the top 6 fragment ions in the +/- 50 Da window throughout the spectrum. The precursor ion mass tolerance was set to 0.02 Da and the MS/MS fragment ion tolerance to 0.02 Da. A molecular network was then created where edges were filtered to have a cosine score above 0.85 and more than 6 matched peaks. Further, edges between two nodes were kept in the network if and only if each of the nodes appeared in each others respective top 10 most similar nodes. Finally, the maximum size of a molecular family was set to 100, and the lowest scoring edges were removed from molecular families until the molecular family size was below this threshold. The analogue search mode was used by searching against MS/MS spectra with a maximum difference of 100.0 in the precursor ion value. The library spectra were filtered in the same manner as the input data. All matches kept between network spectra and library spectra were required to have a score above 0.7 and at least 6 matched peaks. The DEREPLICATOR was used to annotate MS/MS spectra.

The molecular networking job can be publicly accessed at:

Figure 2 – https://gnps.ucsd.edu/ProteoSAFe/status.jsp?task=0836fef437714d9aa089b47c28324138

APPENDIX 3 – Parameter used for feature based networking with the public link to access the molecular networking job.

A molecular network was created with the Feature-Based Molecular Networking (FBMN) workflow on GNPS (https://gnps.ucsd.edu). The mass spectrometry data were first processed with MZMINE3 and the results were exported to GNPS for FBMN analysis. The data was filtered by removing all MS/MS fragment ions within +/- 17 Da of the precursor *m/z*. MS/MS spectra were window filtered by choosing only the top 6 fragment ions in the +/- 50 Da window throughout the spectrum. The precursor ion mass tolerance was set to 0.02 Da and the MS/MS fragment ion tolerance to 0.02 Da. A molecular network was then created where edges were filtered to have a cosine score above 0.7 and more than 6 matched peaks. Further, edges between two nodes were kept in the network if and only if each of the nodes appeared in each others respective top 10 most similar nodes. Finally, the maximum size of a molecular family was set to 100, and the lowest scoring edges were removed from molecular families until the molecular family size was below this threshold. The analogue search mode was used by searching against MS/MS spectra with a maximum difference of 100.0 in the precursor ion value. The library spectra were filtered in the same manner as the input data. All matches kept between network spectra and library spectra were required to have a score above 0.7 and at least 6 matched peaks. The DEREPLICATOR was used to annotate MS/MS spectra. The molecular networks were visualized using Cytoscape software.

The molecular networking job can be publicly accessed at:

Figure 4 - https://gnps.ucsd.edu/ProteoSAFe/status.jsp?task=71164ce15c464e45bc738f87db38d0de

Figure 9 - https://gnps.ucsd.edu/ProteoSAFe/status.jsp?task=83184dc0750646238bad57802a81afc0

Figure 14 - https://gnps.ucsd.edu/ProteoSAFe/status.jsp?task=8675149c90ff462b80b7a6c5c2c60cd8

APPENDIX 4 – Dose-response graph for the lipid-reducing assay. The node shows the mean value, and the line the variation between individuals (n=6).

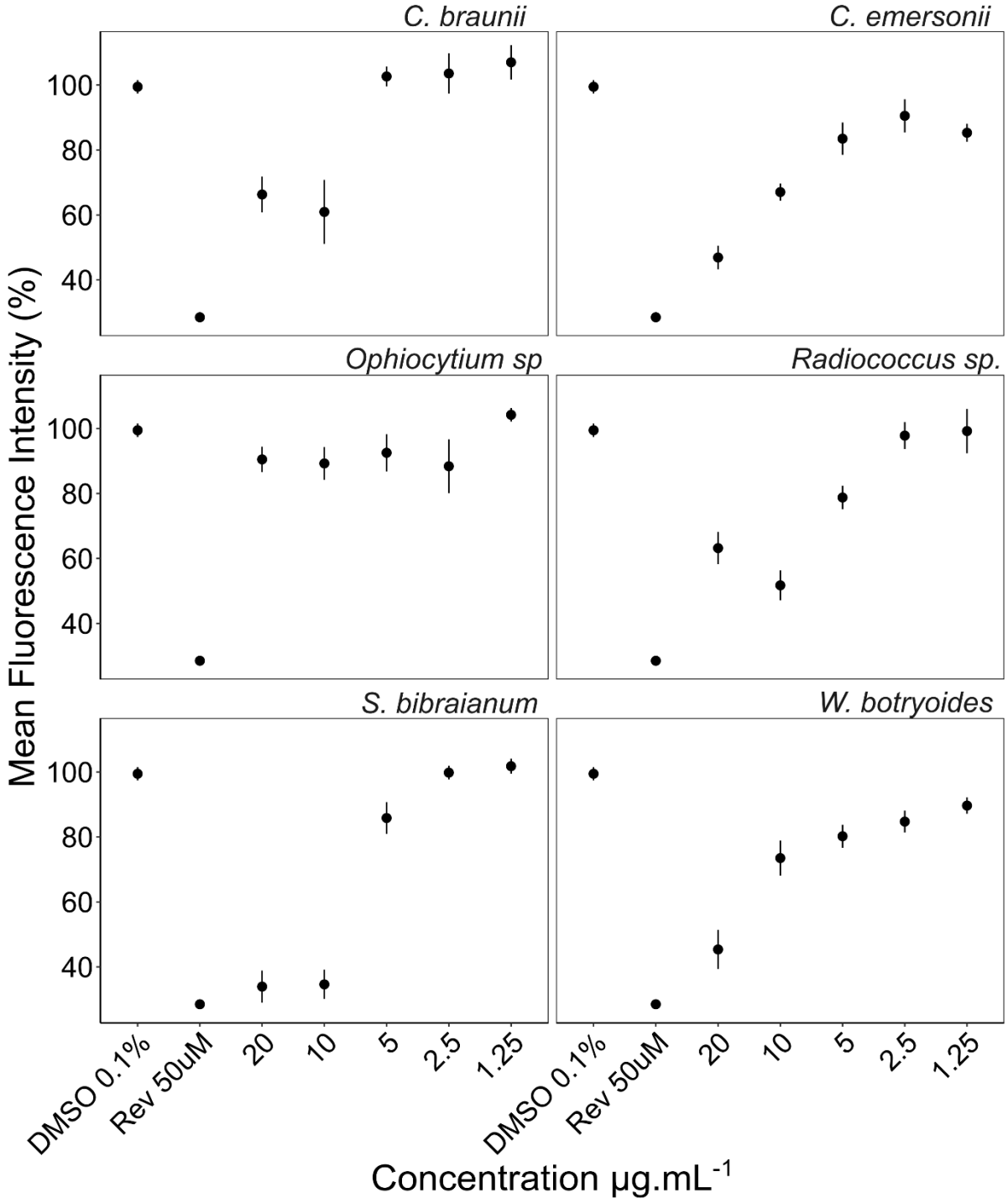

APPENDIX 5 – Dose-response graph for the appetite inhibition assay. The node shows the mean value, and the line the variation between individuals (n=6).